UNIVERSIDADE DE LISBOA
FACULDADE DE CIÊNCIAS
DEPARTAMENTO DE QUÍMICA E BIOQUÍMICA

The role of key post-translational modifications in the nuclear translocation of STAT3 dimers upon cytokine stimulation

Daniela Martins Alves

Mestrado em Bioquímica
Especialização em Bioquímica

Dissertação orientada por:
Dr. Federico Herrera
Dr. Mickael Diallo

2022

Acknowledgments

I would like to express my gratitude to all of those involved in the development of this dissertation:

First, I would like to say thank you to my supervisor Dr. Federico Herrera for the opportunity to work in his laboratory and for the support, patience, and guidance throughout this project. Also, I would like to thank him for helping me achieve one of my goals: to do Erasmus.

I also want to say thank you to my co-supervisor Dr. Mickael Diallo who helped me whenever I needed and taught me so much throughout my dissertation.

To all my colleagues in Herrera's laboratory, specially to Ricardo, Fernanda and Mafalda thank you so much for the help, advice, and company you provided during this time.

I want to say a special thank you to the laboratory of Carmen Rodrígez in the University of Oviedo, Spain, where I did Erasmus. Carmen, Vanesa, Ana, and Maria thank you so much for making me feel so welcome in Oviedo and for teaching me so much in the 3 months I stayed there.

Last, but not least I want to thank my family and my friends for always support me in every phase of my life and for always believe in me even when I doubt myself.

All of you contributed to my personal and scientific growth, so thank you!

This dissertation was mostly carried out at the Cell Structure and Dynamics laboratory (BioISI, Faculdade de Ciências, Universidade de Lisboa) and had an Erasmus component at University of Oviedo, Spain for 3 months. I would like to acknowledge the International FCUL office and Universidade de Lisboa that allowed me to enroll the Erasmus+ 2020/2021 program with the Erasmus scholarship.

Abstract

STAT3 is a pleiotropic transcription factor that plays key roles in development, immunity, response to stress/damage and cancer. Its activity is largely regulated by specific post-translational modifications (PTMs) and protein-protein interactions. Most studies focus only on the phosphorylation at Y705 and/or S727, neglecting almost 80 identified PTMs. Furthermore, it is unlikely that all STAT3 molecules are modified simultaneously exactly in the same residues, existing different pools of STAT3 molecules. The main goal of this work was to determine the influence of key post-translational modifications on STAT3 translocation to the nucleus upon canonical stimulation with cytokines from the IL-6 family. To address this question, we first characterized a STAT3 knockout HeLa cell strain recently developed in our laboratory and created a series of molecular tools to analyze the dynamics of STAT3 homodimers in living cells based on BiFC (i.e., STAT3 expression plasmids with mutations preventing key PTMs, such as Y705F, K49R, K685R, S727A, T236A, Y640F and T714A). STAT3 knockout cells have a distinct gene expression profile and increased oxidative stress. Second, we studied the influence of symmetrically and asymmetrically modified STAT3 homodimers in their response to cytokines. Phosphorylation of only one of the STAT3 monomers is enough to drive STAT3 dimers into the nucleus after LIF stimulation. STAT3 dimers can accumulate in the nucleus independently of their phosphorylation status at Y705 and LIF stimulation. And third, we studied the effect of the disease-associated phosphoresistant Y640F mutation in the behavior of STAT3 dimers. This mutation increases the accumulation of STAT3 in the nucleus in response to LIF but is not related to oxidative stress and gene expression. Our results advance our understanding of STAT3 signaling and could potentially contribute to the study of several human pathologies involving STAT3, such as cancer, hyper-IgE Syndrome, or Inflammatory Hepatocellular Adenoma.

Key words: STAT3, post-translational modifications, bimolecular fluorescence complementation, homodimerization, nuclear translocation.

Resumo

O Transdutor de Sinal e Ativador da Transcrição 3 (STAT3) é um fator de transcrição pleiotrópico que desempenha funções importantes numa variedade de processos fisiológicos, incluindo proliferação celular, sobrevivência, diferenciação, inflamação, angiogénese, apoptose, progressão do ciclo celular e migração celular. O STAT3 está constitutivamente ativo em cerca de 70% dos cancros nos humanos. Esta ativação constitutiva deve-se maioritariamente à desregulação das vias de sinalização a montante. Os cancros incluem tanto tumores hematológicos (ex. leucemia, linfoma ou mieloma múltiplo) como tumores sólidos. Para além disto, mutações ativadoras no STAT3 (ex. Y640F) têm sido associadas a algumas doenças como Leucemia Linfocítica Granular e Adenoma Hepatocelular Inflamatório. Enquanto mutações inativadoras do STAT3 (ex. S636Y, T708S ou T714A) associam-se com a Síndrome de hiper-imunoglobulina E. Apesar do papel claro do STAT3 no cancro, também existem evidências de funções supressoras de tumores para o STAT3. Deste modo as consequências biológicas da ativação do STAT3 no cancro dependem do tipo de tumor e do contexto celular.

O STAT3 é ativado a jusante de muitos tipos de sinais extracelulares, incluindo a família IL-6 de citocinas (ex. IL-6, IL-11, fator inibidor de leucemia (LIF), etc.), hormonas (hormona do crescimento, prolactina e leptina), fatores de crescimento (EGF, PDGF, FGF e IGF), interferões, entre outros. A família IL-6 de citocinas ativa o STAT3 através da via de sinalização canónica JAK-STAT3. Esta via começa com a ligação de uma citocina ao seu recetor na membrana celular. Isto ativa um dos membros da família de *Janus kinase* (JAK) que por sua vez fosforila o recetor da citocina. Os dímeros de STAT3 são recrutados ao recetor ativado e são fosforilados na tirosina 705 (Y705). Isto leva à acumulação dos dímeros de STAT3 fosforilados no núcleo. Os mecanismos moleculares pelos quais a acumulação no núcleo ocorre ainda estão sob discussão. Alguns investigadores defendem que o STAT3 é maioritariamente encontrado no citoplasma de células não estimuladas e que só vai para o núcleo após estimulação com uma citocina. Outros defendem que o STAT3 está permanentemente a mover-se entre o citoplasma e o núcleo e que fica retido no núcleo após a sua fosforilação induzida por uma citocina. Uma vez no núcleo, o STAT3 fosforilado liga-se ao DNA e consegue ativar ou reprimir a expressão génica. Alguns dos genes ativados pelo STAT3 são genes pró-sobrevivência (ex. *BCL2*, *BCL2L1*, *MCL1* e BIRC5); genes de progressão do ciclo celular (ex., *CCND1* e *c-MYC*); e genes pró-migratórios (ex., *MMP2*). O STAT3 fosforilado também reprime a expressão de alguns genes relacionados com a proliferação e sobrevivência celular, como *TP53*, *FAS* e *NDN*. A expressão e ativação do STAT3 é altamente regulada através de uma variedade de proteínas endógenas (ex. SOCS e PIAS) que conseguem silenciar a via de sinalização JAK-STAT3.

Para além desta via canónica, também foram descritas outras vias não canónicas do STAT3 que são independentes da fosforilação do STAT3 no resíduo Y705. Estas vias não canónicas incluem a atividade transcripcional do STAT3 não fosforilado e a atividade do STAT3 na mitocôndria e no retículo endoplasmático. Nestes organelos, o STAT3 desempenha diversas funções como a regulação da respiração e do metabolismo mitocondrial e a regulação de espécies reativas de oxigénio (ROS) e de cálcio (Ca^{2+}).

Ambas as vias de STAT3 canónicas e não canónicas dependem fortemente de interações com outras proteínas e de modificações pós-traducionais (PTMs). A maioria das funções e interações do STAT3 foram estudadas em relação à fosforilação nos resíduos Y705 ou S727. No entanto, o STAT3 tem cerca de 80 PTMs comprovadas experimentalmente, incluindo muitos outros eventos de fosforilação, acetilação, metilação, ubiquitinação e SUMOilação. As funções biológicas destas PTMs são pouco estudadas, e a sua influência nas interações com outras proteínas é mal compreendida. É também improvável que todas as moléculas de STAT3 sejam modificadas simultaneamente nos mesmos resíduos, existindo diferentes conjuntos de moléculas de STAT3 na célula. Recentemente,

descrevemos que dímeros de STAT3 modificados assimetricamente apresentaram alterações no seu comportamento e função. No entanto, estas observações foram realizadas em células que expressavam STAT3 endógeno e em ausência de estímulo de citocinas.

O principal objetivo deste trabalho foi determinar a influência de modificações pós-traducionais importantes na translocação do STAT3 para o núcleo, após estimulação com citocinas da família IL-6. Para responder a esta questão, usámos células HeLa com *knockout* do gene *STAT3* (STAT3-/-) que foram recentemente desenvolvidas no laboratório do Dr. Federico Herrera. Primeiramente, caracterizámos esta linha celular em termos de proliferação, stress oxidativo, níveis de Ca^{2+}, potencial de membrana mitocondrial, expressão génica e níveis de proteínas, usando citometria de fluxo, qPCR e *Western Blot*. Observámos que as células HeLa STAT3-/- têm um perfil genético distinto e maior stress oxidativo. Criámos também uma série de ferramentas moleculares baseadas no ensaio de complementação de fluorescência bimolecular (BiFC) para analisar a dinâmica dos homodímeros de STAT3 nas células. Nestes ensaios BiFC, duas proteínas de interesse são unidas a duas metades complementares não fluorescentes de um repórter fluorescente, como Vénus. Se as proteínas de interesse interagirem, as metades do repórter unem-se reconstituindo o fluoróforo funcional. A fluorescência é, portanto, proporcional à dimerização das proteínas e pode ser facilmente medida por citometria de fluxo ou microscopia. Plasmídeos Venus-STAT3 BiFC, desenvolvidos previamente no laboratório do Dr. Federico Herrera, foram modificados por *site-directed mutagenesis*. Resíduos fosforiláveis (serina (S), treonina (T) e tirosina (Y)) e resíduos lisina (K) (acetiláveis, metiláveis, ubiquitináveis e SUMOiláveis) foram mutados para resíduos estruturalmente semelhantes, não modificáveis [fenilalanina (F), alanina (A) ou arginina (R), a depender do tipo de resíduo]. Deste modo, foram desenvolvidos plasmídeos que expressam STAT3 com mutações que previnem PTMs essenciais ou relacionadas com doenças humanas, como Y705F, K49R, K685R, S727A, T236A, Y640F e T714A. Em segundo lugar, estudámos a influência dos homodímeros de STAT3 modificados simetricamente e assimetricamente na sua resposta a citocinas. As células HeLa STAT3-/- foram transfetadas com combinações de dois plasmídeos Venus-STAT3 BiFC complementares. Foram feitas combinações simétricas de plasmídeos, ou seja, nas quais os dois plasmídeos eram *wild type* ou tinham a mesma mutação. Também foram feitas combinações assimétricas em que os plasmídeos eram diferentes, ou seja, um dos plasmídeos podia ser *wild type* e o outro podia ter uma mutação ou então podiam ser dois plasmídeos mutados, mas com diferentes mutações. Após transfeção e tratamento com LIF, as proteínas nucleares foram extraídas e analisadas por *Western Blot*. Observámos que enquanto os dímeros simétricos de *wild type* STAT3 acumularam-se rapidamente no núcleo em resposta ao LIF, os dímeros simétricos mutantes Y705F não. Os dímeros STAT3 assimétricos onde um dos monómeros era *wild type* STAT3 responderam como os dímeros simétricos de *wild type* STAT3. Deste modo, a fosforilação de apenas um dos monómeros de STAT3 é suficiente para provocar a translocação dos dímeros de STAT3 para o núcleo após estimulação com LIF. Os dímeros de STAT3 podem acumular-se no núcleo independentemente do seu estado de fosforilação no resíduo Y705 e de estimulação com LIF. Em terceiro lugar, estudámos o efeito da mutação fosforesistente Y640F relacionada com doenças no comportamento dos dímeros de STAT3. Esta mutação aumenta a acumulação de STAT3 no núcleo em resposta ao LIF, mas não está relacionada com stress oxidativo e expressão génica. Os nossos resultados permitem aprimorar o nosso conhecimento sobre as vias de sinalização do STAT3 e podem potencialmente contribuir para o estudo de diversas patologias humanas que envolvem o STAT3, como cancro, Síndrome de hiper-imunoglobulina E ou Adenoma Hepatocelular Inflamatório.

Palavras-chave: STAT3, modificações pós-traducionais, complementação de fluorescência bimolecular, homodimerização, translocação nuclear.

Index

List of Figures

List of Tables

List of Abbreviations, Acronyms and Symbols

A	Alanine
AMPK	AMP-activated Protein Kinase
AP-1	Activator Protein 1
BCL2	BCL2 apoptosis regulator
BiFC	Bimolecular Fluorescence Complementation
BRET	Bioluminescence Resonance Energy Transfer
bZIP	Basic leucine zipper
c-MYC	MYC proto-oncogene
Cas9	CRISPR associated protein 9
CBP	CREB-Binding Protein
CCD	Coiled-Coil Domain
CCND1	Cyclin D1
CRISPR	Clustered Regularly Interspaced Short Palindromic Repeats
D	Aspartic acid
DBD	DNA Binding Domain
DMEM	Dulbecco's Modified Eagle Medium
E	Glutamic acid
EGF	Epidermal Growth Factor
EGFP	Enhanced Green Fluorescent Protein
ER	Endoplasmic Reticulum
ETC	Electron Transport Chain
EYFP	Enhanced Yellow Fluorescent Protein
F	Phenylalanine
FGF	Fibroblast Growth Factor
FRET	Förster or Fluorescence Resonance Energy Transfer
G	Glycine

GAPDH Glyceraldehyde-3-phosphate Dehydrogenase

GFP Green Fluorescent Protein

GPX1 Glutathione Peroxidase 1

GRIM-19 Gene associated with Retinoid-IFN-induced Mortality 19

HIES Hyper-Immunoglobulin E Syndrome

I Isoleucine

IFN Interferon

Ig Immunoglobulin

IGF Insulin-like Growth Factor

IGFBP3 Insulin-like Growth Factor Binding Protein 3

IHCAs Inflammatory Hepatocellular Adenomas

IL Interleukin

IP3R3 Inositol 1,4,5-trisphosphate Receptor 3

IRE1 Inositol-Requiring Enzyme 1

IRF Interferon Regulatory Factor

JAK Janus Kinase

K Lysine

KO Knockout

L Leucine

LB Luria Broth

LD Linker Domain

LGL Large Granular Lymphocytic

LIF Leukemia Inhibitory Factor

M Methionine

MAM Mitochondria-associated endoplasmic reticulum membrane

MAPK Mitogen-Activated Protein Kinase

MMP Matrix Metalloproteinases

mTOR Mammalian Target Of Rapamycin

NF-κB	Nuclear Factor kappa-light-chain-enhancer of activated B cells
NTD	N-Terminal Domain
PBS	Phosphate-Buffered Saline
PCAs	Protein-fragment Complementation Assays
PCNA	Proliferating Cell Nuclear Antigen
PCR	Polymerase Chain Reaction
PDGF	Platelet-Derived Growth Factor
PIAS	Protein Inhibitor of Activated STAT
PTMs	Post-Translational Modifications
Q	Glutamine
qPCR	Real-time quantitative Polymerase Chain Reaction
R	Arginine
RELA	REL-associated protein/transcription factor p65
ROS	Reactive Oxygen Species
SDS	Sodium Dodecyl Sulfate
SH2	Src Homology 2 Domain
SLC2A1	Solute carrier family 2 member 1
SOCS	Suppressor Of Cytokine Signaling
SOD	Superoxide Dismutase
STAT	Signal Transducer and Activator of Transcription
T	Threonine
TAD	Transactivation Domain
UPR	Unfolded Protein Response
V	Valine
VC	C-terminal fragment (aa 158-238) of Venus
VDAC	Voltage Dependent Anion-selective Channel
VN	N-terminal fragment (aa 1-157) of Venus
WT	Wild Type

Y	Tyrosine
Y2H	Yeast Two Hybrid
YFP	Yellow Fluorescent Protein

I. Introduction

1.1 The Signal Transducer and Activator of Transcription (STAT) pathway

1.1.1 The STAT family of transcription factors

STATs are dual function proteins which receive an activating signal from the cell surface and carry it toward the nucleus to induce gene transcription **[1]**. In mammals, the STAT protein family consists of seven members (STAT1, STAT2, STAT3, STAT4, STAT5A, STAT5B and STAT6) that share a common structural organization represented by six distinct and functionally conserved domains (from N- to C-termini): N-terminal domain (NTD), coiled-coil domain (CCD), DNA-binding domain (DBD), linker domain (LD), Src homology 2 domain (SH2) and the C-terminally located transactivation domain (TAD) (**Figure 1.1**) **[2]**. The NTD is involved in STAT dimerization and tetramerization and heterologous protein–protein interactions. The CCD is a domain that mediates STAT interactions with other proteins including IRF-9/p48 for STAT1; c-Jun, StIP1 and GRIM-19 for STAT3; and SMRT for STAT5A and STAT5B. In STAT3, CCD is also required for receptor binding. The DBD adopts an immunoglobulin-fold structure and binds to DNA as a dimer. It is also involved in nuclear translocation, probably by maintaining proper conformation so that importins can recognize and bind to the nuclear localization sequences of STATs. The LD is involved in protein–protein interactions (e.g., association between STAT3 and GRIM-19) and it can also be involved in nuclear export and DNA binding. In STAT1, the LD is also associated with transcriptional activation **[2]**. STATs are the only transcription factors containing the phospho-tyrosine binding domain SH2, which is the most conserved domain and is critical for receptor association and phospho-dimer formation. Despite their highly conserved structure, each protein responds to a distinct group of extracellular stimuli and control distinct cellular processes **[2]**.

In mammalian cells, STAT1 and STAT2 were the first proteins identified in interferon signal transduction pathways **[3]**. While STAT1 is activated by type I interferons (IFN-α, -β, -τ, -ω), IFN-γ and other cytokines (e.g., IL-6, IL-2, IL-3) **[4]**, STAT2 is only activated by type I IFN **[3]**. In the IFN-I signaling pathway, heterodimers of STAT2/STAT1 are assembled. These heterodimers associate with the DNA binding protein interferon regulatory factor 9 (IRF9) to form the transcriptional complex interferon stimulated gene factor 3 (ISGF3), activating the expression of IFN-I target genes (e.g., *IRF1*, *IRF2*, *IFNB1*, *OAS*, and *MX1*) **[5]**. STAT1 and STAT2 are involved in anti-viral and -bacterial responses, immunomodulation, growth inhibition, apoptosis regulation, and tumor growth suppression **[3]**. STAT3 is activated by a plethora of stimuli: the IL-6 family of cytokines (IL-6, IL-11, IL-22, IL-27, IL-31, oncostatin M, cardiotrophin-1, ciliary neurotrophic factor, cardiotrophin-like cytokine factor 1, and leukemia inhibitory factor (LIF)); hormones (growth hormone, prolactin, and leptin); growth factors (EGF, PDGF, FGF and IGF); interferons; oncogenic non-receptor tyrosine kinases (Src and ABL1); Toll-like receptors; and G-protein coupled receptors **[6]–[10]**. STAT3 is a pleiotropic transcription factor that plays a key role in a variety of physiological processes, including cell proliferation, survival, differentiation, inflammation, angiogenesis, apoptosis, cell cycle progression and cell migration **[11], [12]**. Some of these roles will be further discussed in the following sections. STAT4 is stimulated by IL-12 and is required for T helper 1 (Th1) cell development and IFN-γ production **[3]**. STAT5A and STAT5B are activated by several cytokines and hormones such as interleukins, erythropoietin, growth hormone, and prolactin and are involved in cell differentiation, lipid mobilization and lymphocyte development. STAT5A and STAT5B are involved in prolactin and

growth hormone signaling, respectively **[3]**. IL-4 and IL-13 activate STAT6, resulting in the proliferation of lymphocytes, differentiation of macrophages, regulation of the IgE class switch in B cells and prevention of apoptosis. STAT6 is also involved in the development of Th2 cells **[3]**.

Among STATs, only the STAT3 knockout in mice leads to early embryonic lethality, which cannot be compensated by other STAT members despite their high homology and shared pathways **[13]**. This indicates a unique role of STAT3 in embryonic development.

Figure 1.1 - Structure of the STAT family of transcription factors. STAT proteins share six distinct and functionally conserved domains: N-terminal domain (NTD), coiled-coil domain (CCD), DNA-binding domain (DBD), linker domain (LD), Src homology 2 domain (SH2) and transactivation domain (TAD). Source: Guanizo *et al.,* 2018 **[14]**.

1.1.2 STAT3 importance at a pathological level

STAT3 is constitutively activated in many human cancers, mostly because of deregulated upstream signaling pathways. Current estimates suggest that persistent STAT3 Y705 phosphorylation -the key activating post-translational modification- is detected in about 70% of human cancers **[15]**. These include both hematological tumors, such as leukemia, lymphoma or multiple myeloma, and solid tumors of the bladder, bone, breast, brain, cervix, colon, esophagus, head-and-neck, kidney, liver, lung, ovary, pancreas, prostate, stomach, and uterus. Most of these tumors frequently become dependent on STAT3 activity and are correlated with a poor clinical outcome **[3]**. In the early stages of cancer development, STAT3 allows tumor initiation without mutations because STAT3 prevents p53-mediated growth control and apoptosis when activated **[16]**. STAT3 facilitates invasiveness and metastasis of cancer cells through the stimulation of angiogenesis, proliferation, survival and expression of matrix metalloproteinases (e.g. MMP-2 and MMP-7) that contribute to invasiveness **[17]–[19]**. Cancer cells and other cell types that are found in the tumor microenvironment release IL-6, which in turn contributes to the activation of STAT3. STAT3 can bind to the promoter of the IL-6 gene and induce its expression, creating a positive-feedback loop. In the tumor microenvironment, STAT3 stimulates the production of other pro-inflammatory cytokines (e.g., IL-1β, IL-8 and CCL2) through the recruitment of immune cells, exacerbating inflammation. STAT3 can also activate immunosuppressive factors such as IL-10 and TGF-β, both of which can stimulate STAT3, creating another positive-feedback loop **[3]**. Despite the clear role of STAT3 in cancer, there is also evidence of tumor suppressive roles for STAT3. For example, activated STAT3 has been shown to suppress proliferation, c-Myc-mediated and spontaneous malignant transformation of mouse embryonic

fibroblasts **[20]**. In phosphatase and tensin homolog deleted on chromosome 10 (PTEN)-proficient mouse astrocytes, STAT3 behaves as a tumor suppressor, preventing astrocyte proliferation and invasiveness. Consistently, simultaneous suppression of PTEN and STAT3 led to astrocyte malignant transformation **[21]**. The biological consequences of STAT3 activation in cancer depend on the tumor type and cellular context.

Activating mutations in STAT3 (e.g. Y640F) have been associated with some diseases such as large granular lymphocytic leukemia (LGL leukemia) **[22]** and inflammatory hepatocellular adenomas (IHCAs) **[23]**, whereas inactivating mutations in STAT3 (e.g. S636Y, T708S or T714A) associate with hyper-Immunoglobulin E syndrome (HIES) **[24]**. LGL leukemia is a rare type of leukemia which can be chronic or aggressive. Most cases are chronic, accounting for 2 to 5% of all chronic lymphoproliferative diseases **[25]**. The most common symptoms are severe neutropenia with or without anemia, and autoimmune-like manifestations including rheumatoid arthritis, autoantibodies, and hyperglobulinemia **[26]**. Patients with aggressive LGL leukemia can also present splenomegaly, hepatomegaly, and lymphadenopathy **[27]**. Both men and women are equally affected, and the median age at diagnosis is 60 years **[25]**. As most cases have an indolent, chronic course, it is common to apply a "watch-and-wait" approach. Current treatment involves a combination of chemotherapy and immune-suppressing drug therapy which includes methotrexate, cyclophosphamide, cyclosporine, fludarabine and alemtuzumab. Bone marrow or stem cell transplantation or splenectomy could also be used to treat LGL leukemia **[25]**. However, there is no cure and patients with the chronic type of the disease are estimated to live an average of 9 years after diagnosis. Life expectancy is likely to be much lower for the aggressive type, as it does not respond well to current therapy **[28]**. LGL leukemia is characterized by enlarged lymphocytes containing noticeable granules, and there are two types depending on the type of white cell expanded: T-cell (T-LGL) and natural killer cell (NK-LGL). T-LGL exhibits expansion of CD3+CD8+CD57+ T-cells and NK-LGL exhibits expansion of CD3−CD16+CD56+ NK cells **[29]**. Heterozygous, somatic STAT3 mutations in the SH2 domain have been reported in approximately 40% of LGL leukemia patients, with Y640F and D661Y being the most common. Studies comparing patients with and without STAT3 mutations showed that the former are more prone to have neutropenia and rheumatoid arthritis. However, no clear relation between STAT3 mutations and the type of LGL leukemia has been established **[29]**.

IHCAs are rare benign liver tumors derived from monoclonal proliferation of hepatocytes, accounting for 40–50% of all adenomas. IHCAs develop predominantly in women (average age: 38 years) with a female/male ratio of 8:1 **[30]**. The therapeutic strategy is determined by tumor size, localization, and sex. In women, when IHCAs are <5 cm, or regress to <5 cm following cessation of oral contraceptives, with no further growth detected, a "watch-and-wait" policy is used. For lesions >5 cm, elective surgical resection is considered. In this case, a laparoscopic approach is preferred instead of open surgery due to fewer complications. When it is not possible to perform surgery, radiofrequency ablation and transcatheter arterial embolization can be performed **[31]**. In men, all IHCAs should be surgically removed because of the high risk of malignant transformation **[30]**. IHCAs are characterized by constitutive uncontrolled activation of the inflammatory IL6/JAK/STAT pathway, which leads to inflammatory infiltrates, dystrophic vessels, and sinusoidal dilatations. IHCAs are associated to several mutations in different oncogenes that belong to this pathway: *GP130* (65%), *FRK* (10%), *STAT3* (5%), *GNAS* (5%), and *JAK1* (2%) **[30]**. Seven STAT3 somatic monoallelic mutations have been reported in IHCAs: Y640F, L78R, D502Y, K658Y, E166Q, Y657_M660dup and G656_Y657insF **[23]**. Besides these mutations, environmental factors can increase the risk of IHCAs, such as hormonal exposure, obesity, metabolic syndrome, and high alcohol consumption **[30]**.

HIES is a rare primary immunodeficiency characterized by a triad of eczema, recurrent skin and pulmonary infections, and elevated IgE levels, although its clinical features might differ widely from person to person. Most cases of HIES are sporadic, but autosomal recessive (AR), autosomal dominant (AD) and X-linked variants were reported **[32]**. AD-HIES is caused mostly by germline, heterozygous mutations with dominant-negative effect in STAT3 that cause its loss-of-function. AD-HIES affects males and females equally in all ethnic groups, affecting fewer than 1 per million people worldwide **[33]**. AD-HIES patients frequently show skeletal and connective tissue abnormalities, including characteristic facial features (broad nasal bridge, prominent forehead, and facial asymmetry), prolonged retention of primary teeth, hyperextensible joints, scoliosis, recurrent pathological fractures, and vascular anomalies **[32]**. Some individuals with AD-HIES also develop lymphomas, suggesting a greater risk of cancer than the general population **[33]**. Although AD-HIES has an early onset in most of the cases, there are adult-onset cases. This complicates diagnostics and treatment. The strategies to treat AD-HIES are purely symptomatic, most frequently involving long-term use of systemic antibiotics and antifungals to prevent and manage infections and a proper skin care. Some patients with low immunoglobulin levels and/or impaired immunity are treated with intravenous immunoglobulin. For more severe cases, surgery is also required (e.g., to treat lung abscesses) **[33]**, and hematopoietic stem cell transplantation is currently being explored, although its efficacy remains unclear **[32]**. AD-HIES is linked with high morbidity and mortality, but with proper care, continuous monitoring, and patient cooperation, the prognosis can be improved, and patients can live more than 50 years **[34]**.

1.1.3 STAT3 isoforms

The *STAT3* gene is composed of 24 exons located on chromosome 17q21, and is highly conserved across species, as the translated protein has only 1 amino acid difference between mouse and human **[33]**. The domains have been clearly defined and are shared with other STATs (see **section 1.1.1**). There are six known isoforms of human STAT3: STAT3α, STAT3β, STAT3ΔS-α, STAT3ΔS-β, STAT3γ and STAT3δ **[35]–[38]**. STAT3α (92 kDa) and STAT3β (83 kDa) are formed by alternative splicing but differ in structure and function. STAT3α is the most abundant isoform, has 770 amino acids and is responsible for most cellular functions attributed to STAT3 **[35]**. In comparison with STAT3α, STAT3β lacks the terminal 55 amino acids which are replaced by a unique 7 amino acid sequence. This truncation eliminates key phosphorylatable residues such as S727 **[35]**. STAT3β activation results in distinct gene expression profiles (e.g. *A2M* and *FOS*) **[39]**. STAT3ΔS-α and STAT3ΔS-β are also STAT3 splice variants that result from the presence or absence of the three nucleotides encoding serine 701 in STAT3α and STAT3β (**Figure 1.2**) **[36], [37]**. There is not much information about the specific roles and importance of STAT3ΔS-α and STAT3ΔS-β. In eosinophils and diffuse large B-cell lymphoma cells, STAT3 isoforms are found in the following proportions: α ~ 75%, β ~ 12%, ΔS-α ~ 10% and ΔS-β ~ 3%. The ΔS variants account for 10–26% of STAT3 transcripts across 16 human tissues, being therefore likely that all cells contain these 4 isoforms of STAT3. Although ΔS variants are less abundant than STAT3α and STAT3β, the ratio between ΔS and the α and β variants remains relatively constant in tissues and is conserved among species **[37]**. This suggests that STAT3ΔS-α and STAT3ΔS-β could have an important biological role. Indeed, it was shown that the expression of all 4 variants (α, β, ΔS-α and ΔS-β) enabled the survival of activated B-cell-like diffuse large B-cell lymphoma cells in culture and activated the target genes *NFKBIA* and *NFKBIZ* **[40]**. STAT3γ (72 kDa) and STAT3δ (64 kDa) are C-terminal truncated forms of full-length STAT3 generated by proteolytic processing. STAT3γ is activated in the terminal stage of granulocytic differentiation whereas STAT3δ is activated in the early stage. These isoforms do not actively mediate

transcription, so they might serve as negative regulators of STAT3 functions **[38], [41]**.

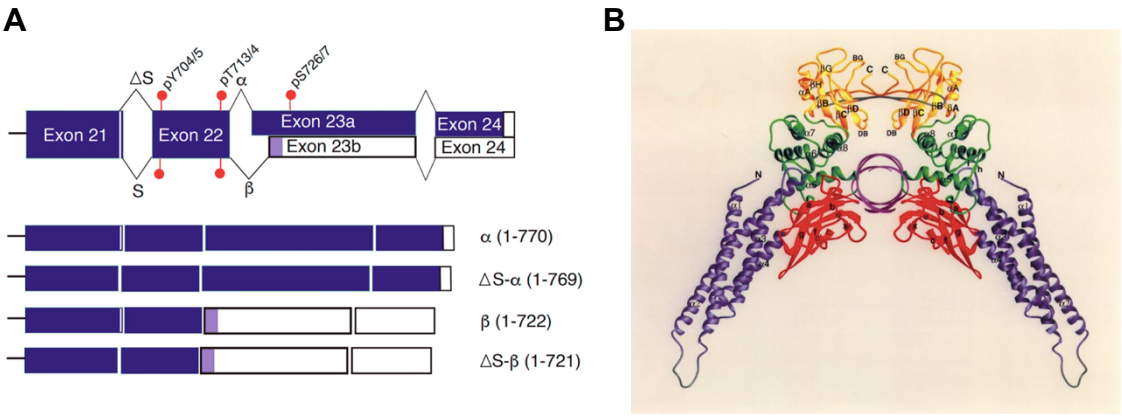

Figure 1.2 - Alternative splicing isoforms of STAT3. A, Scheme of the four STAT3 splice variants. Two splice sites near the 3' end of the STAT3 transcript produce four STAT3 isoforms: α (the longest isoform), β (a shorter isoform with distinct seven residues at the C-terminus), Ser-701-deleted α (ΔS-α), and Ser-701-deleted β (ΔS-β). White boxes indicate the non-coding 3' UTR, and light blue boxes depict coding sequences due to alternative splicing. Phosphorylation sites present in the translated form are also shown on the STAT3 transcript. Source: Zhu *et al.*, 2019 **[42]**. **B**, Model of the STAT3β-DNA complex in a ribbon diagram. Individual domains are color coded: coiled-coil domains (blue), DNA binding domains (red), linker domains (green) and SH2-domains (yellow). PDB: 1BG1. Source: Becker *et al.*, 1998 **[43]**.

1.1.4 Intracellular signaling patterns of STAT3

1.1.4.1 The STAT3 canonical pathway

The canonical STAT3 signaling pathway starts with the binding of a cytokine to its receptor in the cell membrane **[44]**. This activates one of the four receptor-associated kinases of the Janus Kinase (JAK) family (JAK1, JAK2, JAK3 and tyrosine kinase 2 or TYK2), which in turn phosphorylates the cytokine receptor **[45]**. STAT3 dimers are recruited to the activated receptor and phosphorylated on the tyrosine residue 705 (Y705) in the transactivation domain. This leads to the accumulation of phosphorylated STAT3 dimers in the nucleus **[44]**. The molecular mechanisms by which accumulation in the nucleus occurs are still under discussion. Some researchers defend that STAT3 is mainly found in the cytosol of unstimulated cells and only translocate to the nucleus after cytokine stimulation **[46]**. Others defend that STAT3 is permanently shuttling between the cytoplasm and the nucleus, being retained in the nucleus after cytokine-induced phosphorylation **[47]–[49]**.

As mentioned in **section 1.1.1**, the IL-6 family of cytokines can activate STAT3 trough the JAK-STAT3 canonical signaling. LIF stimulation is a paradigmatic example of IL-6 family-mediated STAT3 activation and is especially relevant for this thesis. LIF binds to the LIF receptor (LIFR) at the cell surface, inducing its heterodimerization with signal transducer glycoprotein 130 (gp130). This results in the activation of a gp130-associated kinase (JAK), phosphorylation of gp130 cytoplasmic domain and recruitment of the SH2 domain of STAT3 **[50]**. STAT3 is then phosphorylated at Y705 and accumulated in the nucleus. Once in the nucleus, phosphorylated STAT3 binds the Interferon-γ Activation Site (GAS) sequence $CCT(N)_3GAA$ to activate or repress gene transcription **[33]**. Some of the genes activated by STAT3 are pro-survival genes (e.g., *BCL2*, *BCL2L1*, *MCL1*, and *BIRC5*) **[51]–[54]**; cell-cycle progression genes (e.g., *CCND1* and *c-MYC*) **[55], [56]**; and pro-migratory genes (e.g., *MMP2*) **[18]**. STAT3 also promotes angiogenesis through direct induction of the vascular endothelial growth factor (*VEGF*) promoter **[57]**. Phosphorylated STAT3 was also reported to down-regulate the expression of some genes related to cell proliferation and survival, such as *TP53*, *FAS* and *NDN* **[58]**.

Phosphorylated STAT3 also induces its own gene expression via a STAT3-STAT3 positive autoregulatory loop, producing *de novo* unphosphorylated STAT3 molecules **[59]**. If there is cytokine stimulation, these STAT3 molecules can be phosphorylated at Y705. If not, there will be an increase of unphosphorylated STAT3 which can progressively substitute the phosphorylated STAT3 molecules. During this process, various pools of STAT3 with different post-translational modification profiles can coexist and possibly interact symmetrically or asymmetrically **[60]**.

Expression and activation of STAT3 is tightly regulated through a wide range of endogenously expressed proteins that can silence JAK-STAT3 signaling. These include Suppressors of Cytokine Signaling (SOCS) proteins that bind to activated JAKs or receptor domains and efficiently block STAT3 phosphorylation **[61]**. SOCS3 is a direct transcriptional target of STAT3, providing a negative feedback to control the duration/intensity of STAT3 signaling **[62]**. The Protein Inhibitor of Activated STAT (PIAS) family are small ubiquitin-like modifier (SUMO) E3 ligases that covalently attach SUMO proteins to target substrates, thus promoting their degradation. PIAS3 directly inhibits STAT3 activity through SUMOylation **[63]**. In addition, protein tyrosine phosphatases, Src homology domain-containing tyrosine phosphatases and the protein tyrosine phosphatase receptor T may specifically dephosphorylate STAT3 and upstream kinases in the JAK-STAT3 pathway to terminate STAT3 signaling **[64]**.

Constitutive activation of STAT3 (i.e., persistent phosphorylation at Y705) can affect the balance between glycolytic and oxidative phosphorylation metabolisms, providing the necessary requirements to support the metabolic shift toward aerobic glycolysis in the presence of oxygen, known as the Warburg effect **[65]**. The Warburg effect is a metabolic program used by cancer cells early in oncogenesis that promotes its sustained proliferation and hastens malignant progression **[66]**. Constitutively activated STAT3 induces the transcription of hypoxia-inducible factor 1-alpha (*HIF1A*), which in turn promotes the expression of glycolysis-related genes (e.g., *SLC2A1* and *PDK1*). This allows for rapid proliferation while also significantly increasing glucose consumption, resulting in glucose dependence **[65]**. Constitutively activated STAT3 also reduces the expression of many nuclear genes encoding for mitochondrial proteins, leading to a blunted electron transport chain (ETC) activity. Reduced mitochondrial activity may contribute to a reduction in reactive oxygen species (ROS) accumulation, which is likely to result in high resistance of cells to apoptosis and senescence, two hallmarks of cellular transformation **[65]**. Besides STAT3's nuclear mechanisms, there are other driving processes of the Warburg effect such as activation of oncogenes (e.g., *c-MYC*, *MTOR*C1 and *AKT*), loss of function of tumor suppressors (e.g., mutant p53 and mutant PTEN) and interaction with components of the tumor microenvironment. The Warburg effect is related to resistance to conventional therapies and poor patient outcomes **[66]**.

The effects of STAT3 on glucose metabolism may also be mediated in part by *c-MYC*, a well-known direct transcriptional target, that induces the expression of glycolysis genes such as *SLC2A1*, *HK2*, *ENO1*, and *PFKM* **[67], [68]**. STAT3 also contributes more directly to the inactivation of ROS through the upregulation of the superoxide dismutase 2 (*SOD2*) gene. SOD2 is a mitochondrial antioxidant enzyme that scavenges superoxide radicals providing cytoprotection **[69], [70]**.

1.1.4.2 Non-canonical STAT3 pathways

Non-canonical pathways include several STAT3 functions that have been revealed to be independent of its phosphorylation on Y705. Unphosphorylated STAT3 (U-STAT3) regulates gene expression and drives chromatin structure remodeling **[71]**. U-STAT3, either as dimer or as monomer, can bind to similar DNA sites as tyrosine-phosphorylated STAT3. However, U-STAT3 works in collaboration with transcriptional regulators such as the nuclear factor kappa-light-chain-enhancer of

activated B cells (NF-κB) to control a set of genes not normally affected by tyrosine-phosphorylated STAT3, including *RANTES*, *MET* and *MRAS* **[72]**.

STAT3 can translocate into mitochondria through interaction with GRIM-19, where it promotes mitochondrial respiration and metabolism by interacting with various mitochondrial proteins, as well as the mitochondrial genome. STAT3 phosphorylation at S727, rather than Y705, is required for its mitochondrial activity **[73]**. STAT3 enhances the activity of NADH:ubiquinone oxidoreductase (complex I), succinate oxidoreductase (complex II), ATP synthase (complex V) and lactate dehydrogenase **[74]**. Mitochondrial STAT3 is also implicated in the regulation of ROS. In the mitochondria, STAT3 maintains an optimal ETC activity and can inhibit the opening of the mitochondrial permeability transition pore through the interaction with cyclophilin D **[75]**, reducing ROS production **[76]**, decreasing cell apoptosis, and enhancing cell proliferation and survival **[77]**. STAT3 can also facilitate the formation of respiratory supercomplexes in the mitochondria during ETC process, minimizing electron leakage and reducing the generation of ROS **[78]**. The interaction of mitochondrial STAT3 with GRIM-19 also dampens the ability of GRIM-19 to produce ROS **[79]**. Finally, mitochondrial STAT3 can also contribute to the control of ROS levels by indirectly inducing the gamma-glutamyl cycle and consequently the synthesis of the major cellular ROS scavenger glutathione, via an unknown mechanism **[80]**. Mitochondrial STAT3 has significant effects in normal cellular homeostasis (e.g., cardioprotection, neurite outgrowth) and in pathological conditions (e.g., Ras-driven cancer) **[14]**. Despite these findings, it is still under discussion if STAT3 is in the mitochondria. Recently, Su et al. (2020) **[81]** provided evidence that STAT3 does not exist in mitochondria but localizes in the mitochondria-associated endoplasmic reticulum membrane (MAM). MAM is a cellular structure formed by non-covalent protein interactions between the endoplasmic reticulum (ER) and mitochondria membranes, which have extensive implications in mitochondrial bioenergetics, ROS production, calcium (Ca^{2+}) signaling, lipid transport and dynamics. They also hypothesized that STAT3 can regulate the mitochondrial metabolism via MAM function **[81]**. STAT3 can be found in the ER, where it interacts and facilitates the degradation of inositol 1,4,5-trisphosphate receptor 3 (IP3R3) to control calcium efflux from the ER, enhancing cellular resistance to apoptotic stimuli. For ER STAT3 localization or interaction with IP3R3, phosphorylation at Y705 or at S727 are not strictly needed. However, phosphorylation at S727 is required for the degradation of IP3R3 and regulation of Ca^{2+} efflux **[82]**. IP3R3 has also been found to interact with the voltage dependent anion-selective channel (VDAC) protein at the mitochondrial outer membrane to form the MAM contact site. As a result, MAM STAT3 may control mitochondrial metabolism by regulating calcium transport. Su et al. (2020) also reported that other proteins such as STAT1, MAPK 1/3, MAPK 14, AMPK, mTOR and RELA are localized in the MAM and not in the mitochondria as previously reported. STAT1, MAPK 1, mTOR and RELA are known interactors of STAT3, and AMPK has been reported to suppress the JAK/STAT3 pathway **[81]**.

Finally, STAT3 was also found associated with a variety of other cytosolic structures, including focal adhesions, microtubules, mitotic spindles, lipid rafts and endolysosomal membranes **[14]**. STAT3 promotes cell migration and invasion by regulating the assembly of cytoskeleton networks, such as actin microfilaments and microtubules **[74]**.

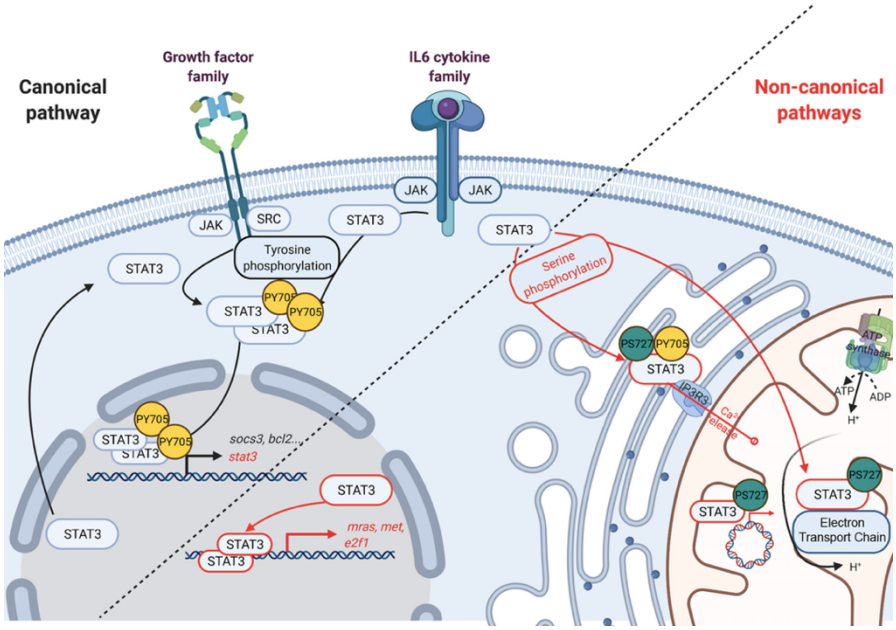

Figure 1.3 - Canonical and noncanonical pathways of STAT3. The canonical pathway (left side of the panel, black arrows) consists of dimerization of STAT3 and its phosphorylation at residue Y705 by JAK family in response to IL-6 cytokine family or growth factors. Activated STAT3 dimers accumulate in the nucleus and induce the transcription of specific genes, including STAT3 gene itself. STAT3 has several noncanonical pathways (right side of the panel, red arrows), regarding the absence or the presence of PTM (i.e., phosphorylation) and the cellular localization. *De novo* unphosphorylated STAT3 accumulates within the nucleus and induces a second wave of a distinct set of genes. STAT3 phosphorylated at S727 is found in the endoplasmic reticulum where it interacts with IP3R3 and blocks the ER calcium release to mitochondria. STAT3 is also found in the inner mitochondrial compartment where it has transcriptional and non-transcriptional activities. Bcl2, B cell lymphoma 2; JAK, janus kinase; mras, muscle ras; socs3, suppressor of cytokine signaling 3; IP3R3, inositol trisphosphate receptor 3. Source: Diallo *et al.,* 2021 **[60]**.

1.1.5 STAT3 post-translational modifications

According to PhosphoSitePlus, STAT3 has 80 identified post-translational modifications (PTMs) **[83]**. Most studies only focus on the phosphorylation at Y705 and S727. However, other PTMs including other phosphorylation events, acetylation, methylation, ubiquitination and SUMOylation were found to play key roles on STAT3 functions (**Figure 1.4**).

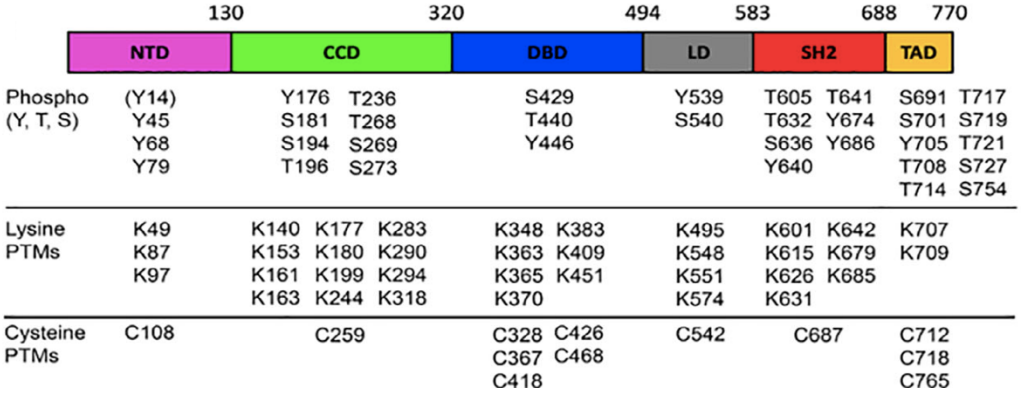

Figure 1.4 – STAT3 Post-Translational Modifications. Experimentally proven post-translational modifications of STAT3 and their localization in the domains of STAT3. NTD, N-terminal domain; CCD, coiled-coil domain; DBD, DNA binding domain; LD, linker domain; SH2, Src homology 2 domain; TAD, transactivation domain; Y, tyrosine; T, threonine; S, serine; K, lysine; C, cysteine. Source: Diallo *et al.*, 2021 **[60]**.

1.1.5.1 Phosphorylation

The most common PTM in STAT3 is phosphorylation, which consists in the covalent addition of a phosphate group to a specific amino acid (tyrosine, serine, and threonine). In total, STAT3 can be phosphorylated at 41 different residues across its domains **[60]**. Many of them are rarely found and could be background derived from the extremely high sensitivity of mass spectrometry approaches. However, some of them have demonstrated biological relevance. This is the case of the SH2 domain residue Y640. Y640 can be phosphorylated via the TK domain of TYK2. Y640 along with Y705 are buried in the STAT3 dimerization interface, but while the phosphorylation at Y705 promotes STAT3 dimerization, phosphorylation at Y640 interferes with it **[84]**. This occurs because the phosphate at Y640 partially occupies the binding site for T708, a threonine previously implicated in STAT3-DNA complex formation **[85]**. In accordance with these findings, the Y640F mutation, which prevents the phosphorylation at this residue, was found to enhance phosphorylation of STAT3 at Y705, resulting in an increased formation and stability of STAT3 homodimers. This was demonstrated in cells stimulated with interferon alpha 2 (IFNα2) and LIF. The effect is more pronounced for IFNα2, which is consistent with TYK2 being a crucial JAK kinase of the IFN receptor (IFNAR) complex **[84]**. Interestingly, even when the cells are not stimulated, a significant fraction of STAT3 Y640F is constitutively phosphorylated and dimerized **[23], [84]**. Moreover, STAT3 Y640F showed increased nuclear translocation compared with STAT3 wild type after stimulation with IFNα2 **[84]**. As mentioned in the **section 1.1.2**, the mutation Y640F has been associated with LGL leukemia and IHCAs. In these diseases, STAT3 Y640F increases the hydrophobicity of the STAT3 dimerization site, resulting in a more stable STAT3 dimer, constitutive Y705 phosphorylation and improved nuclear stability and transcriptional activity **[23], [86]**. In LGL leukemia, constitutive STAT3 activation eventually leads to the activation of a LGL leukemia tumor cell survival network via immune dysregulation of Fas/FasL or activation of antiapoptotic genes **[86]**. In IHCAs, JAK1 is required for maximal activation of STAT3 Y640F mutant, whereas Src is required for constitutive activation **[23]**.

Other residues that suffer phosphorylation but have barely been studied are T714, located in the TAD, and T236, located in the CCD. In response to simultaneous activation of epidermal growth factor receptor (EGFR) and protease-activated receptor 1 (PAR-1), glycogen synthase kinase 3α and -β (GSK-3α/β) phosphorylates simultaneously T714 and S727, inducing the expression of *MCL1* and *EGR1*. The levels of double phosphorylated STAT3 are increased in renal tumors, implying that the GSK-3α/β/STAT3 signaling axis is active in the disease **[87]**. The 714 phosphorylation could also have a relevant role in the study of HIES, since the T714I and T714A mutations, which prevent phosphorylation at this residue, have been reported in patients with this disease **[24], [88]**. The phosphoresistant T236M mutation has been associated with adenocarcinomas in the biliary tract and in the prostate **[89]**.

1.1.5.2 Acetylation

STAT3 can be acetylated at 10 different lysine residues **[60]**. This PTM consists in the transfer of an acetyl group from acetyl-coenzyme A to the ε-amino group of lysine residues. In the N-terminal domain, STAT3 is acetylated at K49 and K87 by the histone acetyltransferase p300/CBP, in response to IL-6 and oncostatin M **[90]**. Studies using K49R and K87R mutations, which block acetylation, found that acetylation of the N-terminus of STAT3 enhances its interaction with p300 and is required for STAT3-dependent transcription. However, K49 and K87 acetylation do not influence the DNA binding activity of STAT3 **[90]**. It was hypothesized that the acetylation at K49 and K87 causes the p300 bromodomain to recognize the N-terminal domain, resulting in a stronger recruitment of p300 to

the promoter of the STAT3 target gene, and facilitating subsequent enhanceosome assembly **[91]**. Acetylated STAT3 is deacetylated by histone deacetylases 1 and 4 (HDACs 1 and 4). Deacetylation reduces STAT3's affinity for the p300 co-activator, resulting in STAT3 dephosphorylation, ubiquitination, and/or cytoplasmic redistribution **[90]**.

The most studied acetylation of STAT3 is at the K685 residue in the SH2 domain. K685 is acetylated by the histone acetyltransferase p300/CBP **[92], [93]** and deacetylated by HDACs 1,2,3,6 and sirtuins (SIRTs) 1-3 **[92], [94]**. Phosphorylation at Y705 stabilizes the acetyl group at K685, protecting it from deacetylation. Studies *in vivo* demonstrated that K685 acetylation promotes STAT3 dimerization and transcriptional activity, implying an acetylation-dependent mode of DNA binding and transcriptional activity **[92], [93]**. However, a more recent study *in vitro* did not find any direct influence of K685 acetylation on STAT3 DNA binding affinity or specificity. It was hypothesized that the results observed *in vivo* could depend on other factors or conditions found in the cellular environment, such as additional post-translational modifications, protein-protein interactions, and sub-cellular compartmentalization **[94]**.

1.1.5.3 Methylation

Methylation consists in the addition of a methyl group to proteins by methyltransferases that use S-adenosyl-L-methionine as a cofactor. The primary acceptors of methyl groups in the protein are lysine and arginine residues. STAT3 can be methylated in its N-terminal domain (K49) and coiled-coil domain (K140 and K180) **[95]–[97]**. In response to IL-6 and after phosphorylation at Y705, STAT3 is dimethylated at K49 by the enhancer of zeste homolog 2 (EZH2). This dimethylation is essential for the expression of a major fraction of STAT3 target genes such as *SERPINA1*, *SOCS3*, and *GADD45G* **[95]**. STAT3 is also dimethylated at K140 by SET domain containing lysine methyltransferase 9 (SET9) **[96]** and trimethylated at K180 by EZH2 **[97]**.

1.1.5.4 Ubiquitination and SUMOylation

Ubiquitin and SUMO proteins can be covalently attached to lysine residues of target proteins, respectively. Ubiquitination is a three-step enzymatic reaction that requires three types of enzymes: E1 ubiquitin-activator, E2 ubiquitin-conjugator and E3 ubiquitin ligase **[98]**. SUMOylation is similar to ubiquitination but the process is carried out by SUMO-specific enzymes and involves fewer enzymatic components. The best-known SUMO E3 ligases are the PIAS 1–4 **[99]**. Both ubiquitination and SUMOylation are reversible processes that determine the fate of modified proteins, including proteasomal degradation, cellular re-localization, and binding partner alteration **[98]**. STAT3 has been reported to have 31 sites for ubiquitination and 3 sites for SUMOylation **[60]**. Most studies about STAT3 ubiquitination or SUMOylation only emphasize the role of these PTMs in STAT3's degradation and stability. For example, STAT3 is poly-ubiquitinated after activation and transcriptional activity, which promotes its degradation by the 26S proteasome **[100]**. In granulomatous inflammation, the nuclear ubiquitin E3 ligase PDLIM2 promotes the poly-ubiquitination and proteasomal degradation of STAT3, inhibiting T helper 17 cell development **[101]**. Nonetheless, ubiquitination and SUMOylation also play important roles in STAT3 canonical phosphorylation and transcriptional activity. STAT3 can be mono-ubiquitinated at K97 in the N-terminal domain. Mono-ubiquitinated STAT3 recruits the bromodomain-containing protein 4 (BRD4) to promote the expression of SOCS3, a negative STAT3 regulator, and pro-proliferative and anti-apoptotic genes such as *CCND1*, *BCL2L1*, *APEX1*, *SOD2*, *BCL2*, *MYC*. Mono-ubiquitination of STAT3 has, therefore, a crucial role in cell survival **[102]**. Contrary to ubiquitination of STAT3, SUMOylation has been reported to negatively regulate STAT3's transcriptional activity. STAT3 can

be SUMOylated at K451 in the DNA binding domain. This SUMOylation promotes the interaction between STAT3 and the nuclear phosphatase TC45, restraining STAT3 Y705 phosphorylation in the nucleus. In contrast, the deSUMOylation by the sentrin/SUMO2/3-specific protease (SENP3) enhances Y705 phosphorylation and STAT3's transcriptional activity (upregulation of *c-MYC*, *CCND1*, *BCL2L1*, *MCL1*, *VEGF* and *BIRC5*) **[103]**.

1.2 STAT3 protein-protein interactions

The human genome comprises approximately 20 000 genes which can encode for more than 100 000 transcripts (and subsequent proteins) due to genomic recombination, transcription initiation at alternative promoters, differential transcription termination and alternative splicing. Post-translational modifications of proteins can further increase the total number of proteoforms in the human proteome to over 1 million **[104]**. As described for STAT3 in the previous sections, PTMs can modulate and expand the range of possible functions for proteins, and so do protein-protein interactions. Protein-protein interactions are defined as specific, direct, or indirect, physical contacts between proteins that occur by selective molecular docking in a particular biological context **[105]**. A protein-protein interaction is direct if the molecular interfaces of two proteins contact with each other and is indirect if the proteins are physically separated but interact through other intermediates building a complex **[105]**. Proteins can interact with different proteins (heterodimerization) or proteins of the same kind, forming homodimers. In this sense, homodimerization occurs more frequently in nature than expected by chance, suggesting that it plays key biological roles **[106]**. Both hetero- and homodimerization are rate-limiting events that control STAT3 signaling. Whether homodimerization occurs between identically modified monomers (symmetric interaction) or monomers with different post-translational modifications (asymmetric interaction) is unclear, but certainly possible considering the heterogeneous pools of molecules that can coexist during cell signaling events. Herrera's laboratory recently reported a surprisingly strong effect of STAT3 asymmetric homodimers in its subcellular localization in the absence of cytokine stimuli, but their role in canonical STAT3 pathways remains unknown **[107]**.

1.2.1 Methods to study protein-protein interactions

Protein-protein interactions can be studied by means of biochemical techniques such as crosslinking, co-immunoprecipitation and co-fractionation by chromatography. These techniques require the lysis of cells and the purification of proteins for analysis *in vitro*. Some protein-protein interactions may be lost or abolished, whereas other proteins can be brought close enough to the potential interacting proteins, causing interactions that would never occur under physiological conditions **[108]**.

In 1989, Stanley Fields and Ok-kyu Song developed the yeast two-hybrid system (Y2H) to study protein-protein interactions *in vivo* **[109]**, overcoming some of the limitations of the methods mentioned before. In their genetic system, the glucose sensor SNF1 (protein of interest X) was fused to the DNA binding domain (DBD) of the transcriptional activator Gal4, a construct called bait. The bait binds the upstream activator sequence of the promoter. The regulatory protein SNF4 (potential interacting protein Y) was fused to the activation domain (AD) of Gal4 and was called prey (**Figure 1.5A**). The two proteins, SNF1 and SNF4, interacted and reconstituted Gal4, leading to transcription of a *GAL1-lacZ* fusion gene (**Figure 1.5B**). This reporter gene encoded the enzyme beta galactosidase which labeled the yeast cells where interaction occurred upon incubation with a colorimetric substrate **[109], [110]**. Other DNA-binding proteins (e.g., DBD of *Escherichia coli* repressor protein LexA), transcriptional activators (e.g., AD of Herpes simplex virus VP16) and reporter genes can be used in the classic Y2H system **[110]**. This system can be easily used to identify interacting proteins for a

given protein, to check direct interactions between two known proteins, or to map interacting domains **[111]**. The main advantages of Y2H assays are simplicity, time efficiency and low cost **[108]**. The biggest limitations of the classic Y2H are the obligatory nuclear localization of the interaction partners, the use of a non-physiological yeast environment and the forced protein co-expression. This system is also prone to yield relatively high false-positive and false-negative interactions **[110]**. To overcome these limitations, many improvements, and variations of the classical Y2H have been developed. Currently two-hybrid (2H)-based methods include a large series of different technologies to be used not only in yeast cells but also in mammalian and bacterial cells **[112]**. Additionally, new variants of 2H methodologies have been developed to overcome the limitations of the classic 'nuclear' Y2H, allowing the visualization of interactions in cytosolic and membrane proteins **[110]**; or to allow the screen for novel DNA-protein **[113]**, RNA-protein **[114]**, and small molecule-protein interactions **[115]**.

Further methods were later developed to study protein-protein interactions, which include fluorescence or bioluminescence resonance energy transfer (FRET or BRET) and protein-fragment complementation assays (PCAs).

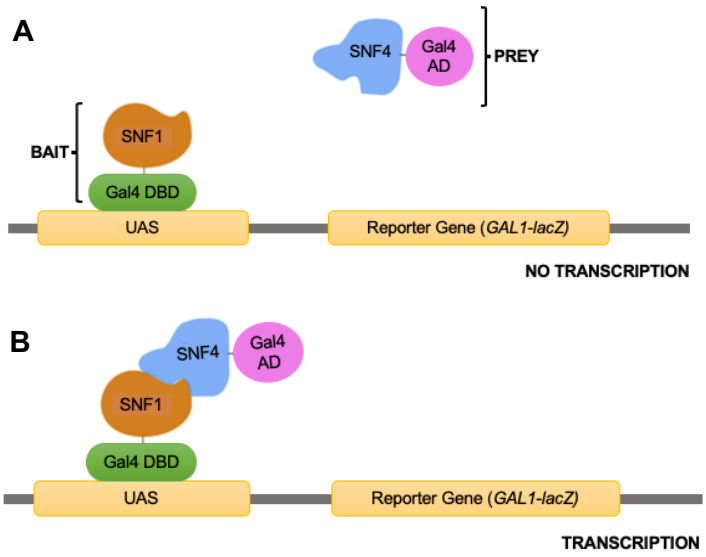

Figure 1.5 – The classical yeast two-hybrid system. A, SNF1 is fused to the DNA binding domain (DBD) of Gal4, a construct called bait. The potential interacting protein SNF4 is fused to the activation domain (AD) of Gal4 and is called prey. **B**, The bait binds the upstream activator sequence (UAS) of the promoter. The interaction of the bait with the prey, recruits the AD and thus reconstitutes the functional transcription factor Gal4, leading to the subsequent transcription of the reporter gene (*GAL1-lacZ*).

1.2.1.1 FRET and BRET

FRET is a physical phenomenon of energy transfer that occurs between two compatible light-sensitive molecules (fluorochromes). The fluorescence emitted by one of them (donor) upon excitation at the corresponding wavelength is absorbed by and excites the other (acceptor) when they are close enough. In FRET setups, the fluorescent donor molecule is fused to one of the proteins of interest and the acceptor to the other protein. If there is no interaction, only the fluorescence of the donor should be detected. However, if an interaction takes place the energy relaxation of the excited fluorescent donor protein is not emitted via its own fluorescence but instead is emitted through non radiative transfer of this energy to the nearby acceptor molecule **[116]**. For FRET to occur, the spectral overlap of donor emission and acceptor absorption must be sufficient for effective energy transfer; the distance between

the fluorescent proteins (donor and acceptor) must be below 10 nm; and the dipole orientation of the fluorescent proteins must be aligned. The FRET ratio (emission of the acceptor divided by emission of the donor) is normally used for quantification. A significant increase in the ratio indicates an interaction between the two proteins of interest **[116]**. A limitation of FRET is the requirement for external illumination to initiate the fluorescence transfer. This could result in direct excitation of the acceptor, photobleaching or autofluorescence, which leads to high background noise and consequently low signal-to-noise ratios **[117]**. BRET is similar to FRET, but instead of using a fluorescent protein as a donor it uses an enzyme (e.g., luciferase). The enzyme catalyzes a substrate to become bioluminescent, thus exciting the acceptor **[117]**. Unlike FRET, this method does not require an external light to excite the donor and therefore has a very small background noise. However, BRET signals are very weak and dim, and BRET experiments do not provide spatial information of protein-protein interactions since the substrate cannot be allocated to a specific cellular region **[117]**.

1.2.1.2 Protein complementation assays

Protein-fragment complementation assays (PCAs) are a family of simple and direct assays for detecting protein-protein interactions in any living cell, multicellular organism, or *in vitro*. PCAs can be used to detect protein-protein interactions between proteins of any molecular weight and expressed at their endogenous levels **[118]**. In this method, each of the proteins of interest is fused to complementary N- or C-terminal fragments of a reporter protein. If the proteins of interest interact, the reporter fragments reassemble, and the reporter recovers its native structure and activity **[118]**. The first PCA method was described by Johnsson and Varshavsky in 1994 **[119]**, who used ubiquitin as the reporter protein. Subsequently many other types of reporter proteins have been used such as β-galactosidase, dihydrofolate reductase (DHFR), β-lactamase, Tobacco Etch Virus (TEV) protease, various fluorescent proteins, luciferase, thymidine kinase, Cas9, horseradish peroxidase, RNA polymerase, aminoacyl tRNA synthetase and miniSOG **[120]–[122]**. The types of readouts for these assays include fluorescence, bioluminescence, cell survival, gene transcription, protein translation, positron emission, genome editing, and electron microscopy **[120], [122]**. Among these, one type of assay stands out since it enables to monitor the intracellular localization and dynamics of protein-protein interactions in living cells: Bimolecular Fluorescence Complementation (BiFC) (**Figure 1.6**) **[123]**.

1.2.1.2.1 Bimolecular Fluorescence Complementation

BiFC was originally described *in vitro* and *in vivo* (*Escherichia coli*) by Ghosh, Hamilton, and Regan in 2000 **[124]**. They demonstrated that complementary fragments of the green fluorescent protein (GFP) fused to leucine zippers could reassemble upon interaction, reconstituting the fluorescence of GFP **[124]**. Subsequently, in 2002, Hu *et al.* **[125]** described a BiFC assay using the yellow fluorescent protein (YFP) as a reporter to investigate interactions between bZIP and Rel transcription factors in living mammalian cells. BiFC has the advantage that the assembled complex has strong intrinsic fluorescence that can be easily quantified in living cells by conventional methods, such as flow cytometry and microscopy **[126]**. Therefore, the interaction can be directly visualized without the requirement for staining with exogenous molecules (as in other PCAs), lysis or cell fixation that could affect the detection of the interaction. This ensures minimal perturbation of the normal cellular environment **[127]**.

Although BiFC has advantages in comparison with other methods, it also has some limitations that are important to consider. One of the biggest limitations is the virtual irreversibility of the BiFC

complexes in live cells, although the reporter fragments do not form covalent bonds and they can be separated by mild denaturalizing agents *in vitro*. This can be advantageous to detect transient or weak protein-protein interactions **[123]**. However, the irreversible reconstitution of the fluorophore prevents the observation of transitions between different complexes in real time and can interfere with the function of the interacting proteins under investigation **[128], [129]**. Furthermore, proper reporter protein folding, and fluorophore maturation require some time, making difficult to use these systems to visualize real-time dynamics of protein-protein interactions **[128]**. Finally, the two non-fluorescent fragments have an inherent binding affinity for each other independent of the interaction of their fusion proteins. This spontaneous self-assembly leads to higher background fluorescence, an increase in false-positives and a consequent decrease in the signal-to-noise ratio **[120]**.

Every BiFC assay should be set up and adjusted empirically for each protein of interest or experimental condition. To choose the fluorescent reporter protein, it is important to consider what is the purpose of the experiment, the tools available and the properties of the fluorescent reporter protein **[126]**. Some of the parameters to consider are the relative location of the protein of interest *versus* the reporter protein, physical–chemical properties of the reporter protein of choice, temperature of incubation, or the ability to self-assemble of the reporter protein. Furthermore, if the BiFC system will be combined with other fluorescent markers, it is important to consider the excitation and emission wavelengths of the reporter protein **[126]**. The fluorescent reporter protein chosen can be of first- or second-generation, such as GFP and YFP, or enhanced green fluorescent protein (EGFP) and enhanced yellow fluorescent protein (EYFP), respectively. However, these proteins are less bright and require a conformational maturation at a temperature of 30 ºC to efficiently reconstruct the functional fluorophore. This is a low temperature for mammalian cells and consequently can elicit undesirable intracellular pathways that could cover biologically important events **[126]**. The third generation of fluorescent proteins is usually much brighter than the first generation and have intrinsically improved folding efficiency, being able to reconstruct the fluorophore very efficiently even at 37 ºC (e.g. Venus, Cerulean,…). Besides that, third generation fluorescent proteins enable the use of weaker promoters and therefore, to approximate the expression of the interactors at physiological levels. Nevertheless, they may produce more background and lower signal-to-noise ratios **[126]**.

One of the most widely used third-generation fluorescent protein in BiFC assays is Venus. Venus was generated from EYFP by introducing several point mutations: F46L, F64L, M153T, V163A, and S175G **[130]**. Venus is less sensitive to the environment (e.g., temperature) **[130]** and the fluorescence intensity of the Venus-based BiFC was approximately 10 times higher than that of EYFP-based BiFC **[131]**. It also has faster and more efficient maturation **[132]**. However, it has higher levels of spontaneous binding and lower signal-to-noise (S/N) ratios than its antecessors YFP and EYFP **[126]**. Several groups tried to overcome this problem by mutating Venus. The mutations V150L, V150A, I152L, L201V, and L207V can increase S/N ratios in the Venus-based BiFC system **[133]**. The use of Venus' fragments with different sizes (e.g. fragments 1-210 and 210-238) was also shown to improve the spontaneous binding and lower S/N ratio **[128]**.

Besides proteins derived from the GFP, there is another type of proteins that can be used as fluorescent reporters in BiFC called bacterial phytochromes **[134]**. These proteins have excitation wavelengths in the near-infrared region (>600 nm) and use biliverdin, which is an intermediate of normal mammalian heme metabolism, as their chromophore. The higher excitation wavelengths of phytochromes compared with GFP-derived proteins make them more suitable to do BiFC assays in animal tissues **[134]**.

After the choice of the fluorescent reporter protein, it is necessary to develop a series of constructs, where the fragments of the reporter protein are fused to either the N- or the C-terminal of the proteins of interest to know what are the combinations which will allow their interaction **[126]**. Finally, the constructs must be tested for their functionality in living cells and their physiological relevance **[126]**.

The basic principle of the BiFC assay has also been utilized to investigate post-translational modifications (e.g., ubiquitination of the JUN transcription factor **[135]**); protein folding and aggregation (e.g., study of the aggregation of huntingtin **[136]**, synuclein **[137]** and tau **[138]** *in vivo*); protein conformational changes (e.g., conformational changes in the maltose binding protein **[139]**); and protein topology (e.g., study of the topology of TGBp2 proteins **[140]**).

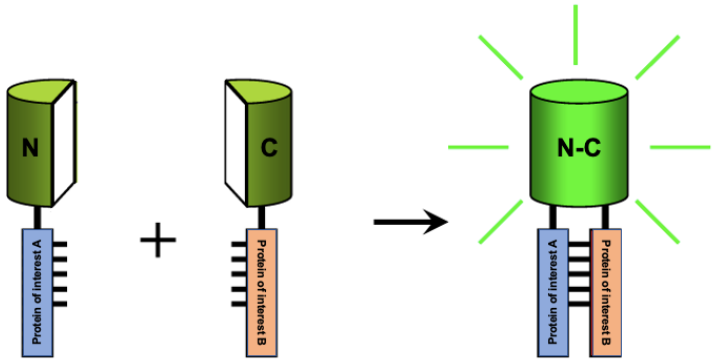

Figure 1.6 – Bimolecular Fluorescence Complementation (BiFC). In BiFC assays two proteins of interest are fused to two complementary non-fluorescent N- or C-terminal fragments of a fluorescent reporter. If the proteins of interest interact, they bring the reporter fragments back together, reconstituting the functional fluorophore. Fluorescence is therefore proportional to the dimerization of the proteins and can be easily measured by flow cytometry or microscopy. Source: Kerppola, 2006 **[127]**.

A multicolor BiFC version has been developed to allow the visualization of multiple protein interactions (**Figure 1.7A)**. In this assay, the N-terminal fragments of two different fluorescent proteins are fused to two proteins, and a C-terminal fragment that can complement with the two N-terminal fragments is fused to a third protein (a shared interaction partner of the two proteins). Any interaction that occurs between the third protein and either of the two interacting proteins will lead to the reconstitution of fluorescence, and its interaction partner can be determined based on which spectrum is obtained **[141]**. Some of the applications of this assay until now are the study of dimerization selectivity and subcellular sites of interactions of the bZIP family proteins, the AP-1 and the Myc/Max/Mad families of transcription factors, among others **[141]**. BiFC-based FRET also allows the visualization and identification of ternary complexes in living cells (**Figure 1.7B)**. In this assay, two interacting proteins are fused to non-fluorescent fragments of Venus. A third protein is fused to a full-length Cerulean, an improved version of enhanced cyan fluorescent protein (ECFP). The interaction between the first two proteins reconstitutes an intact Venus, which serves as a FRET acceptor. If the third protein is interacting with the protein complex, Cerulean, the FRET donor, is brought into proximity to the reconstituted Venus and allows FRET to occur **[141]**. Using such a BiFC-FRET assay, the p65 subunit of the transcription factor NF-kB was shown to form a ternary complex with the FOS-JUN heterodimer **[141]**.

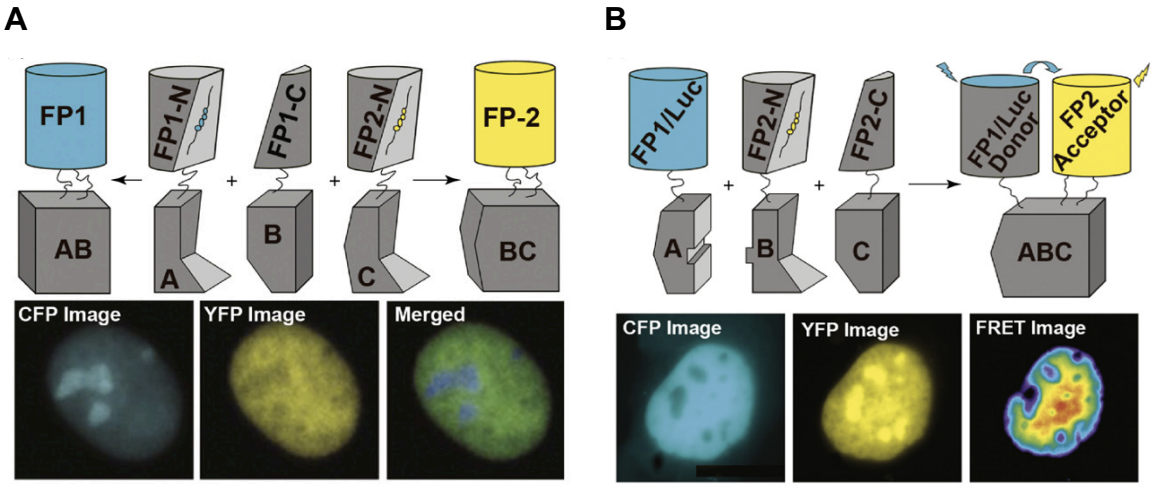

Figure 1.7 - **Visualization of multiple protein interactions and complexes using BiFC. A,** Multicolor BiFC system. Proteins A and C are fused to N-terminal fragments of two different fluorescent proteins (FPs): FP1-N and FP2-N. Protein B, a common partner of proteins A and C, is fused to the C-terminal fragment of FP1 (FP1-C). When coexpressed in the same cells, A–B interaction reconstitutes FP1 and B–C interaction reconstitutes FP2, allowing the simultaneous visualization of two distinct interactions in the same cell. The images below show subcellular localization of bFOS-bJUN (CFP Image) and bFOS-JUN (YFP Image) in the same cell. **B,** BiFC-based FRET/BRET system. Protein A is fused to a donor chromophore, such as a full-length FP (FP1) or a Renilla luciferase (Luc), and proteins B and C are fused to the N- and C-terminal fragments (FP2-N and FP2-C) of a second FP. B–C interaction reconstitutes an intact FP2, which serves as a FRET acceptor. If protein A interacts with either B or C, or with both, FP1 (or Luc) is brought into proximity to FP2, allowing FRET or BRET to occur. Images below show the subnuclear localization of ternary complexes between FOS, JUN and p65. Source: Shyu *et al.*, *2008* **[141]**.

II. Aims

The main goal of this work is to determine the influence of key post-translational modifications on STAT3 translocation to the nucleus upon canonical stimulation with cytokines from the IL-6 family. To address this question, we will use STAT3 knockout HeLa cells recently developed in Herrera´s laboratory. First, we will characterize the features of this cell strain and create a series of molecular tools to analyze the dynamics of STAT3 homodimers in living cells based on BiFC (i.e., STAT3 expression plasmids with mutations preventing key PTMs, such as Y705F, K49R, K685R, S727A, T236A, Y640F and T714A). Second, we will study the influence of symmetrically and asymmetrically modified STAT3 homodimers in their response to cytokines. And third, we will study the effect of the disease-associated phosphoresistant Y640F mutation in the behavior of STAT3 dimers.

III. Materials and methods

3.1 STAT3 BiFC Constructs

The original Venus-STAT3 BiFC constructs (**Figure 3.1**) were previously designed as described in **[107]** and were already available in Herrera's laboratory. The single or double mutant constructs were produced by polymerase chain reaction (PCR)-based site-directed mutagenesis using the original Venus-STAT3 BiFC or the mutant Venus-STAT3-Y705F BiFC constructs as templates. The primers used for the mutagenesis were designed using PrimerX free software (https://www.bioinformatics.org/primerx/) (**Table 3.1**). The original tyrosines (Y) on position 640 and 705 were replaced by phenylalanine (F), the lysines (K) on position 49 and 685 were replaced by arginine (R), and serine (S) 727 and threonines (T) 236 and 714 were replaced by alanine (A). The Venus-STAT3 BIFC constructs Y705F (Addgene plasmid #123172 and #123173), Y705F/K49R, Y705F/K685R and Y705F/S727A (Addgene plasmid #123176 and #123177) were already available in Herrera's laboratory. PCR was carried out using 20 ng of the template plasmid, 0.2 μM of forward and reverse primers, 200 μM of deoxynucleotide triphosphates (dNTP) mix (NZYTech, Lisbon, Portugal) and 2.5 U of PfuTurbo DNA Polymerase (Agilent, Santa Clara, CA, USA). The conditions were 30 sec at 95 ºC and 12 cycles of 30 sec at 95 ºC, 1 min at 67 ºC and 10 min at 68 ºC. The template DNA was digested with 10 U of Dpn I (NZYTech, Lisbon, Portugal) for 1 hour at 37 ºC. Transformation of the Dpn I-treated DNA was carried using chemically competent *Escherichia coli* cells (Thermo Fisher Scientific, Waltham, MA, USA). The mix of DNA and competent cells was incubated at 4 ºC for 30 min, followed by heat shock at 42 ºC for 45 sec and incubated again at 4 ºC for 2 min. Then Luria Broth (LB) medium (1% w/v tryptone, 0.5% w/v yeast extract, 171 mM NaCl) without antibiotics was added to the bacteria suspension and incubated in agitation at 180 rpm, 37ºC for 1 hour. Transformed bacteria were seeded on LB agar (1% w/v tryptone, 0.5% w/v yeast extract, 171 mM NaCl, 1.5% w/v Agar) petri dishes (Thermo Fisher Scientific, Waltham, MA, USA) containing 100 μg/mL of ampicillin (ITW Reagents, Chicago, IL, USA) and incubated overnight at 37ºC. In the next day, the colonies were poked and grown in 3 mL of LB medium containing 100 μg/mL of ampicillin at 180 rpm, 37 ºC, overnight. DNA was then extracted and purified using the ZR Plasmid Miniprep™-Classic D4016 (Zymo Research, Irvine, CA, USA), following the manufacturer's instructions. DNA was quantified using Nanodrop 1000 (Thermo Fisher Scientific, Waltham, MA, USA) and sent for sequencing to STAB VIDA (Caparica, Portugal).

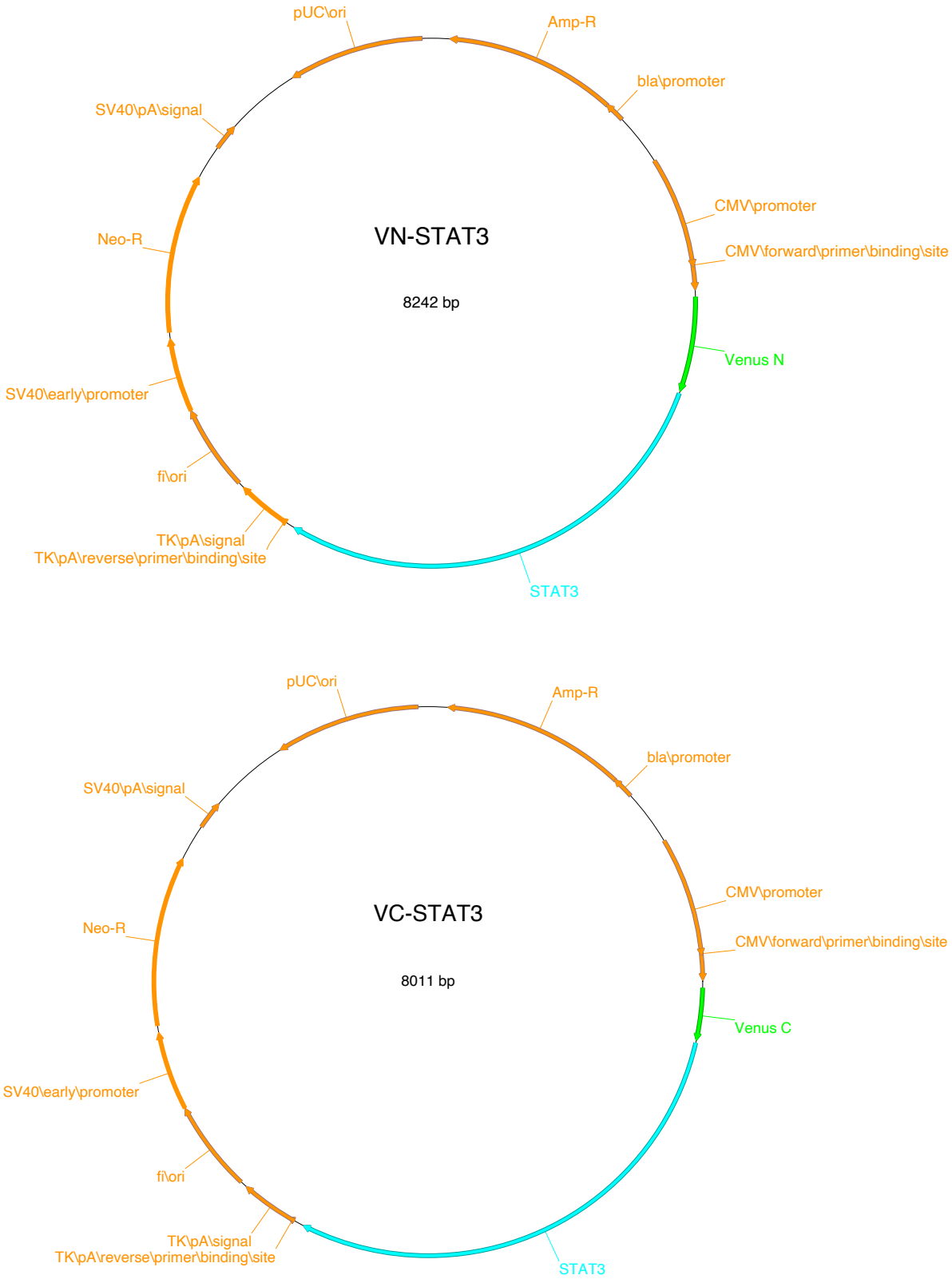

Figure 3.1 - Venus-STAT3 BiFC constructs. VN-STAT3 corresponds to the fusion of the fragment 1-157 of Venus to STAT3 (Addgene plasmid #123164). VC-STAT3 corresponds to the fusion of the fragment 158-238 of Venus to STAT3 (Addgene plasmid #123165).

Table 3.1 - Sequence of the primers used to perform PCR-based site-directed mutagenesis. Fwd: forward. Rev: reverse

Mutation	Template Plasmid	Primers	Resulting Construct
Y705F	Venus-STAT3 BiFC constructs	Fwd: 5' CAGGTAGCGCTGCCCCATTCCTGAAGACCAAGTTTATC 3'	Venus-STAT3-Y705F
		Rev: 5' GATAAACTTGGTCTTCAGGAATGGGGCAGCGCTACCTG 3'	
K49R	Venus-STAT3-Y705F BiFC constructs	Fwd: 5' CATATGCGGCCAGCAGAGAATCACATGCCAC 3'	Venus-STAT3-Y705F/K49R
		Rev: 5' GTGGCATGTGATTCTCTGCTGGCCGCATATG 3'	
K685R	Venus-STAT3-Y705F BiFC constructs	Fwd: 5' GAGGCATTCGGAAGGTATTGTCGGCC 3'	Venus-STAT3-Y705F/K685R
		Rev: 5' GGCCGACAATACCTTCCGAATGCCTC 3'	
S727A	Venus-STAT3-Y705F BiFC constructs	Fwd: 5' CATTGACCTGCCGATGGCACCCCGCACTTTAGATTC 3'	Venus-STAT3-Y705F/S727A
		Rev: 5' GAATCTAAAGTGCGGGGTGCCATCGGCAGGTCAATG 3'	
T236A	Venus-STAT3 BiFC constructs	Fwd: 5' CAGAAAACTCTCGCGGACGAGGAGC 3'	Venus-STAT3-T236A
		Rev: 5' GCTCCTCGTCCGCGAGAGTTTTCTG 3'	
Y640F	Venus-STAT3 BiFC constructs	Fwd: 5' GTCCGTGGAACCATTCACAAAGCAGCAG 3' Rev: 5' CTGCTGCTTTGTGAATGGTTCCACGGAC 3'	Venus-STAT3-Y640F
Y640F	Venus-STAT3-Y705F BiFC constructs		Venus-STAT3-Y705F/Y640F
T714A	Venus-STAT3 BiFC constructs	Fwd: 5' GTTTATCTGTGTGGCACCAACGACCTGC 3'	Venus-STAT3-T714A
		Rev: 5' GCAGGTCGTTGGTGCCACACAGATAAAC 3'	

3.2 Cell Cultures

HeLa cells (ATCC, Manassas, VA, USA) were cultivated and maintained in Dulbecco's Modified Eagle Medium (DMEM) Low Glucose with stable Glutamine (862 mg/L) and Sodium Pyruvate (110 mg/L) (biowest, Nuaillé, France), supplemented with 10% v/v fetal bovine serum (biowest, Nuaillé, France) and 1% v/v of a penicillin/streptomycin commercial antibiotic mixture (Cytiva, Marlborough, MA, USA) at 37°C in a humidified atmosphere containing 5% CO_2. Medium was changed every other day and cells were passed once a week by trypsinization (TrypLE Express, Thermo Fisher Scientific,

Waltham, MA, USA) for 5 min at 37ºC. For all the experiments, cells were counted using a Neubauer Chamber (Glaswarenfabrik Karl Hecht, Sondheim vor der Rhön, Germany) and seeded in different types of dishes according to the type of assay. Transfection was performed 24 hours after seeding, with the transfection reagent jetPRIME (Polyplus-transfection, Illkirch-Graffenstaden, France) in a 1:3 proportion (1 µg of DNA: 3 µL jetPRIME) or with the Lipofectamine 3000 Reagent (Thermo Fisher Scientific, Waltham, MA, USA) in a 1:2 proportion (1 µg of DNA: 2 µL Lipofectamine 3000 Reagent). Conditions and protocols were used according to the manufacturer's instructions. STAT3 knockout (STAT3-/-) HeLa cells transfected with the corresponding Venus-STAT3 BiFC constructs were stimulated with LIF (R&D systems, Minneapolis, MN, USA) at 200 ng/mL for 20 minutes or 2 hours, as indicated in the corresponding figures (**Figure 3.2)**. Prior to LIF stimulation, STAT3-/- HeLa cells were maintained in DMEM without fetal bovine serum for 2 hours to avoid unwanted stimulation by the serum components.

Knockout of the endogenous STAT3 gene from HeLa cells was previously done by Ricardo Vilela, a PhD student from Herrera's laboratory. HeLa cells at 80% confluence were transfected with the STAT3 CRISPR/Cas9 Knockout plasmid (Santa Cruz Biotechnology, Dallas, TX, USA) according to the manufacturer's instructions. Cells transfected with CRISPR/Cas9 constructs expressed temporarily GFP. Forty-eight hours after transfection, positive clones were selected by fluorescence-assisted cell sorting by means of a BD FACSAria III sorter (BD Biosciences, Franklin Lakes, NJ, USA) at Instituto de Medicina Molecular (Lisbon, Portugal). Single cells were distributed into 96-well plates (VWR International, Radnor, PA, USA) to grow. When cells reached confluence, the proteins were extracted to confirm the knockout by Western Blot. A STAT3-knockout clone was selected for further growth and experiments.

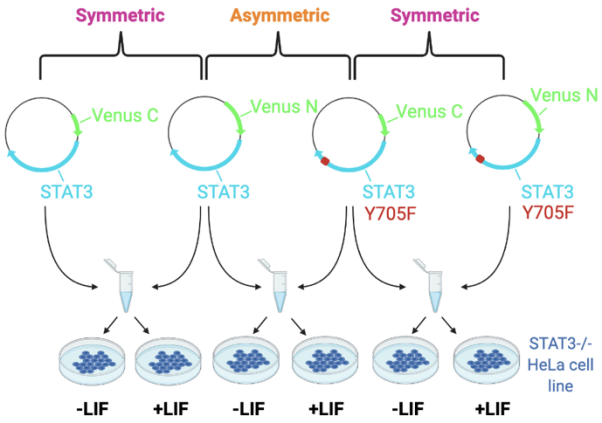

Figure 3.2 - Representative scheme of transfection of STAT3-/- HeLa cells with Venus-STAT3 BiFC constructs. STAT3-/- HeLa cells were transfected with symmetric or asymmetric combinations of BiFC plasmids: symmetric wild type STAT3 pair; symmetric STAT3-Y705F pair, and an asymmetric wild type STAT3 + STAT3-Y705F pair. Cells were then treated with leukemia inhibitory factor (LIF) at 200 ng/mL for 20 min or 2 hours.

3.3 Protein Extraction

For total protein extraction, 1.10 x 10^6 cells were seeded in 100 mm dishes (Orange Scientific, Braine-l'Alleud, Belgium). Cells were trypsinized for 5 min and collected into a microcentrifuge tube. Cells were centrifuged at 500 x g for 5 min at room temperature. The supernatant was discarded, and the pellet was resuspended in 100-200 µL (depending on the size of the pellet) of lysis buffer [150 mM NaCl and CelLytic M (Sigma-Aldrich, St. Louis, MO, USA)] containing a cocktail of protease

and phosphatase inhibitors (1 mM PMSF, 1X pepstatin, 5 μg/mL leupeptin and 1 mM Na_3VO_4). Cells were sonicated (Fisher Scientific, Waltham, MA, USA) for 10 seconds and incubated on ice for 45 min. Cells were then centrifuged at 15000 x g for 15 min at 4 ºC. The supernatant corresponding to the total proteins was collected and stored at -30ºC.

For nuclear and cytoplasmatic protein extraction, 375 000 cells were seeded in 60 mm dishes (Orange Scientific, Braine-l'Alleud, Belgium). The protein extraction was carried out using the NE-PER Nuclear and Cytoplasmic Extraction Reagents kit (Thermo Fisher Scientific, Waltham, MA, USA), 24 hours after transfection and the corresponding treatments with LIF. Cells were washed with PBS, trypsinized for 5 min, and collected into a microcentrifuge tube. Cells were then centrifuged at 500 x g for 5 min at room temperature. The supernatant was discarded, and the pellet was resuspended in PBS. The suspension was centrifuged at 500 x g for 3 minutes. The supernatant was discarded, and the pellet was resuspended in ice-cold Cytoplasmic Extraction Reagent I with protease inhibitors (Protease Inhibitor Cocktail EDTA Free, abcam, Cambridge, UK) and phosphatase inhibitors (Halt Phosphatase Inhibitor Single-Use Cocktail, Thermo Fisher Scientific, Waltham, MA, USA). To fully suspend the cell pellet, the suspension was vortexed for 15 seconds and incubated on ice for 10 minutes. Next, ice-cold Cytoplasmic Extraction Reagent II was added, and the suspension was vortexed for 5 seconds and incubated on ice for 1 minute. The mixture was once again vortexed for 5 seconds and centrifuged at 16000 x g for 5 min at 4ºC. The supernatant, which corresponded to the cytoplasmic extract, was collected into a new sterile eppendorf, and stored at -30ºC. The pellet was resuspended in ice-cold Nuclear Extraction Reagent with protease and phosphatase inhibitors and homogenized by vortex 4 times for 15 seconds every 10 minutes. Then, the suspension was centrifuged at 16000 x g for 10 minutes at 4ºC. The supernatant corresponding to the nuclear extract was collected into a new sterile eppendorf and stored at -30ºC.

Protein concentrations were quantified using the Bradford assay **[142]**. A standard curve with known concentrations of bovine serum albumin (BSA, 0.125 to 2 μg/μL) was used to determine protein concentration. Samples were incubated with 200 μL of Bradford reagent (Alfa Aesar, Ward Hill, MA, USA) for 10 minutes and read at 595 nm in the absorbance microplate reader Sunrise (Tecan, Männedorf, Switzerland).

3.4 Western Blot

Forty micrograms of total protein or 7.5-10 μg of nuclear extracts were mixed with 4x loading buffer (250 mM Tris-HCl pH 6.8, 10% w/v sodium dodecyl sulphate (SDS), 40% v/v glycerol, 20% v/v β-mercaptoethanol, 0.008% w/v bromophenol blue). Samples were heated for 5 minutes at 95ºC and then incubated at 4ºC for 5 minutes. Samples were resolved in 10% w/v SDS-polyacrylamide gel electrophoresis at 120V in running buffer (25 mM Tris, 190 mM glycine, 0.1% SDS); and transferred to a nitrocellulose membrane (Cytiva, Marlborough, MA, USA) at 100V for 1 hour in transfer buffer (25 mM Tris, 190 mM glycine, 20% methanol). Transfer efficiency and equal sample loading was confirmed by staining with Ponceau S solution [0,1% w/v Ponceau S (Amresco, Solon, OH, USA), 5% v/v acetic acid and ddH_2O (double-distilled water)]. Ponceau solution was later removed from the membranes by washing them with Tris-Buffered Saline with Tween 20 (TBS-T) (150 mM NaCl, 20 mM Tris pH 7.5, 0.05% v/v Tween 20). Membranes were blocked with 5% w/v skim milk (Nestlé, Vevey, Switzerland) in TBS-T for 1 hour at room temperature and then washed 3 times, 10 minutes each, with TBS-T before incubation with the primary antibodies overnight (**Table 3.2**). The membranes were then washed 3 times with TBS-T and incubated for 2 hours with the appropriate secondary antibodies (**Table 3.2**). Next, the membranes were washed 3 times, 10 minutes each, with TBS-T and incubated for 5 min with chemiluminescent HRP substrate (Thermo Fisher Scientific,

Waltham, MA, USA) before imaging in an Amersham Imager 680 RGB (Cytiva, Marlborough, MA, USA). The primary antibodies were diluted in a solution with 5% w/v BSA, 0.05% sodium azide and TBS-T. The secondary antibodies were diluted in 5% w/v skim milk in TBS-T.

Table 3.2 - Antibodies used in Western Blot. Identification of the primary and secondary antibodies used with the respective dilution, manufacturer, and reference.

Primary Antibody	Dilution	Manufacturer	Reference
Anti-phospho-STAT3 Y705 (rabbit)	1:1000	Cell Signaling Technology, Danvers, MA, USA	#9131
Anti-phospho-STAT3 Y705 (mouse)	1:1000	Santa Cruz Biotechnology, Dallas, TX, USA	sc-8059
Anti-acetyl-STAT3 K49 (rabbit)	1:1000	St John's Laboratory, London, UK	STJ193228
Anti-acetyl-STAT3 K685 (rabbit)	1:1000	Thermo Fisher Scientific, Waltham, MA, USA	PA5-17429
Anti-STAT3 (rabbit)	1:1000	Cell Signaling Technology, Danvers, MA, USA	#12640
Anti-STAT3 (mouse)	1:1000	Santa Cruz Biotechnology, Dallas, TX, USA	sc-8019
Anti-phospho-IRE1-S724 (rabbit)	1:1000	ABclonal, Woburn, MA, USA	AP0878
Anti-Calnexin (rabbit)	1:1000	ABclonal, Woburn, MA, USA	A15631
Anti-VDAC (rabbit)	1:3000	Millipore, Burlington, MA, USA	AB10527
Anti-GAPDH (rabbit)	1:2000	Santa Cruz Biotechnology, Dallas, TX, USA	sc-25778
Anti-PCNA (rabbit)	1:500	Cell Signaling Technology, Danvers, MA, USA	#13110
Anti-PCNA (mouse)	1:500	Cell Signaling Technology, Danvers, MA, USA	#2586
Secondary Antibody	**Dilution**	**Manufacturer**	**Reference**
Goat anti-Rabbit IgG (H+L)	1:10 000	Thermo Fisher Scientific, Waltham, MA, USA	A16096
Goat anti-Mouse IgG (H+L)	1: 10 000	Thermo Fisher Scientific, Waltham, MA, USA	A16066

3.5 Proliferation Assay

For this assay, 100 000 cells per well were seeded in a 6-well plate (Orange Scientific, Braine-l'Alleud, Belgium). After 48 hours, cells were trypsinized for 5 min at 37ºC. Trypsin was neutralized with complete DMEM medium, and cells were collected into a microcentrifuge tube. Cells were then centrifuged at 500 x g for 5 min at room temperature. The supernatant was discarded, and the pellet was resuspended in PBS. Cells were counted using a Neubauer Chamber.

3.6 Flow Cytometry and Fluorimetry

For this assay, 200 000 cells were seeded per well in a 6-well plate. Cells were trypsinized for 5 min at 37ºC and collected into microcentrifuge tubes. Cells were then centrifuged at 500 x g for 5 min

at room temperature. The supernatant was discarded, and the pellet was resuspended in a specific reporter solution according to the type of assay, followed by incubation in a 37ºC bath in agitation in the dark, as described in **Table 3.3**. The reporter solutions were prepared in PBS except for Fluo-3 AM and MitoSOX Red. Fluo-3 AM was prepared in DMEM with 1% fetal bovine serum and MitoSOX Red was prepared in CPBS (PBS, 0.5 mM $MgCl_2$, 0.7 mM $CaCl_2$, 5 mM glucose). Cells were then centrifugated at 500 x g for 5 min. The supernatant was discarded, and the pellet was resuspended in PBS. In the assay using MitoSOX Red, the pellet was resuspended in CPBS. The resuspension was transferred to cytometer tubes (VWR International, Radnor, PA, USA) or to a quartz 96-well plate (Thermo Fisher Scientific, Waltham, MA, USA) to measure the fluorescence intensity of cells by flow cytometry (Cytomics FC500, Beckman Coulter, Brea, CA, USA) or fluorimetry (FL_X800, BioTek Instruments, Winooski, VT, USA), respectively.

Table 3.3 – Flow cytometry and Fluorimetry Assays. Compounds used in each assay with the respective properties: wavelength of excitation (λ_{ex}) and of emission (λ_{em}) in nanometers (nm), concentration, time of incubation in minutes (min) and manufacturer.

Type of Assay	Compound used	λ_{ex}/ λ_{em} (nm)	Concentration	Time of incubation (min)	Description	Manufacturer
Measure of intracellular Ca^{2+} levels	Fluo-3, AM (F1242)	506/526	1 µg/mL	20	Fluo-3AM is a permeable molecule. Inside the cell, it is split by esterases originating Fluo-3 which can ligate to free Ca^{2+} ions, producing fluorescence.	Thermo Fisher Scientific, Waltham, MA, USA
Measure of intracellular ROS	$DCFH_2$-DA (D6883)	492/517	10 µM	20	$DCFH_2$-DA (2'-7'dichlorohidrofluorescin diacetate) is a non-polar, non-fluorescent molecule that enters the cell and is converted to $DCFH_2$ by esterases. $DCFH_2$ is oxidated by intracellular ROS and converts into DCF, which is fluorescent.	Sigma-Aldrich, St. Louis, MO, USA
Measure of mitochondrial Ca^{2+} levels	Rhod-2, AM (R1244)	552/581	3 µM	30	In physiological conditions, Rhod-2 presents a net positive charge which facilitates its capture inside the mitochondria, due to the electrochemical gradient that occurs trough the mitochondrial membrane. Rhod-2 exhibits a fluorescence which depends on the calcium but only after its oxidation (process that occurs inside the mitochondria).	Thermo Fisher Scientific, Waltham, MA, USA
Measure of mitochondrial superoxide levels	MitoSOX Red (M36008)	510/580	5 µM	20	MitoSOX Red enters quickly and selectively in the mitochondria of alive cells, where it is oxidized by superoxide, producing fluorescence.	Thermo Fisher Scientific, Waltham, MA, USA

Measure of mitochondrial membrane potential	Rhodamine 123 (R8004)	488/515-575	2.63 µM	20	Rhodamine 123 is a lipophilic and fluorescent cation that is sequestered by the mitochondria and retained in the inner membrane. The ability of cells to retain this compound in their inner membrane depends directly on the electrochemical potential in said membranes, in this way, a decrease in the mitochondrial membrane potential would imply less retention of Rhodamine 123 and therefore a decrease in the fluorescence emitted by cells.	Sigma-Aldrich, St. Louis, MO, USA

3.7 Real-Time Quantitative PCR (qPCR)

For this assay, 1.10 x 10^6 cells were seeded in 100 mm dishes. Total RNA was isolated using the GenElute Mammalian Total RNA Miniprep Kit (Sigma-Aldrich, St. Louis, MO, USA), according to manufacturer's instructions. RNA was quantified using Nanodrop 1000 (Thermo Fisher Scientific, Waltham, MA, USA). Then, reverse transcription of total RNA (2 µg) to single-stranded cDNA was performed using the High-Capacity cDNA Reverse Transcription Kit (Thermo Fisher Scientific, Waltham, MA, USA), according to manufacturer's instructions. The resulting solution containing cDNA was diluted with nuclease-free water (dilution ratio 1:6). qPCR was done using the equipment QuantStudio5 (Thermo Fisher Scientific, Waltham, MA, USA). The reaction had a final volume of 10 µL, with 5 µL of Power SYBR Green PCR Master Mix (Thermo Fisher Scientific, Waltham, MA, USA), 0.25 µL of each primer (forward and reverse) and 4.5 µL of cDNA. The qPCR conditions were 50°C for 2 min, 95°C for 10 min, followed by 40 cycles of 95°C for 15 sec and 60°C for 1 min. The dissociation curve was analyzed to confirm the desired genetic product: one cycle of 95°C for 15 sec, 60°C for 1 min, and 95°C for 15 sec. Comparative quantification was carried out using the ΔΔCq method, where the Cq values for the genes were normalized using a reference gene (*GAPDH*) and a calibrator (wild type HeLa cell samples). All the primers used (**Table 3.4**) were kindly lend to us by Carmen Rodrígez' laboratory at University of Oviedo, Spain.

Table 3.4 – Sequence of the primers used to perform qPCR. Fwd: forward. Rev: reverse.

Target Gene	Primers
CCND1	Fwd: 5' GCTGCGAAGTGGAAACCATC 3'
	Rev: 5' CCTCCTTCTGCACACATTTGA 3'
BCL2	Fwd: 5' GGAGGATTGTGGCCTTCTTT 3'
	Rev: 5' GCCCAATACGACCAAATCCGTTGA 3'
c-MYC	Fwd: 5' GCCACGTCTCCACACATCAG 3'
	Rev: 5' TGGTGCATTTTCGGTTGTTG 3'
SOD1	Fwd: 5' AAGGCCGTGTGCGTGCTGAA 3'
	Rev: 5' CAGGTCTCCAACATGCCTCT 3'

SOD2	Fwd: 5’ GCACATTAACGCGCAGATCA 3’
	Rev: 5’ AGCCTCCAGCAACTCTCCTT 3’
GPX1	Fwd: 5’ GTGTATGCCTTCTCGGCGCG 3’
	Rev: 5’ CGTTGCGACACACCGGAGAC 3’
SLC2A1	Fwd: 5’ GCTGTGCTTATGGGCTTCTC 3’
	Rev: 5’ CACATACATGGGCACAAAGC 3’
IGFBP3	Fwd: 5’ GACACACTGAATCACCTGAAGT 3’
	Rev: 5’ TATCCACACACCAGCAGAAG 3’
GAPDH	Fwd: 5’ CGGAGTCAACGGATTTGGTC 3’
	Rev: 5’ AATCATATTGGAACATGTAAACCATGTAGT 3’

3.8 Statistical Analysis

All the data were presented as the arithmetic mean ± Standard Error of the Mean (SEM). The minimum number of biological replicates was 1 (n=1). Statistical comparison between two groups was performed using unpaired t test with Welch’s correction and between more than two groups was performed using Ordinary one-way ANOVA test. All statistical analyses were performed with GraphPad Prism 8 (GraphPad Software Inc., San Diego, CA, USA). P-values less than 0.05 were considered statistically significant (*$P < 0.05$; **$P < 0.01$; ***$P < 0.001$).

IV. Results

4.1 Characterization of STAT3-/- HeLa cells

STAT3-/- HeLa cells were characterized in comparison to wild type (WT) HeLa cells. First, STAT3 knockout was confirmed by extracting total proteins from WT and STAT3-/- HeLa cells and analyzing them by Western Blot. As shown in **Figure 4.1A**, the bands corresponding to phospho-STAT3 (Y705) and STAT3 only appeared in the sample from WT HeLa cells, as expected. This confirms the absence of endogenous STAT3 in STAT3-/- HeLa cells. To assess if STAT3 had an impact in the proliferation of cells, WT and STAT3-/- HeLa cells were seeded and counted 48 h later. No significant difference between the two groups was evident, suggesting that STAT3 does not have a critical role in the proliferation of HeLa cells (**Figure 4.1B**). ROS and Ca^{2+} homeostasis are fundamental for the survival of cells and STAT3 has been implicated in both, as described in **section 1.1.4**. As shown in **Figure 4.1C**, STAT3-/- HeLa cells presented higher levels of intracellular ROS, and consequently higher oxidative stress than WT HeLa cells. To determine if mitochondria contributed to elevated ROS observed in STAT3-/- cells, the fluorescent probe MitoSOX Red was used. Unlike DCF, MitoSOX Red selectively fluoresces in mitochondria and is retained there in response to superoxide production (**Figure 4.1D**). There were no significant alterations in the levels of superoxide in the mitochondria of STAT3-/- HeLa cells. As the measurement of mitochondrial superoxide was performed only with 3 technical replicates and no biological replicates, more assays are needed to do a more accurate interpretation of the results. Intracellular and mitochondrial Ca^{2+} levels were obtained by measuring Fluo-3 AM and Rhod-2 AM fluorescence, respectively. As shown in **Figure 4.1E** and **Figure 4.1F**, there is no significant difference in the intracellular and mitochondrial Ca^{2+} levels between the two cell lines. The results regarding the intracellular Ca^{2+} levels are still preliminary, and further optimization is required. **Figure 4.1G** shows that although there is a slight decrease in the mitochondrial membrane potential in STAT3 -/- HeLa cells, the difference is not significant.

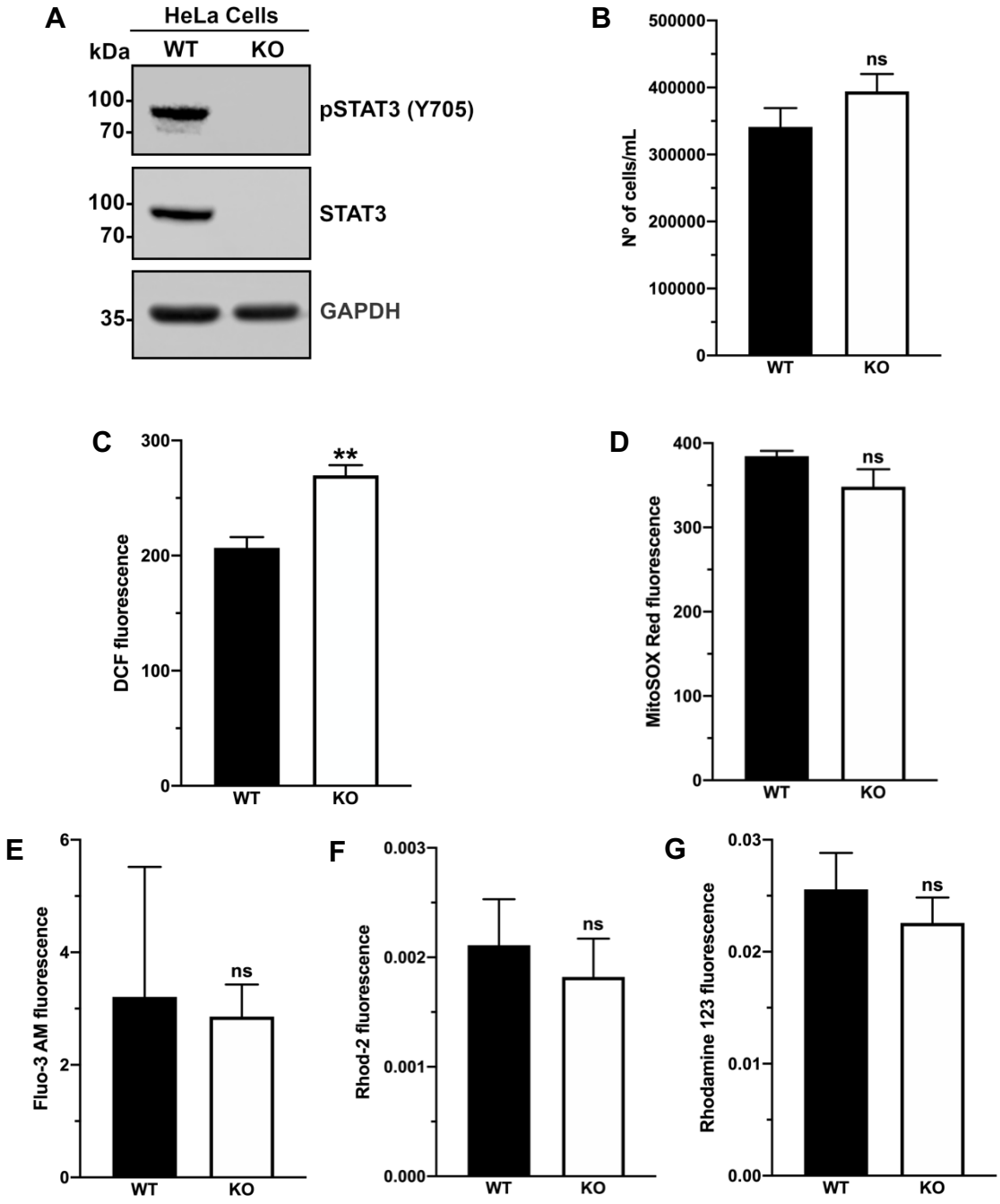

Figure 4.1 - Characterization of STAT3-/-HeLa cells. A, Proteins from wild type (WT) and STAT3 -/- (KO) HeLa cells were collected and analyzed by Western Blot. The antibodies used were anti-phospho-STAT3 (Y705), anti-STAT3 and anti-GAPDH. GAPDH levels were used as loading control. **B**, WT and KO HeLa cells were counted 48 h after seeding. Statistical analysis was carried out on the mean ± SEM of 2 independent experiments carried out in triplicate. **C**, Measurement of intracellular oxidative stress using 2'-7'dichlorofluorescin (DCF) fluorescence in WT and KO HeLa cells. Statistical analysis was carried out on the mean ± SEM of 4 independent experiments carried out in triplicate. **D**, Measurement of mitochondrial oxidative stress using MitoSOX Red fluorescence in WT and KO HeLa cells. Statistical analysis was carried out on the mean ± SEM of 1 experiment carried out in triplicate. **E**, Measurement of intracellular Ca^{2+} levels using Fluo-3 AM fluorescence in WT and KO HeLa cells. Statistical analysis was carried out on the mean ± SEM of 2 independent experiments carried out in triplicate. **F**, Measurement of mitochondrial Ca^{2+} levels using Rhod-2 AM fluorescence in WT and KO HeLa cells. Statistical analysis was carried out on the mean ± SEM of 3 independent experiments carried out in triplicate. **G**, Measurement of the mitochondrial membrane potential using Rhodamine 123 fluorescence in WT and KO HeLa cells. Statistical analysis was carried out on the mean ± SEM of 3 independent experiments carried out in triplicate. **, Significant *vs* the WT cells, $P < 0.01$; ns, $P > 0.05$. In this figure all ns corresponds to $P > 0.2$.

4.1.1 Effect of STAT3 knockout on HeLa cells gene expression

Further characterization of STAT3-/- cells was performed by measuring the expression of a set of genes that are induced by STAT3 (*CCND1*, *BCL2* and *c-MYC*). *CCND1* and *c-MYC* are cell-cycle progression genes and *BCL2* is a pro-survival gene **[51], [55], [56]**. As STAT3 regulates the production of ROS in the cell and it was shown that STAT3-/- HeLa cells presented higher levels of intracellular oxidative stress (**Figure 4.1C)**, it was also measured the expression of antioxidant genes (*SOD1, SOD2* and *GPX1*). Among these, only *SOD2* was shown to be upregulated by STAT3 **[69], [70]**. STAT3 also affects glucose metabolism **[67]**, so the expression of *SLC2A1* (commonly known as GLUT1) which encodes the glucose transporter protein type 1 was also measured. According to the dataset "CHEA Transcription Factor Targets" **[143]**, *IGFBP3* is also a target gene of STAT3. However, if STAT3 up or down regulates *IGFBP3* is still unknown. *IGFBP3* encodes for insulin like growth factor binding protein 3 which binds to insulin-like growth factor-1 (IGF-1). This binding can inhibit or enhance IGF-1's activity in promoting cell proliferation and survival. *IGFBP3* has also been linked to the pathogenesis of cancers **[144]**. As shown in **Figure 4.2**, only the expression of *CCND1* was significantly reduced in STAT3-/- cells compared with WT cells. The other six genes were more expressed in STAT3-/- cells, but the differences were only statistically significant for *SOD1*, *SLC2A1* and *IGFBP3*.

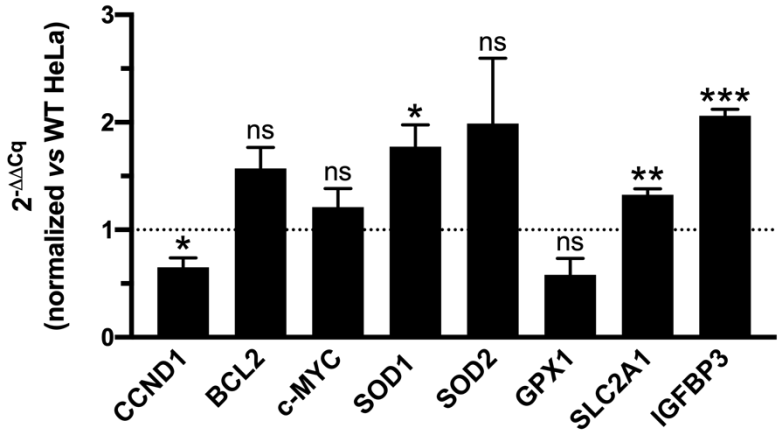

Figure 4.2 - Gene expression levels in WT and STAT3-/- HeLa cells. The expression levels for eight genes were determined by real time quantitative polymerase chain reaction (qPCR) in WT and STAT3-/- HeLa cells. These genes are cyclin D1 (*CCND1*), BCL2 apoptosis regulator (*BCL2*), MYC proto-oncogene (*c-MYC*), superoxide dismutase 1 (*SOD1*), superoxide dismutase 2 (*SOD2*), glutathione peroxidase 1 (*GPX1*), solute carrier family 2 member 1 (*SLC2A1*) and insulin like growth factor binding protein 3 (*IGFBP3*). Comparative quantification was carried out using the $\Delta\Delta C_q$ method, where the C_q values for the genes were normalized using a reference gene (*GAPDH*) and a calibrator (wild type HeLa cell (WT HeLa) samples). In WT HeLa cells, $2^{-\Delta\Delta Cq} = 1$ for all genes. Statistical analysis was carried out on the mean ± SEM of data (n=4). *, Significant *vs* the WT cells, $P < 0.05$; **, Significant *vs* the WT cells, $P < 0.01$; ***, Significant *vs* the WT cells, $P < 0.001$; ns, $P > 0.05$.

4.1.2 Levels of ER and mitochondria related proteins in WT and STAT3-/- HeLa cells

To know if the elevated oxidative stress observed in STAT3-/- cells (**Figure 4.1C)** could lead to ER stress and mitochondrial dysfunction, the levels of three proteins related to these phenomena were analyzed. Inositol-requiring enzyme 1 (IRE1) and calnexin are ER-resident proteins that maintain the good functioning of this organelle. In conditions of ER stress, IRE1 is phosphorylated (pIRE1) during the unfolded protein response (UPR) and calnexin is up-regulated **[145]**. Voltage dependent anion-selective channel (VDAC) is a protein localized in the outer mitochondrial membrane that participates in mitochondrial stress response **[146]**. As show in **Figure 4.3**, the levels of the three proteins (pIRE1, calnexin and VDAC) did not show a significant difference between WT and STAT3-/- cells. However, there seems to be a tendency of higher levels of calnexin and VDAC in STAT3-/- cells. Further assays are necessary to confirm or dismiss this tendency. The level of STAT3 was also observed to ensure the absence of STAT3 in STAT3-/- cells.

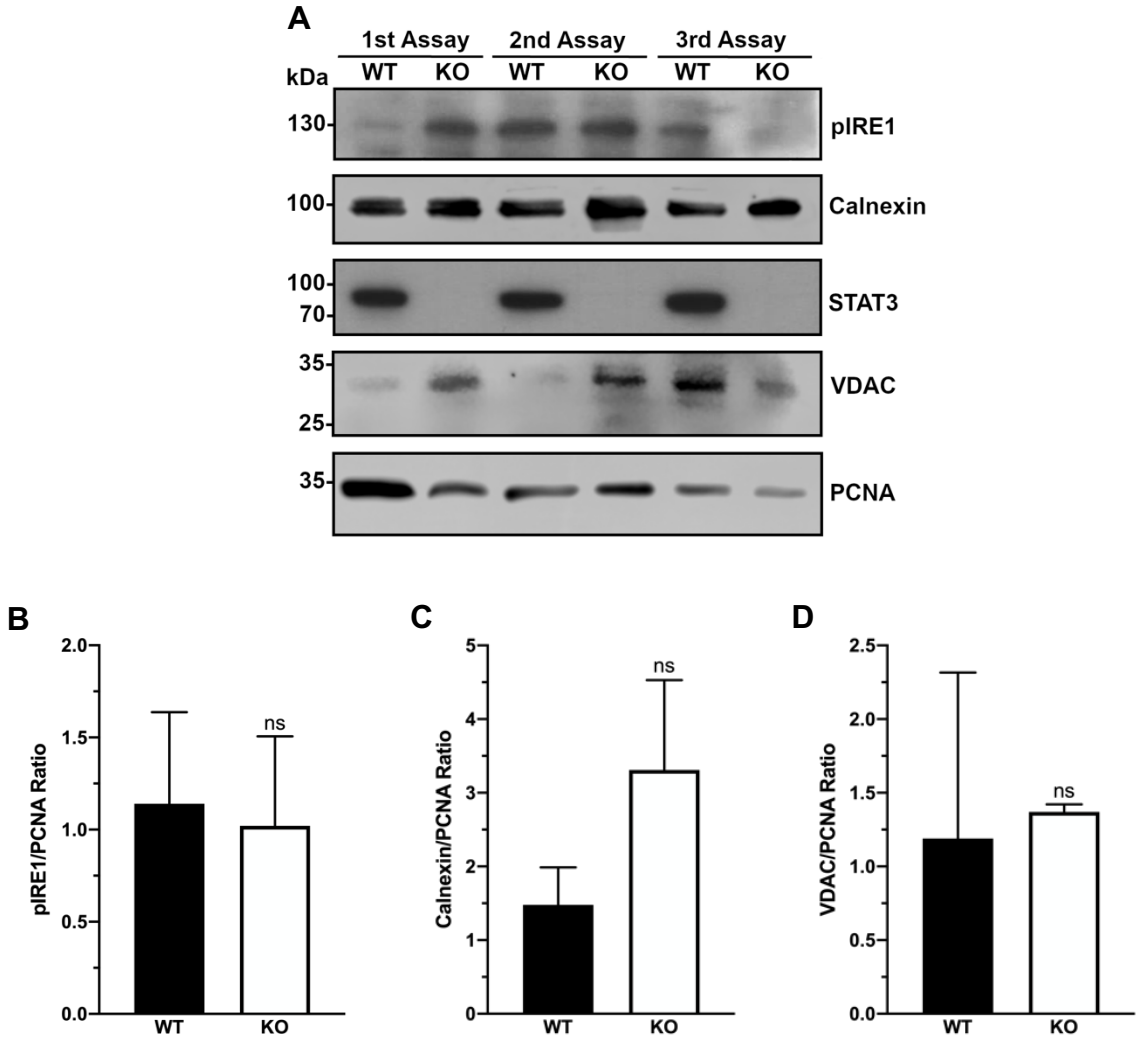

Figure 4.3 - Levels of ER and mitochondria related proteins in WT and STAT3-/- HeLa cells. A, Total proteins from wild type (WT) and STAT3 knockout (KO) HeLa cells of three different assays were extracted and analyzed by Western Blot. The antibodies used were anti-phospho-IRE1 (S724), anti-Calnexin, anti-STAT3, anti-VDAC and anti-PCNA. PCNA levels were used as loading control to ensure that the same amount of protein was used in all samples. **B, C, D**, Semi-quantification of Western Blot bands was performed by calculating the ratio P-IRE1/PCNA (**B**), Calnexin/PCNA (**C**) and VDAC/PCNA (**D**). Statistical analysis was carried out on the mean ± SEM of 3 independent experiments. ns, $P > 0.05$.

4.2 Effects of post-translational modifications in the translocation of STAT3 homodimers to the nucleus

4.2.1 Phosphorylation of one of the STAT3 monomers is enough to drive STAT3 dimers into the nucleus after LIF stimulation

STAT3 homodimers are phosphorylated at Y705 and accumulate in the nucleus upon stimulation with various cytokines, such as LIF **[44]**. A question that our laboratory is currently investigating is whether Y705 phosphorylation and other post-translational modifications must occur on the two monomers of the STAT3 dimer for it to become active. To address this question, STAT3 -/- HeLa cells were transfected with combinations of two complementary Venus-STAT3 BiFC plasmids, either wild type or carrying the phosphoresistant Y705F mutation in both constructs (**symmetric**), or an **asymmetric** mixture of one wild type monomer and a Y705F monomer 1:1 (**Figure 4.4A)**. Twenty-four hours later, cells were treated with LIF for 20 min or 2 hours and their nuclear proteins analyzed by Western Blot. As shown in **Figure 4.4A**, there is accumulation of phospho- and total wild type STAT3 in the nucleus after only 20 minutes of stimulation with LIF, but not of symmetric STAT3-Y705F dimers. Asymmetric STAT3 dimers (i.e., formed by one wild type molecule and one Y705F molecule) responded as wild type STAT3 symmetric dimers, suggesting that phosphorylation of only one of the STAT3 molecules is enough to drive STAT3 dimers into the nucleus.

Nuclear accumulation of wild type STAT3 dimers after 2 hours of stimulation with LIF was not higher than at 20 min. Regarding STAT3-Y705F symmetric dimers, there was more quantity in the nucleus comparing to 20 min. However, this was not related to the presence of LIF because the intensity of the bands is similar with or without LIF. This supports previous reports that unphosphorylated STAT3 dimers can translocate to the nucleus or shuttle freely between cytoplasm and nucleus in the absence of cytokine stimuli **[47]–[49]**. Asymmetric dimers did not accumulate in the nucleus in response to LIF, as wild type symmetric dimers, indicating that the effect observed at 20 min was transient. Since the aim of this work was to see a more immediate response of STAT3 to LIF stimulation, the following experiments were done after 20 minutes of stimulation with LIF, and the same experimental design and workflow was used.

The previous result suggests that phosphorylation of only one of the STAT3 molecules is enough to drive STAT3 dimers into the nucleus. To investigate if this was still observed when adding an additional inactivating mutation to the STAT3-Y705F construct, double mutant plasmids were designed and produced. STAT3 -/- HeLa cells were transfected with asymmetric combinations of two complementary Venus-STAT3 BiFC plasmids, one wild type and the other carrying the phosphoresistant Y705F mutation or carrying a double PTM-resistant mutation (Y705F/K49R, Y705F/K685R, Y705F/S727A) (**Figure 4.4B**). The mutations K49R and K685R prevent the acetylation, methylation, ubiquitination and/or SUMOylation of these residues and the mutation S727A prevents its phosphorylation. Twenty-four hours after transfection, cells were treated with LIF for 20 minutes and their nuclear proteins analyzed by Western Blot. As shown in **Figure 4.4B**, there is accumulation of STAT3 in the nucleus in all the asymmetric combinations with double mutants. The addition of the mutations K685R and S727A appeared to reduce slightly the accumulation of wild type STAT3 in the nucleus. However, the levels of the loading control (PCNA) used were also reduced compared to the other samples. This suggests that the decrease in STAT3 accumulation could be due to unequal sample loading. Therefore, even if one of the STAT3 monomers carries the phosphoresistant Y705F mutation or the double inactivating mutations Y705F/K49R, Y705F/K685R, Y705F/S727A, the presence of one phosphorylatable wild type STAT3 monomer is sufficient to drive STAT3 accumulation in the nucleus.

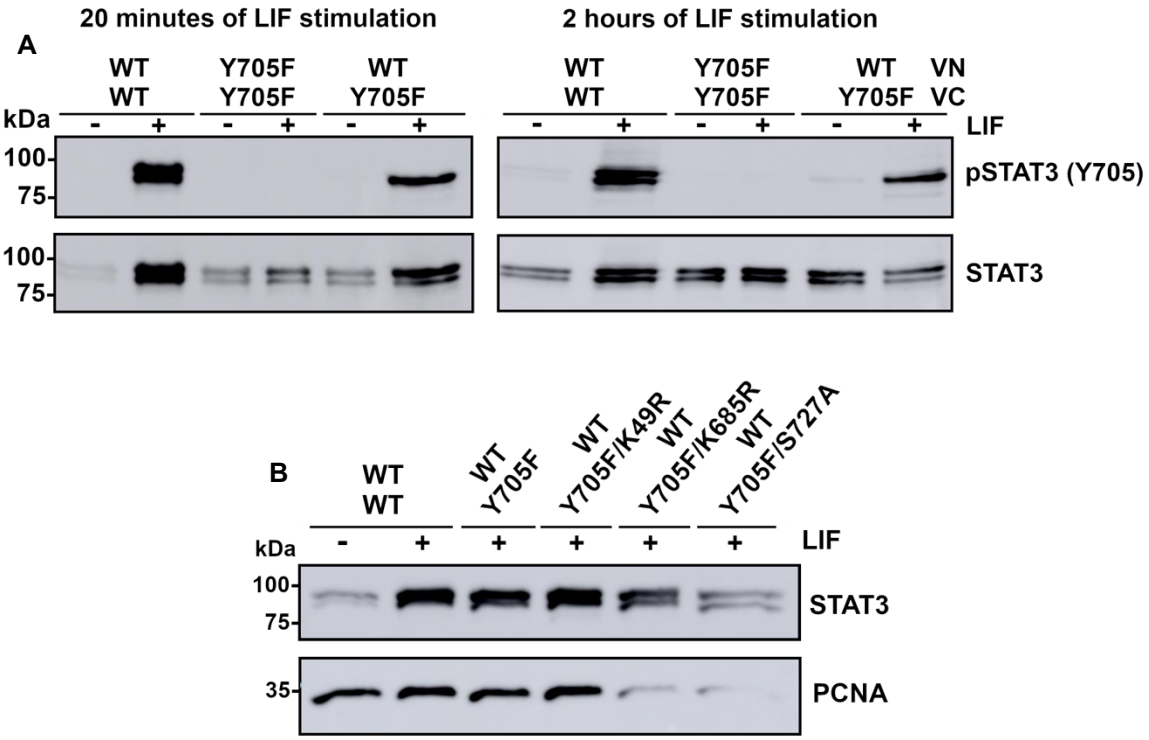

Figure 4.4 - Nuclear translocation of STAT3 dimers after LIF stimulation. A, STAT3-/- HeLa cells were transfected with symmetric or asymmetric combinations of BiFC plasmids: symmetric wild type STAT3 pair (WT); symmetric STAT3-Y705F pair (Y705F), and an asymmetric STAT3-WT / STAT3-Y705F pair (WT+Y705F). Cells were then treated with leukemia inhibitory factor (LIF) at 200 ng/mL for 20 min or 2 hours, and nuclear extracts collected. Figure corresponding to 20 min of LIF stimulation is representative of 4 experiments. Figure corresponding to 2 hours of LIF stimulation is representative of 2 experiments. **B**, STAT3-/- HeLa cells were transfected with symmetric or asymmetric combinations of BiFC plasmids: symmetric wild type STAT3 pair (WT); an asymmetric STAT3-WT / STAT3-Y705F pair; an asymmetric STAT3-WT / STAT3-Y705F/K49R pair; an asymmetric STAT3-WT / STAT3-Y705F/K685R pair and an asymmetric STAT3-WT / STAT3-Y705F/S727A pair. Cells were then treated with LIF at 200 ng/mL for 20 min, and nuclear extracts collected. Representative image of 2 experiments. Nuclear extracts were analyzed by Western blot, using anti-phospho-STAT3 (Y705), anti-STAT3 and anti-PCNA antibodies. PCNA levels were used as loading control to ensure that the same amount of protein was used in all samples.

4.2.2 Influence of inactivating mutations on the nuclear accumulation of unphosphorylated STAT3

As shown above, symmetric STAT3-Y705F dimers can translocate to the nucleus independently of LIF stimulation. To investigate if an additional mutation could affect the accumulation of STAT3 in the nucleus, STAT3 -/- HeLa cells were transfected with symmetric and asymmetric combinations of two complementary Venus-STAT3 BiFC plasmids. The symmetric dimers were formed by two wild type monomers, by two STAT3-Y705F monomers and by two double mutant Y705F/K49R, Y705F/K685R or Y705F/S727A STAT3 monomers. The asymmetric dimers were formed by one STAT3-Y705F monomer with one double mutant (Y705F/K49R, Y705F/K685R or Y705F/S727A) monomer. Twenty-four hours later, cells were treated with LIF for 20 minutes and their nuclear proteins analyzed by Western Blot. As shown in **Figure 4.5A**, the mutation K49R does not affect the nuclear accumulation of Y705-unphosphorylated STAT3 because the intensity of the bands corresponding to the dimers bearing the mutation Y705F is similar. This is not observed for the mutation K685R, as the dimers containing this mutation present a decrease in the intensity of bands compared to the Y705-unphosphorylated dimer, suggesting a reduced accumulation in the nucleus. This effect is more accentuated in the asymmetric dimer (**Figure 4.5B**). The phosphoresistant mutation S727A appears to only affect the accumulation of Y705-unphosphorylated STAT3 in the nucleus when it is present in both monomers (**Figure 4.5C**).

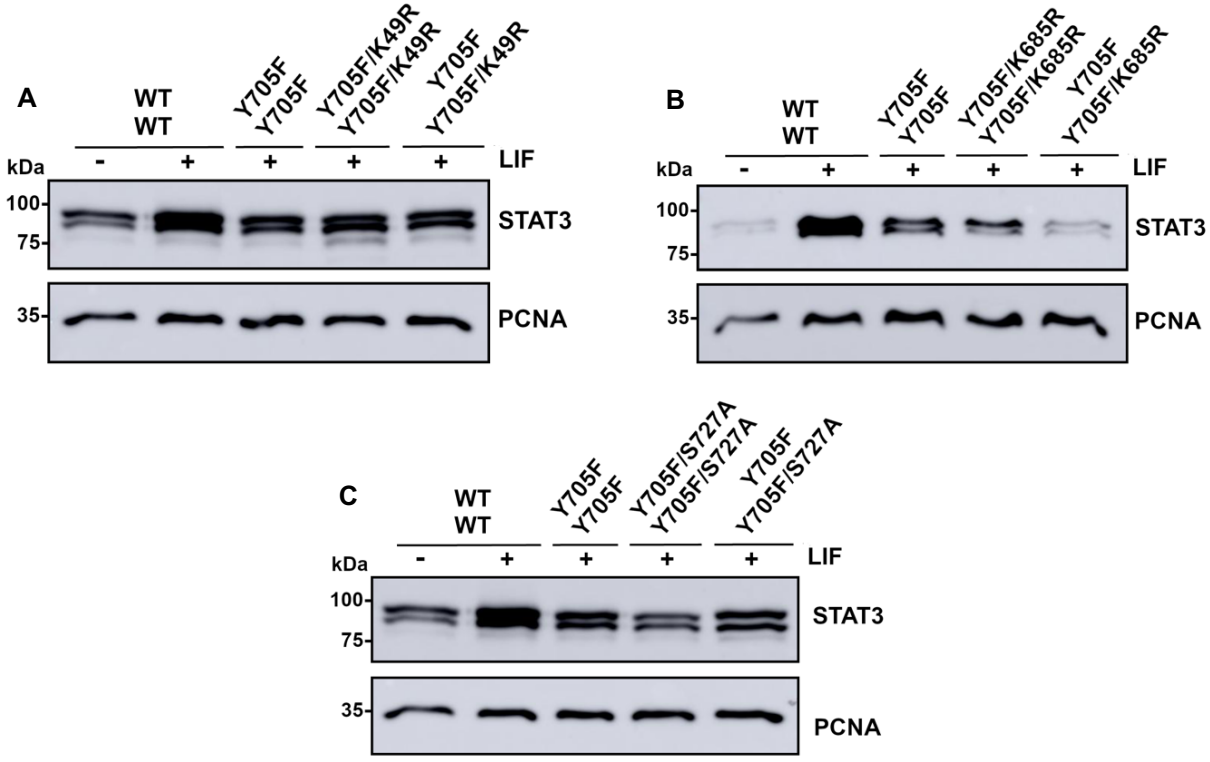

Figure 4.5 - Nuclear accumulation of Y705-unphosphorylated STAT3 dimers. STAT3-/- HeLa cells were transfected with symmetric or asymmetric combinations of BiFC plasmids. Cells were then treated with leukemia inhibitory factor (LIF) at 200 ng/mL for 20 min, and nuclear extracts collected. Nuclear extracts were analyzed by Western blot, using anti-STAT3 and anti-PCNA antibodies. PCNA levels were used as loading control to ensure that the same amount of protein was used in all samples. **A**, Transfection with a symmetric wild type (WT) STAT3 pair; symmetric STAT3-Y705F pair, symmetric STAT3-Y705F/K49R pair and an asymmetric STAT3-Y705F + STAT3-Y705F/K49R pair. **B**, Transfection with a symmetric WT STAT3 pair; symmetric STAT3-Y705F pair, symmetric STAT3-Y705F/K685R pair and an asymmetric STAT3-Y705F + STAT3-Y705F/K685R pair. **C**, Transfection with a symmetric WT STAT3 pair; symmetric STAT3-Y705F pair, symmetric STAT3-Y705F/S727A pair and an asymmetric STAT3-Y705F + STAT3-Y705F/S727A pair. Representative images of 2 experiments.

4.2.3 The role of the disease-related Y640F mutation in STAT3 nuclear translocation, intracellular oxidative stress, and gene expression

As mentioned before, the STAT3 Y640F mutation has been found in patients with LGL leukemia and IHCAs. To observe how this mutation impacts the translocation of STAT3 to the nucleus, STAT3 -/- HeLa cells were transfected with symmetric combinations of two complementary Venus-STAT3 BiFC plasmids, either wild type, carrying the phosphoresistant Y705F or Y640F mutations or carrying the double mutation Y705F/Y640F in both constructs (symmetric combinations, **Figure 4.6A**). Twenty-four hours later, cells were treated with LIF for 20 min and their nuclear proteins analyzed by Western Blot. As shown in **Figure 4.6A**, symmetric wild type and mutant Y640F dimers can be phosphorylated and accumulate in the nucleus in response to LIF. Interestingly, the accumulation was higher in Y640F mutant symmetric dimers in terms of both phospho- and total STAT3, confirming previous reports that this mutation increases the accumulation of STAT3 in the nucleus **[23], [84]**. As expected, the Y705F mutant and Y705F/Y640F double mutant symmetric dimers could not be phosphorylated. These mutant symmetric dimers did not display any alterations in the absence or presence of LIF, suggesting that these dimers do not respond to LIF stimulation. In the double mutants, the mutation Y705F prevents the effect of the Y640F mutation.

To further characterize the function of STAT3 Y640F, STAT3-/- HeLa cells were transfected with one wild type Venus-STAT3 BiFC plasmid or with one Venus-STAT3-Y640F BiFC plasmid. As shown in **Figure 4.6B**, both cells transfected with wild type STAT3 or STAT3-Y640F presented significantly higher levels of ROS than WT cells, instead of restoring the levels of oxidative stress of WT HeLa cells. The difference between STAT3-/- cells transfected with wild type STAT3 and with STAT3-Y640F was not significant, which suggests that the mutation Y640F was not the cause of the higher oxidative stress observed.

The gene expression profile of transfected STAT3-/- was also determined for the same gene set described before (**Figure 4.6C**). Both STAT3-/- cells transfected with wild type STAT3 and with STAT3-Y640F plasmids presented significantly higher expression of the genes *BCL2*, *c-MYC* and *IGFBP3* in comparison to WT HeLa cells. The expression of *GPX1* was significantly decreased in both STAT3-/- transfected cells and the expression of *CCND1* and *SOD2* was not significantly different comparing with WT HeLa cells. However, the differences between STAT3-/- cells transfected with wild type STAT3 and with Y640F STAT3 were not significant, suggesting that the mutation Y640F did not have influence in the transcriptional activity of STAT3 or in the expression alterations observed in this gene set. Since these measurements were carried out in the absence of cytokine stimuli, we cannot rule out the possibility that the Y640F mutation had an effect on the canonical STAT3 pathway.

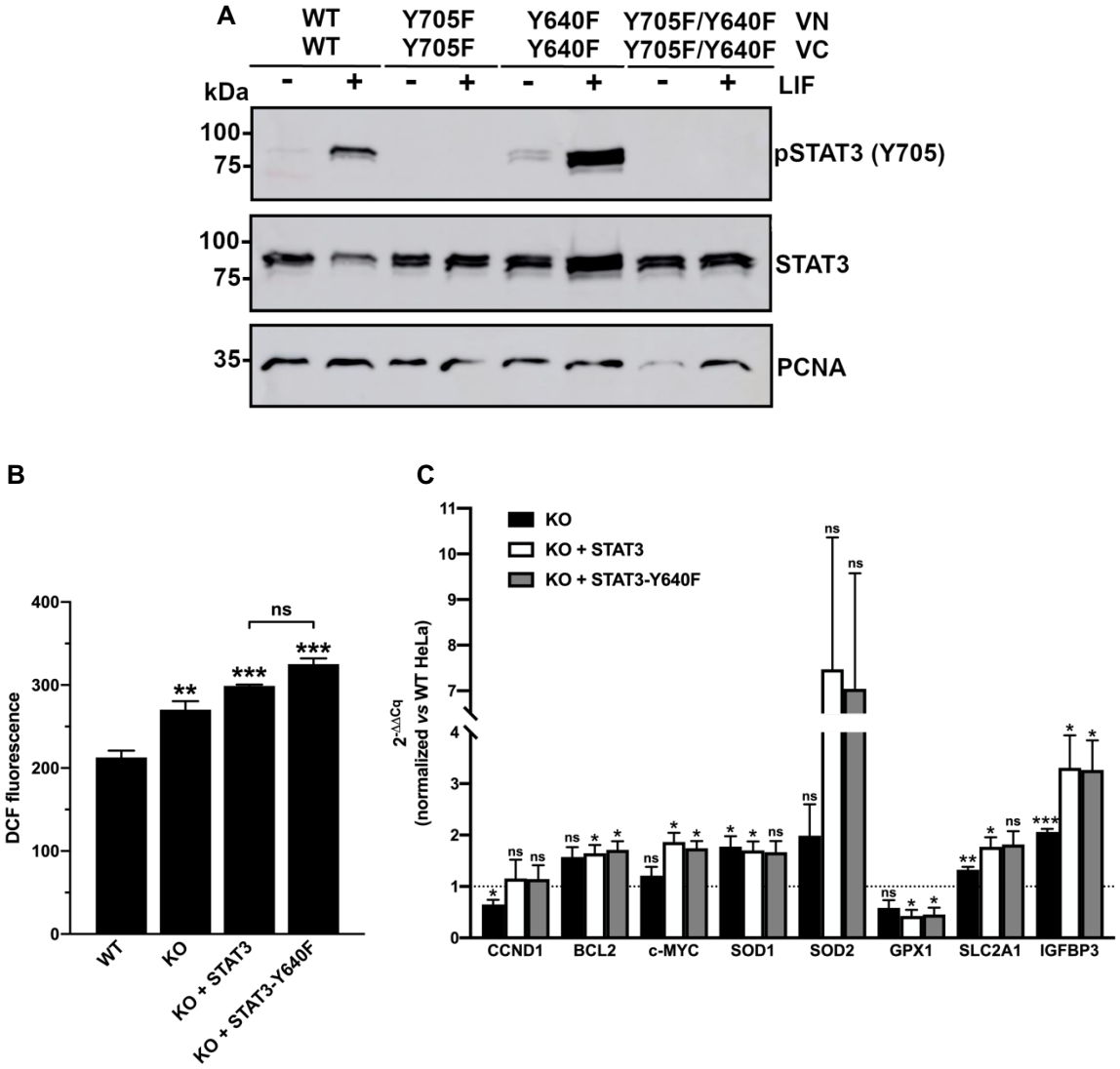

Figure 4.6 - The role of mutation Y640F in STAT3 nuclear translocation, intracellular oxidative stress, and gene expression. A, STAT3-/- HeLa cells were transfected with symmetric combinations of BiFC plasmids: wild type STAT3 pair (WT); STAT3-Y705F pair (Y705F); STAT3-Y640F pair (Y640F), and STAT3-Y705F/Y640F pair (Y705F/Y640F). Cells were then treated with leukemia inhibitory factor (LIF) at 200 ng/mL for 20 min, and nuclear extracts collected. Nuclear extracts were analyzed by Western blot, using anti-phospho-STAT3 (Y705), anti-STAT3 and anti-PCNA antibodies. PCNA levels were used as loading control to ensure that the same amount of protein was used in all samples. Representative image of 2 experiments. **B**, Measurement of intracellular oxidative stress using DCF fluorescence in wild type (WT) cells, STAT3-/- (KO) cells, STAT3-/- cells transfected with one wild type STAT3 plasmid (KO + STAT3) and STAT3-/- cells transfected with one STAT3-Y640F plasmid (KO + STAT3-Y640F). Statistical analysis was carried out on the mean ± SEM of 3 independent experiments carried out in triplicate. **C**, The expression levels for eight genes were determined by real time quantitative polymerase chain reaction (qPCR) in WT, KO and STAT3-/- transfected HeLa cells (KO + STAT3 and KO + STAT3-Y640F). These genes are cyclin D1 (*CCND1*), BCL2 apoptosis regulator (*BCL2*), MYC proto-oncogene (*c-MYC*), superoxide dismutase 1 (*SOD1*), superoxide dismutase 2 (*SOD2*), glutathione peroxidase 1 (*GPX1*), solute carrier family 2 member 1 (*SLC2A1*) and insulin like growth factor binding protein 3 (*IGFBP3*). Comparative quantification was carried out using the $\Delta\Delta C_q$ method, where the C_q values for the genes were normalized using a reference gene (*GAPDH*) and a calibrator (wild type HeLa cell (WT HeLa) samples). In WT HeLa cells, $2^{-\Delta\Delta Cq} = 1$ for all genes. Statistical analysis was carried out on the mean ± SEM of data (n=4). *, Significant *vs* the WT cells, $P < 0.05$; **, Significant *vs* the WT cells, $P < 0.01$; ***, Significant *vs* the WT cells, $P < 0.001$; ns, $P > 0.05$.

V. Discussion

In the present work, the influence of key post-translational modifications on the nuclear translocation of symmetric and asymmetric STAT3 dimers was analyzed upon LIF stimulation. A previous study by Herrera's laboratory had already reported that asymmetric dimers could be formed and observed striking changes in the intracellular distribution of unstimulated asymmetric STAT3 dimers **[107]**. However, this study was carried out in cells that expressed endogenous STAT3. Thus, there was a need to expand these observations on cells lacking STAT3 to avoid the interference of endogenous STAT3 and in the presence of cytokines to determine the possible influence of asymmetric PTMs on the canonical STAT3 pathway.

We started by characterizing STAT3-/- HeLa cells recently developed in Herrera´s laboratory. As expected, STAT3-/- cells did not express STAT3 protein. However, we observed that WT HeLa cells presented levels of phosphorylated STAT3 at Y705 in the absence of LIF stimulus (**Figure 4.1A**). This could be explained by the fact that HeLa cells were not subjected to serum starvation prior to protein extraction, and fetal bovine serum used is rich in growth factors and cytokines. Therefore, WT HeLa cells presented heterogeneous pools of Y705-phosphorylated and -unphosphorylated STAT3. Removal of serum 2 hours before cytokine stimuli seemed to decrease substantially the basal levels of phospho-STAT3 **(Figure 4.4)**.

STAT3 knockout did not impact HeLa cell proliferation (**Figure 4.1B**). Previous reports indicated that STAT3 promotes the expression of genes involved in cell proliferation such as *CCND1* and *c-MYC* and has been shown to be essential for the proliferation of cutaneous squamous cell carcinoma cell lines, glioblastoma stem cells, and other cell lines **[147]–[149]**. However, other studies show that STAT3 expression does not necessarily correlate with cell proliferation and can even inhibit proliferation of specific cell types **[150], [151]**. Consistently, STAT3 deletion did not change the expression of *c-MYC* in HeLa cells (**Figure 4.2**), which could explain the similar levels of proliferation between WT and STAT3-/- cells.

STAT3 knockout increased intracellular oxidative stress (**Figure 4.1C**), which is consistent with the role of STAT3 on ROS homeostasis. As mentioned in **section 1.1.4.**, both nuclear and mitochondrial STAT3 can reduce ROS production and increase ROS scavenging in different cellular contexts. The increased oxidative stress in STAT3-/- cells could correlate to the slightly decrease of *GPX1* expression in the same cell line (**Figure 4.2**). *GPX1* encodes for the enzyme glutathione peroxidase 1 which main role is to protect the organism from oxidative damage **[152]**. Since STAT3-/- cells have less *GPX1*, they could be more susceptible to oxidative damage and thus have an increase in oxidative stress comparing to the WT cells. The increased intracellular oxidative stress in STAT3-/- cells could also be due to the significant higher expression of *IGFBP3* in this cell line compared to WT cells (**Figure 4.2**). Overexpression of *IGFBP3* increases production of ROS, potentiating oxidative stress **[153], [154]**. Moreover, the mechanism by which *IGFBP3* increases ROS production may involve, at least in part, decreased STAT3 activation because overexpression of *IGFBP3* leads to a decrease in pSTAT3 levels and an increase in SOCS3 levels, which is one of the negative regulators of STAT3 **[154]**. On the contrary, STAT3 knockout did not alter significantly the mitochondrial oxidative stress (**Figure 4.1D**). Since the staining used was specific for mitochondrial superoxide radicals, these results could suggest that the elevated intracellular ROS in STAT3-/- cells were produced by sources other than the mitochondria or that the ROS altered are other than superoxide radicals. These results are preliminary and need confirmation, but we could also carry out experiments with the Dihydroethidium (DHE) staining which also detects specifically superoxide radicals from any source. However, the fact that superoxide radicals are not increased could be explained by the higher expression of *SOD1* and *SOD2* in STAT3-/- cells (**Figure 4.2**). SOD1 protein is localized in the

cytosol, in the intermembrane space of the mitochondria and in the nucleus, while SOD2 is only expressed in the mitochondria. Both proteins efficiently convert superoxide to the less reactive hydrogen peroxide, which can freely diffuse across the mitochondrial membrane, decreasing mitochondrial oxidative stress **[155], [156]**. The elevated intracellular oxidative stress of STAT3-/- cells did not lead to ER stress or mitochondrial dysfunction (**Figure 4.3**). There is a tendency for higher levels of calnexin and VDAC in STAT3-/- cells, but further assays are needed to confirm this tendency. Also, other assays measuring the levels of other proteins involved in ER and mitochondrial stress/dysfunction should be measure (e.g., phosphorylated PERK, ATF6 and mtHSP60). Since oxidative stress can trigger ER stress by affecting the protein folding process **[145]**, it could be expected a more significant difference in the levels of pIRE1 and calnexin between WT and STAT3-/- cells. Both pIRE1 and calnexin help in decreasing ER stress: pIRE1 as a part of the UPR and calnexin as a chaperone contributing to the reduction of misfolded proteins in the ER **[145]**. Oxidative stress can also trigger mitochondrial dysfunction and lead to necrosis and apoptosis **[157]**. Levels of VDAC are related to apoptosis since up-regulation of VDAC promotes mitochondria-mediated apoptosis in several cell lines **[158]**. In our work, VDAC levels were similar between WT and STAT3-/- cells, suggesting that the oxidative stress observed did not correlate with mitochondrial dysfunction and apoptosis. This is consistent to the similar levels of mitochondrial membrane potential between both cell lines (**Figure 4.1G**). If VDAC was up-regulated in STAT3-/- cells, a significant decrease in the mitochondrial membrane potential was expected, according to literature **[159]**. It was not possible to recover from oxidative stress by transfecting STAT3-/- HeLa cells with a wild type STAT3 plasmid (**Figure 4.6B**). Since the knockout of STAT3 increased the production of ROS (**Figure 4.1C**), it was expected that the restoring of STAT3 in the cells would lower the levels of ROS to similar ROS levels of WT HeLa cells.

STAT3 knockout slightly decreased intracellular and mitochondrial Ca^{2+} levels, but the decrease was not statistically significant (**Figures 4.1E and 4.1F**). The data about intracellular Ca^{2+} levels must be interpreted with caution because further optimization of the protocol is needed. According to literature, it was expected that the WT HeLa cells presented lower levels of mitochondrial Ca^{2+} comparing to the STAT3-/- cells because STAT3-mediated IP3R3 downregulation in the ER prevents the release of Ca^{2+} into the mitochondria **[82]**. Nevertheless, previous studies also demonstrate that STAT3 must be phosphorylated at S727 to degrade IP3R3 and regulate Ca^{2+} efflux from the ER **[82]**. If STAT3 is not phosphorylated at S727 in WT HeLa cells, this could explain the similar levels of mitochondrial Ca^{2+} in both cell lines.

STAT3 knockout significantly reduces the expression of *CCND1* (**Figure 4.2**). This finding is consistent with several studies that report STAT3 as an up-regulator of *CCND1* **[55]**. Consistently, STAT3-/- cells transfected with wild type STAT3 and with STAT3-Y640F plasmids recovered the expression of *CCND1* (**Figure 4.6C**). *BCL2*, *c-MYC*, *SOD1*, *SOD2*, *SLC2A1* and *IGFBP3* were more expressed in STAT3-/- cells than in WT cells but only the increases in *SOD1*, *SLC2A1* and *IGFBP3* were statistically significant (**Figure 4.2**). Since STAT3 up-regulates the expression of *BCL2*, *c-MYC* and *SOD2* **[51], [56], [69], [70]**, it was surprising to find that the knockout of STAT3 did not inhibit the expression of these genes. Possible explanations for this phenomenon might be the absence of cytokine stimuli or functional compensation by other transcriptions factors, such as other STATs. Consistently, previous studies demonstrate that NF-κB can up-regulate *BCL2* **[160]** and *c-MYC* **[161]**, while Sp1 transcription factor is essential for transcription of *SOD2* **[162]**. Interestingly, NF-κB binds to unphosphorylated STAT3 to regulate gene expression **[72]**. The higher expression of *SLC2A1* could be a consequence of *c-MYC* expression since previous studies reported that *c-MYC* induces the expression of *SLC2A1* **[67]**.

After characterization of STAT3-/- HeLa cells, we tested different combinations of Venus-STAT3 BiFC plasmids in this cell line. We observed that Y705 phosphorylation and the subsequent STAT3

accumulation in the nucleus was visible after 20 min of incubation with LIF (**Figure 4.4A**). This is consistent with previous studies that report rapid STAT3 phosphorylation upon only 5 minutes of stimulation with LIF **[163], [164]**. In this work, we assume the possible existence of asymmetric dimers produced from pools of STAT3 molecules with different PTMs. This possibility has been barely studied and literature simply assumes that STAT3 dimers are formed by two identical STAT3 molecules. As described in **section 1.1.5**, STAT3 has several possible PTMs, so it is possible that different STAT3 molecules could have different PTMs, and that these molecules could form dimers with one another, forming symmetric or asymmetric dimers. Moreover, dominant STAT3 mutations have been reported in patients with AD-HIES **[33]**, meaning that mutant and normal STAT3 can coexist in cells, increasing the chances of asymmetric combinations. In this sense, we observed that phosphorylation of only one of the STAT3 monomers is enough to drive STAT3 dimers into the nucleus (**Figure 4.4**). The non-phosphorylated monomer at Y705 can have a single (Y705F) or a double (Y705F/K49R, Y705F/K685R, Y705F/S727A) PTM-resistant mutation and still translocate to the nucleus in response to LIF (**Figure 4.4B**). This contradicts some studies that assume that STAT3 dimers only become active when both monomers are phosphorylated at Y705 **[165]**. Further studies should be carried out to determine if asymmetric STAT3 dimers actually happen in nature, their frequency, and putative roles.

STAT3 dimers are present in the nucleus independently of Y705 phosphorylation and LIF stimulation, but the nuclear levels of unphosphorylated STAT3 do not change substantially in the absence or presence of LIF (**Figure 4.4A)**. The K685R and S727A PTM-resistant mutations, but not the K49R mutation, decreased the accumulation of unphosphorylated STAT3 in the nucleus (**Figure 4.5**). This is consistent to what is described in the literature, since both K685 acetylation and S727 phosphorylation increase STAT3 nuclear localization **[93], [166]**. K49 acetylation is associated to the interaction with p300 and both K49 acetylation and methylation are associated with STAT3-dependent transcription rather than to the translocation of STAT3 to the nucleus **[90], [91], [95]**. Our results contradict the signaling model where STAT3 dimers can only translocate to the nucleus after cytokine stimulation and phosphorylation at Y705 **[46], [165]**. On the other hand, they support the model where STAT3 can shuttle between the cytoplasm and the nucleus independently of cytokine stimulation and phosphorylation at Y705 and is retained in the nucleus upon phosphorylation **[47]–[49]**. This could happen by some unknown mechanism that blocks the export of phosphorylated STAT3 from the nucleus. However, if the stimulation with LIF is prolonged (e.g., for 2 hours), this "blockage" could fade and STAT3 dimers can exit the nucleus easily. Consistently, Dr. Mickael Diallo, a post-doc investigator in Herrera's laboratory has observed, by using Venus-STAT3 BiFC dimers, that after stimulation with LIF there is an increase of fluorescence in the nucleus compared to the fluorescence in the cytoplasm. He also observed that there is still fluorescence in the cytoplasm indicating that not all STAT3 dimers accumulate in the nucleus after stimulation with LIF (**data not published**).

The disease-related mutation Y640F was studied to observe if it could influence the nuclear translocation of STAT3, the intracellular oxidative stress and gene expression in STAT3-/- HeLa cells. The mutation Y640F increases the accumulation of STAT3 in the nucleus in response to LIF (**Figure 4.6A**). This is consistent with a previous study that reports that the Y640F mutation enhances STAT3 phosphorylation at Y705 by preventing phosphorylation at Y640, resulting in an increased formation and stability of STAT3 homodimers **[84]**. The same study also demonstrated that even when the cells are not stimulated, a significant fraction of STAT3 is constitutively phosphorylated and dimerized when carrying the mutation Y640F **[84]**. In our hands, however, the symmetric Y640F mutant dimer is barely phosphorylated at Y705 in the absence of LIF stimulation (**Figure 4.6A**). LIF-dependent nuclear accumulation of symmetric Y640F dimers was prevented by the introduction of the Y705F mutation, indicating that STAT3-Y640F nuclear accumulation is dependent on Y705 phosphorylation.

Transfection of STAT3-/- cells with STAT3-Y640F did not produce significantly higher intracellular oxidative stress than the transfection with the wild type STAT3 version (**Figure 4.6B**). This was not expected, since it was previously observed an increase in oxidative stress in T-LGL leukemia patients' cells harboring STAT3 Y640F mutation compared with both healthy controls and patients without STAT3 mutations **[167]**. We also observed that the mutation Y640F does not influence the transcriptional activity of STAT3, or the expression alterations observed in the gene set studied in this work (**Figure 4.6C)**. Consistently, an Electrophoretic Mobility Shift Assay (EMSA) performed by Dr. Sandra Viegas, a collaborator from ITQB (Oeiras, Portugal) has shown that mutant Y640F symmetric STAT3 dimers did not bind to DNA at the same level as wild type symmetric STAT3 dimers (**data not published**). It could be interesting to analyze the same genes in the presence of LIF stimulus, to determine if the Y640F mutation influences the canonical STAT3 pathway.

VI. Conclusions

In this work we showed that:

1. STAT3 knockout increases oxidative stress and alters gene expression in HeLa cells.
2. Phosphorylation of only one of the STAT3 monomers is enough to drive STAT3 dimers into the nucleus after LIF stimulation.
3. STAT3 dimers can accumulate in the nucleus independently of their phosphorylation status at Y705 and LIF stimulation.
4. The Y640F disease-related mutation increases the accumulation of STAT3 in the nucleus in response to LIF but is not related to oxidative stress and gene expression.

Our results advance our understanding of STAT3 signaling and could potentially contribute to the study of several human pathologies involving STAT3, such as cancer, hyper-IgE Syndrome, or Inflammatory Hepatocellular Adenoma.

Further studies using other mutations that prevent key PTMs such as T236A and T714A should be considered to continue the study of how PTMs can influence STAT3 behavior and function.

References

[1] G. R. Stark and J. E. Darnell, "The JAK-STAT Pathway at Twenty," *Immunity*, vol. 36, no. 4, pp. 503–514, Apr. 2012, doi: 10.1016/j.immuni.2012.03.013.

[2] C. P. Lim and X. Cao, "Structure, function, and regulation of STAT proteins," *Mol. Biosyst.*, vol. 2, no. 11, p. 536, 2006, doi: 10.1039/b606246f.

[3] Y. Verhoeven *et al.*, "The potential and controversy of targeting STAT family members in cancer," *Semin. Cancer Biol.*, vol. 60, pp. 41–56, Feb. 2020, doi: 10.1016/j.semcancer.2019.10.002.

[4] R. P. Sharma, C. Rosen, J. K. Melbourne, B. Feiner, and K. A. Chase, "Activated Phosphorylated STAT1 Levels as a Biologically Relevant Immune Signal in Schizophrenia," *Neuroimmunomodulation*, vol. 23, no. 4, pp. 224–229, 2016, doi: 10.1159/000450581.

[5] Z. Hojati, M. Kay, and F. Dehghanian, "Mechanism of Action of Interferon Beta in Treatment of Multiple Sclerosis," in *Multiple Sclerosis*, Elsevier, 2016, pp. 365–392. doi: 10.1016/B978-0-12-800763-1.00015-4.

[6] J. F. Bromberg, "Activation of STAT proteins and growth control," *BioEssays News Rev. Mol. Cell. Dev. Biol.*, vol. 23, no. 2, pp. 161–169, Feb. 2001, doi: 10.1002/1521-1878(200102)23:2<161::AID-BIES1023>3.0.CO;2-0.

[7] G. S. Campbell, D. J. Meyer, R. Raz, D. E. Levy, J. Schwartz, and C. Carter-Su, "Activation of Acute Phase Response Factor (APRF)/Stat3 Transcription Factor by Growth Hormone," *J. Biol. Chem.*, vol. 270, no. 8, pp. 3974–3979, Feb. 1995, doi: 10.1074/jbc.270.8.3974.

[8] L. DaSilva *et al.*, "Prolactin recruits STAT1, STAT3 and STAT5 independent of conserved receptor tyrosines TYR402, TYR479, TYR515 and TYR580," *Mol. Cell. Endocrinol.*, vol. 117, no. 2, pp. 131–140, Mar. 1996, doi: 10.1016/0303-7207(95)03738-1.

[9] C. W. Schindler, "Series Introduction: JAK-STAT signaling in human disease," *J. Clin. Invest.*, vol. 109, no. 9, pp. 1133–1137, May 2002, doi: 10.1172/JCI0215644.

[10] J. Yuan, F. Zhang, and R. Niu, "Multiple regulation pathways and pivotal biological functions of STAT3 in cancer," *Sci. Rep.*, vol. 5, no. 1, p. 17663, Nov. 2016, doi: 10.1038/srep17663.

[11] D. E. Levy and C. Lee, "What does Stat3 do?," *J. Clin. Invest.*, vol. 109, no. 9, pp. 1143–1148, May 2002, doi: 10.1172/JCI0215650.

[12] E. B. Haura, J. Turkson, and R. Jove, "Mechanisms of Disease: insights into the emerging role of signal transducers and activators of transcription in cancer," *Nat. Clin. Pract. Oncol.*, vol. 2, no. 6, pp. 315–324, Jun. 2005, doi: 10.1038/ncponc0195.

[13] K. Takeda *et al.*, "Targeted disruption of the mouse Stat3 gene leads to early embryonic lethality," *Proc. Natl. Acad. Sci.*, vol. 94, no. 8, pp. 3801–3804, Apr. 1997, doi: 10.1073/pnas.94.8.3801.

[14] A. C. Guanizo, C. D. Fernando, D. J. Garama, and D. J. Gough, "STAT3: a multifaceted oncoprotein," *Growth Factors*, vol. 36, no. 1–2, pp. 1–14, Mar. 2018, doi: 10.1080/08977194.2018.1473393.

[15] M. Boudný and M. Trbušek, "The Important Role of STAT3 in Chronic Lymphocytic Leukaemia Biology," *Klin. Onkol.*, vol. 33, no. 1, Feb. 2020, doi: 10.14735/amko202032.

[16] G. Niu *et al.*, "Role of Stat3 in Regulating p53 Expression and Function," *Mol. Cell. Biol.*, vol. 25, no. 17, pp. 7432–7440, Sep. 2005, doi: 10.1128/MCB.25.17.7432-7440.2005.

[17] H. Yu and R. Jove, "The STATs of cancer — new molecular targets come of age," *Nat. Rev. Cancer*, vol. 4, no. 2, pp. 97–105, Feb. 2004, doi: 10.1038/nrc1275.

[18] T. Xie *et al.*, "Stat3 activation regulates the expression of matrix metalloproteinase-2 and tumor invasion and metastasis," *Oncogene*, vol. 23, no. 20, pp. 3550–3560, Apr. 2004, doi: 10.1038/sj.onc.1207383.

[19] M. Shi *et al.*, "Catecholamine up-regulates MMP-7 expression by activating AP-1 and STAT3 in gastric cancer," *Mol. Cancer*, vol. 9, no. 1, p. 269, Dec. 2010, doi: 10.1186/1476-4598-9-269.

[20] A. Ecker, "The dark and the bright side of Stat3: proto-oncogene and tumor-suppressor," *Front. Biosci.*, vol. Volume, no. 14, p. 2944, 2009, doi: 10.2741/3425.

[21] N. de la Iglesia *et al.*, "Identification of a PTEN-regulated STAT3 brain tumor suppressor pathway," *Genes Dev.*, vol. 22, no. 4, pp. 449–462, Feb. 2008, doi: 10.1101/gad.1606508.

[22] H. L. M. Koskela *et al.*, "Somatic *STAT3* Mutations in Large Granular Lymphocytic Leukemia," *N. Engl. J. Med.*, vol. 366, no. 20, pp. 1905–1913, May 2012, doi: 10.1056/NEJMoa1114885.

[23] C. Pilati *et al.*, "Somatic mutations activating STAT3 in human inflammatory hepatocellular adenomas," *J. Exp. Med.*, vol. 208, no. 7, pp. 1359–1366, Jul. 2011, doi: 10.1084/jem.20110283.

[24] C. Woellner *et al.*, "Mutations in STAT3 and diagnostic guidelines for hyper-IgE syndrome," *J. Allergy Clin. Immunol.*, vol. 125, no. 2, pp. 424-432.e8, Feb. 2010, doi: 10.1016/j.jaci.2009.10.059.

[25] T. Lamy, A. Moignet, and T. P. Loughran, "LGL leukemia: from pathogenesis to treatment," *Blood*, vol. 129, no. 9, pp. 1082–1094, Mar. 2017, doi: 10.1182/blood-2016-08-692590.

[26] M. Sakata-Yanagimoto, T. Enami, Y. Yokoyama, and S. Chiba, "Disease-specific mutations in mature lymphoid neoplasms: Recent advances," *Cancer Sci.*, vol. 105, no. 6, pp. 623–629, Jun. 2014, doi: 10.1111/cas.12408.

[27] R. Suzuki *et al.*, "Aggressive natural killer-cell leukemia revisited: large granular lymphocyte leukemia of cytotoxic NK cells," *Leukemia*, vol. 18, no. 4, pp. 763–770, Apr. 2004, doi: 10.1038/sj.leu.2403262.

[28] M. V. Shah, C. C. Hook, T. G. Call, and R. S. Go, "A population-based study of large granular lymphocyte leukemia," *Blood Cancer J.*, vol. 6, no. 8, pp. e455–e455, Aug. 2016, doi: 10.1038/bcj.2016.59.

[29] K. C. Olson *et al.*, "Large granular lymphocyte leukemia serum and corresponding hematological parameters reveal unique cytokine and sphingolipid biomarkers and associations with STAT3 mutations," *Cancer Med.*, vol. 9, no. 18, pp. 6533–6549, Sep. 2020, doi: 10.1002/cam4.3246.

[30] A.-L. Védie, O. Sutter, M. Ziol, and J.-C. Nault, "Molecular classification of hepatocellular

adenomas: impact on clinical practice," *Hepatic Oncol.*, vol. 5, no. 1, p. HEP04, Jan. 2018, doi: 10.2217/hep-2017-0023.

[31] M. G. Thomeer *et al.*, "Hepatocellular adenoma: when and how to treat? Update of current evidence," *Ther. Adv. Gastroenterol.*, vol. 9, no. 6, pp. 898–912, Nov. 2016, doi: 10.1177/1756283X16663882.

[32] T. Al-Shaikhly and H. D. Ochs, "Hyper IgE syndromes: clinical and molecular characteristics," *Immunol. Cell Biol.*, vol. 97, no. 4, pp. 368–379, Apr. 2019, doi: 10.1111/imcb.12209.

[33] T. P. Vogel, J. D. Milner, and M. A. Cooper, "The Ying and Yang of STAT3 in Human Disease," *J. Clin. Immunol.*, vol. 35, no. 7, pp. 615–623, Oct. 2015, doi: 10.1007/s10875-015-0187-8.

[34] W. Hafsi and S. N. Yarrarapu, "Job Syndrome," *StatPearls*, Aug. 2021, Accessed: Sep. 04, 2021. [Online]. Available: https://www.statpearls.com/ArticleLibrary/viewarticle/23814

[35] D. Maritano *et al.*, "The STAT3 isoforms α and β have unique and specific functions," *Nat. Immunol.*, vol. 5, no. 4, pp. 401–409, Apr. 2004, doi: 10.1038/ni1052.

[36] M. Hiller *et al.*, "Phylogenetically widespread alternative splicing at unusal GYNGYN donors," *Genome Biol.*, vol. 7, no. 7, p. R65, 2006, doi: 10.1186/gb-2006-7-7-r65.

[37] K. B. Turton, D. S. Annis, L. Rui, S. Esnault, and D. F. Mosher, "Ratios of Four STAT3 Splice Variants in Human Eosinophils and Diffuse Large B Cell Lymphoma Cells," *PLOS ONE*, vol. 10, no. 5, p. e0127243, May 2015, doi: 10.1371/journal.pone.0127243.

[38] D. L. Hevehan, W. M. Miller, and E. T. Papoutsakis, "Differential expression and phosphorylation of distinct STAT3 proteins during granulocytic differentiation," *Blood*, vol. 99, no. 5, pp. 1627–1637, Mar. 2002, doi: 10.1182/blood.V99.5.1627.

[39] J.-Y. Yoo, D. L. Huso, D. Nathans, and S. Desiderio, "Specific Ablation of Stat3β Distorts the Pattern of Stat3-Responsive Gene Expression and Impairs Recovery from Endotoxic Shock," *Cell*, vol. 108, no. 3, pp. 331–344, Feb. 2002, doi: 10.1016/S0092-8674(02)00636-0.

[40] M. Zheng *et al.*, "A mix of S and ΔS variants of STAT3 enable survival of activated B-cell-like diffuse large B-cell lymphoma cells in culture," *Oncogenesis*, vol. 5, no. 1, pp. e184–e184, Jan. 2016, doi: 10.1038/oncsis.2015.44.

[41] A. Chakraborty and D. J. Tweardy, "Granulocyte colony-stimulating factor activates a 72-kDa isoform of STAT3 in human neutrophils," *J. Leukoc. Biol.*, vol. 64, no. 5, pp. 675–680, Nov. 1998, doi: 10.1002/jlb.64.5.675.

[42] F. Zhu, K. B. Wang, and L. Rui, "STAT3 Activation and Oncogenesis in Lymphoma," *Cancers*, vol. 12, no. 1, p. 19, Dec. 2019, doi: 10.3390/cancers12010019.

[43] S. Becker, B. Groner, and C. W. Müller, "Three-dimensional structure of the Stat3β homodimer bound to DNA," *Nature*, vol. 394, no. 6689, pp. 145–151, Jul. 1998, doi: 10.1038/28101.

[44] W. X. Li, "Canonical and non-canonical JAK–STAT signaling," *Trends Cell Biol.*, vol. 18, no. 11, pp. 545–551, Nov. 2008, doi: 10.1016/j.tcb.2008.08.008.

[45] D. Guschin *et al.*, "A major role for the protein tyrosine kinase JAK1 in the JAK/STAT signal

transduction pathway in response to interleukin-6," *EMBO J.*, vol. 14, no. 7, pp. 1421–1429, Apr. 1995.

[46] J. Ma and X. Cao, "Regulation of Stat3 nuclear import by importin α5 and importin α7 via two different functional sequence elements," *Cell. Signal.*, vol. 18, no. 8, pp. 1117–1126, Aug. 2006, doi: 10.1016/j.cellsig.2005.06.016.

[47] A. L. Pranada, S. Metz, A. Herrmann, P. C. Heinrich, and G. Müller-Newen, "Real Time Analysis of STAT3 Nucleocytoplasmic Shuttling," *J. Biol. Chem.*, vol. 279, no. 15, pp. 15114–15123, Apr. 2004, doi: 10.1074/jbc.M312530200.

[48] T. Meyer and U. Vinkemeier, "Nucleocytoplasmic shuttling of STAT transcription factors," *Eur. J. Biochem.*, vol. 271, no. 23–24, pp. 4606–4612, Dec. 2004, doi: 10.1111/j.1432-1033.2004.04423.x.

[49] A. Herrmann *et al.*, "Nucleocytoplasmic shuttling of persistently activated STAT3," *J. Cell Sci.*, vol. 120, no. 18, pp. 3249–3261, Sep. 2007, doi: 10.1242/jcs.03482.

[50] U. Graf, E. A. Casanova, and P. Cinelli, "The Role of the Leukemia Inhibitory Factor (LIF) — Pathway in Derivation and Maintenance of Murine Pluripotent Stem Cells," *Genes*, vol. 2, no. 1, pp. 280–297, Mar. 2011, doi: 10.3390/genes2010280.

[51] P. J. Real, A. Sierra, A. de Juan, J. C. Segovia, J. M. Lopez-Vega, and J. L. Fernandez-Luna, "Resistance to chemotherapy via Stat3-dependent overexpression of Bcl-2 in metastatic breast cancer cells," *Oncogene*, vol. 21, no. 50, pp. 7611–7618, Oct. 2002, doi: 10.1038/sj.onc.1206004.

[52] R. Catlett-Falcone *et al.*, "Constitutive Activation of Stat3 Signaling Confers Resistance to Apoptosis in Human U266 Myeloma Cells," *Immunity*, vol. 10, no. 1, pp. 105–115, Jan. 1999, doi: 10.1016/S1074-7613(00)80011-4.

[53] P. K. Epling-Burnette *et al.*, "Inhibition of STAT3 signaling leads to apoptosis of leukemic large granular lymphocytes and decreased Mcl-1 expression," *J. Clin. Invest.*, vol. 107, no. 3, pp. 351–362, Feb. 2001, doi: 10.1172/JCI9940.

[54] T. Gritsko *et al.*, "Persistent Activation of Stat3 Signaling Induces Survivin Gene Expression and Confers Resistance to Apoptosis in Human Breast Cancer Cells," *Clin. Cancer Res.*, vol. 12, no. 1, pp. 11–19, Jan. 2006, doi: 10.1158/1078-0432.CCR-04-1752.

[55] D. Sinibaldi, W. Wharton, J. Turkson, T. Bowman, W. J. Pledger, and R. Jove, "Induction of p21WAF1/CIP1 and cyclin D1 expression by the Src oncoprotein in mouse fibroblasts: role of activated STAT3 signaling," *Oncogene*, vol. 19, no. 48, pp. 5419–5427, Nov. 2000, doi: 10.1038/sj.onc.1203947.

[56] N. Kiuchi *et al.*, "STAT3 Is Required for the gp130-mediated Full Activation of the c-myc Gene," *J. Exp. Med.*, vol. 189, no. 1, pp. 63–73, Jan. 1999, doi: 10.1084/jem.189.1.63.

[57] G. Niu *et al.*, "Constitutive Stat3 activity up-regulates VEGF expression and tumor angiogenesis," *Oncogene*, vol. 21, no. 13, pp. 2000–2008, Mar. 2002, doi: 10.1038/sj.onc.1205260.

[58] R. Carpenter and H.-W. Lo, "STAT3 Target Genes Relevant to Human Cancers," *Cancers*, vol. 6, no. 2, pp. 897–925, Apr. 2014, doi: 10.3390/cancers6020897.

[59] M. Narimatsu *et al.*, "Tissue-Specific Autoregulation of the *stat3* Gene and Its Role in Interleukin-6-Induced Survival Signals in T Cells," *Mol. Cell. Biol.*, vol. 21, no. 19, pp. 6615–6625, Oct. 2001, doi: 10.1128/MCB.21.19.6615-6625.2001.

[60] M. Diallo and F. Herrera, "The role of understudied post-translational modifications for the behavior and function of Signal Transducer and Activator of Transcription 3," *FEBS J.*, p. febs.16116, Jul. 2021, doi: 10.1111/febs.16116.

[61] R. Starr *et al.*, "A family of cytokine-inducible inhibitors of signalling," *Nature*, vol. 387, no. 6636, pp. 917–921, Jun. 1997, doi: 10.1038/43206.

[62] D. L. Krebs and D. J. Hilton, "SOCS Proteins: Negative Regulators of Cytokine Signaling," *STEM CELLS*, vol. 19, no. 5, pp. 378–387, Sep. 2001, doi: 10.1634/stemcells.19-5-378.

[63] C. D. Chung *et al.*, "Specific Inhibition of Stat3 Signal Transduction by PIAS3," *Science*, vol. 278, no. 5344, pp. 1803–1805, Dec. 1997, doi: 10.1126/science.278.5344.1803.

[64] D. Xu, "Protein tyrosine phosphatases in the JAK/STAT pathway," *Front. Biosci.*, vol. Volume, no. 13, p. 4925, 2008, doi: 10.2741/3051.

[65] M. Demaria *et al.*, "A STAT3-mediated metabolic switch is involved in tumour transformation and STAT3 addiction," *Aging*, vol. 2, no. 11, pp. 823–842, Nov. 2010, doi: 10.18632/aging.100232.

[66] P. Vaupel and G. Multhoff, "Revisiting the Warburg effect: historical dogma *versus* current understanding," *J. Physiol.*, vol. 599, no. 6, pp. 1745–1757, Mar. 2021, doi: 10.1113/JP278810.

[67] R. C. Osthus *et al.*, "Deregulation of Glucose Transporter 1 and Glycolytic Gene Expression by c-Myc," *J. Biol. Chem.*, vol. 275, no. 29, pp. 21797–21800, Jul. 2000, doi: 10.1074/jbc.C000023200.

[68] J. Kim, P. Gao, Y.-C. Liu, G. L. Semenza, and C. V. Dang, "Hypoxia-Inducible Factor 1 and Dysregulated c-Myc Cooperatively Induce Vascular Endothelial Growth Factor and Metabolic Switches Hexokinase 2 and Pyruvate Dehydrogenase Kinase 1," *Mol. Cell. Biol.*, vol. 27, no. 21, pp. 7381–7393, Nov. 2007, doi: 10.1128/MCB.00440-07.

[69] D. J. Dauer *et al.*, "Stat3 regulates genes common to both wound healing and cancer," *Oncogene*, vol. 24, no. 21, pp. 3397–3408, May 2005, doi: 10.1038/sj.onc.1208469.

[70] J. E. Jung, G. S. Kim, P. Narasimhan, Y. S. Song, and P. H. Chan, "Regulation of Mn-Superoxide Dismutase Activity and Neuroprotection by STAT3 in Mice after Cerebral Ischemia," *J. Neurosci.*, vol. 29, no. 21, pp. 7003–7014, May 2009, doi: 10.1523/JNEUROSCI.1110-09.2009.

[71] J. Srivastava and J. DiGiovanni, "Non-canonical Stat3 signaling in cancer," *Mol. Carcinog.*, vol. 55, no. 12, pp. 1889–1898, Dec. 2016, doi: 10.1002/mc.22438.

[72] J. Yang, X. Liao, M. K. Agarwal, L. Barnes, P. E. Auron, and G. R. Stark, "Unphosphorylated STAT3 accumulates in response to IL-6 and activates transcription by binding to NFκB," *Genes Dev.*, vol. 21, no. 11, pp. 1396–1408, Jun. 2007, doi: 10.1101/gad.1553707.

[73] P. Tammineni, C. Anugula, F. Mohammed, M. Anjaneyulu, A. C. Larner, and N. B. V. Sepuri, "The Import of the Transcription Factor STAT3 into Mitochondria Depends on GRIM-19, a Component of the Electron Transport Chain," *J. Biol. Chem.*, vol. 288, no. 7, pp. 4723–4732, Feb. 2013, doi: 10.1074/jbc.M112.378984.

[74] R. Cocchiola *et al.*, "STAT3 Post-Translational Modifications Drive Cellular Signaling Pathways in Prostate Cancer Cells," *Int. J. Mol. Sci.*, vol. 20, no. 8, p. 1815, Apr. 2019, doi: 10.3390/ijms20081815.

[75] K. Boengler, D. Hilfiker-Kleiner, G. Heusch, and R. Schulz, "Inhibition of permeability transition pore opening by mitochondrial STAT3 and its role in myocardial ischemia/reperfusion," *Basic Res. Cardiol.*, vol. 105, no. 6, pp. 771–785, Nov. 2010, doi: 10.1007/s00395-010-0124-1.

[76] J. A. Meier *et al.*, "Stress-induced dynamic regulation of mitochondrial STAT3 and its association with cyclophilin D reduce mitochondrial ROS production," *Sci. Signal.*, vol. 10, no. 472, p. eaag2588, Mar. 2017, doi: 10.1126/scisignal.aag2588.

[77] V. Poli and A. Camporeale, "STAT3-Mediated Metabolic Reprograming in Cellular Transformation and Implications for Drug Resistance," *Front. Oncol.*, vol. 5, Jun. 2015, doi: 10.3389/fonc.2015.00121.

[78] R. Yang *et al.*, "Mitochondrial Ca2+ and membrane potential, an alternative pathway for Interleukin 6 to regulate CD4 cell effector function," *eLife*, vol. 4, p. e06376, May 2015, doi: 10.7554/eLife.06376.

[79] K.-S. Chun, J.-H. Jang, and D.-H. Kim, "Perspectives Regarding the Intersections between STAT3 and Oxidative Metabolism in Cancer," *Cells*, vol. 9, no. 10, p. 2202, Sep. 2020, doi: 10.3390/cells9102202.

[80] D. J. Garama *et al.*, "A Synthetic Lethal Interaction between Glutathione Synthesis and Mitochondrial Reactive Oxygen Species Provides a Tumor-Specific Vulnerability Dependent on STAT3," *Mol. Cell. Biol.*, vol. 35, no. 21, pp. 3646–3656, Nov. 2015, doi: 10.1128/MCB.00541-15.

[81] Y. Su, X. Huang, Z. Huang, T. Huang, Y. Xu, and C. Yi, "STAT3 Localizes in Mitochondria-Associated ER Membranes Instead of in Mitochondria," *Front. Cell Dev. Biol.*, vol. 8, p. 274, Apr. 2020, doi: 10.3389/fcell.2020.00274.

[82] L. Avalle *et al.*, "STAT3 localizes to the ER, acting as a gatekeeper for ER-mitochondrion Ca2+ fluxes and apoptotic responses," *Cell Death Differ.*, vol. 26, no. 5, pp. 932–942, May 2019, doi: 10.1038/s41418-018-0171-y.

[83] P. V. Hornbeck, B. Zhang, B. Murray, J. M. Kornhauser, V. Latham, and E. Skrzypek, "PhosphoSitePlus, 2014: mutations, PTMs and recalibrations," *Nucleic Acids Res.*, vol. 43, no. D1, pp. D512–D520, Jan. 2015, doi: 10.1093/nar/gku1267.

[84] R. Mori *et al.*, "TYK2-induced phosphorylation of Y640 suppresses STAT3 transcriptional activity," *Sci. Rep.*, vol. 7, no. 1, p. 15919, Dec. 2017, doi: 10.1038/s41598-017-15912-6.

[85] J. Sasse *et al.*, "Mutational analysis of acute-phase response factor/Stat3 activation and dimerization," *Mol. Cell. Biol.*, vol. 17, no. 8, pp. 4677–4686, Aug. 1997, doi: 10.1128/MCB.17.8.4677.

[86] M. Shi *et al.*, "STAT3 mutation and its clinical and histopathologic correlation in T-cell large granular lymphocytic leukemia," *Hum. Pathol.*, vol. 73, pp. 74–81, Mar. 2018, doi: 10.1016/j.humpath.2017.12.014.

[87] M. S. Waitkus *et al.*, "Signal Integration and Gene Induction by a Functionally Distinct STAT3

Phosphoform," *Mol. Cell. Biol.*, vol. 34, no. 10, pp. 1800–1811, May 2014, doi: 10.1128/MCB.00034-14.

[88] J. Wu *et al.*, "Clinical Manifestations and Genetic Analysis of 17 Patients with Autosomal Dominant Hyper-IgE Syndrome in Mainland China: New Reports and a Literature Review," *J. Clin. Immunol.*, vol. 37, no. 2, pp. 166–179, Feb. 2017, doi: 10.1007/s10875-017-0369-7.

[89] J. G. Tate *et al.*, "COSMIC: the Catalogue Of Somatic Mutations In Cancer," *Nucleic Acids Res.*, vol. 47, no. D1, pp. D941–D947, Jan. 2019, doi: 10.1093/nar/gky1015.

[90] S. Ray, I. Boldogh, and A. R. Brasier, "STAT3 NH2-Terminal Acetylation Is Activated by the Hepatic Acute-Phase Response and Required for IL-6 Induction of Angiotensinogen," *Gastroenterology*, vol. 129, no. 5, pp. 1616–1632, Nov. 2005, doi: 10.1053/j.gastro.2005.07.055.

[91] T. Hou, S. Ray, C. Lee, and A. R. Brasier, "The STAT3 NH2-terminal Domain Stabilizes Enhanceosome Assembly by Interacting with the p300 Bromodomain," *J. Biol. Chem.*, vol. 283, no. 45, pp. 30725–30734, Nov. 2008, doi: 10.1074/jbc.M805941200.

[92] Z. Yuan, Y. Guan, D. Chatterjee, and Y. E. Chin, "Stat3 Dimerization Regulated by Reversible Acetylation of a Single Lysine Residue," *Science*, vol. 307, no. 5707, pp. 269–273, Jan. 2005, doi: 10.1126/science.1105166.

[93] R. Wang, P. Cherukuri, and J. Luo, "Activation of Stat3 Sequence-specific DNA Binding and Transcription by p300/CREB-binding Protein-mediated Acetylation," *J. Biol. Chem.*, vol. 280, no. 12, pp. 11528–11534, Mar. 2005, doi: 10.1074/jbc.M413930200.

[94] Y. Belo *et al.*, "Unexpected implications of STAT3 acetylation revealed by genetic encoding of acetyl-lysine," *Biochim. Biophys. Acta BBA - Gen. Subj.*, vol. 1863, no. 9, pp. 1343–1350, Sep. 2019, doi: 10.1016/j.bbagen.2019.05.019.

[95] M. Dasgupta, J. K. T. Dermawan, B. Willard, and G. R. Stark, "STAT3-driven transcription depends upon the dimethylation of K49 by EZH2," *Proc. Natl. Acad. Sci.*, vol. 112, no. 13, pp. 3985–3990, Mar. 2015, doi: 10.1073/pnas.1503152112.

[96] J. Yang *et al.*, "Reversible methylation of promoter-bound STAT3 by histone-modifying enzymes," *Proc. Natl. Acad. Sci.*, vol. 107, no. 50, pp. 21499–21504, Dec. 2010, doi: 10.1073/pnas.1016147107.

[97] E. Kim *et al.*, "Phosphorylation of EZH2 Activates STAT3 Signaling via STAT3 Methylation and Promotes Tumorigenicity of Glioblastoma Stem-like Cells," *Cancer Cell*, vol. 23, no. 6, pp. 839–852, Jun. 2013, doi: 10.1016/j.ccr.2013.04.008.

[98] S. Su, Y. Zhang, and P. Liu, "Roles of Ubiquitination and SUMOylation in DNA Damage Response," *Curr. Issues Mol. Biol.*, pp. 59–84, 2020, doi: 10.21775/cimb.035.059.

[99] M. M. Rytinki, S. Kaikkonen, P. Pehkonen, T. Jääskeläinen, and J. J. Palvimo, "PIAS proteins: pleiotropic interactors associated with SUMO," *Cell. Mol. Life Sci.*, vol. 66, no. 18, pp. 3029–3041, Sep. 2009, doi: 10.1007/s00018-009-0061-z.

[100] E. Perry *et al.*, "TMF/ARA160 is a BC-box-containing protein that mediates the degradation of Stat3," *Oncogene*, vol. 23, no. 55, pp. 8908–8919, Nov. 2004, doi: 10.1038/sj.onc.1208149.

[101] T. Tanaka *et al.*, "PDLIM2 Inhibits T Helper 17 Cell Development and Granulomatous Inflammation Through Degradation of STAT3," *Sci. Signal.*, vol. 4, no. 202, Dec. 2011, doi: 10.1126/scisignal.2001637.

[102] S. Ray, Y. Zhao, M. Jamaluddin, C. B. Edeh, C. Lee, and A. R. Brasier, "Inducible STAT3 NH2 terminal mono-ubiquitination promotes BRD4 complex formation to regulate apoptosis," *Cell. Signal.*, vol. 26, no. 7, pp. 1445–1455, Jul. 2014, doi: 10.1016/j.cellsig.2014.03.007.

[103] Z. Zhou *et al.*, "SUMOylation and SENP3 regulate STAT3 activation in head and neck cancer," *Oncogene*, vol. 35, no. 45, pp. 5826–5838, Nov. 2016, doi: 10.1038/onc.2016.124.

[104] G. Duan and D. Walther, "The Roles of Post-translational Modifications in the Context of Protein Interaction Networks," *PLOS Comput. Biol.*, vol. 11, no. 2, p. e1004049, Feb. 2015, doi: 10.1371/journal.pcbi.1004049.

[105] X. Peng, J. Wang, W. Peng, F.-X. Wu, and Y. Pan, "Protein–protein interactions: detection, reliability assessment and applications," *Brief. Bioinform.*, p. bbw066, Jul. 2016, doi: 10.1093/bib/bbw066.

[106] I. Ispolatov, "Binding properties and evolution of homodimers in protein-protein interaction networks," *Nucleic Acids Res.*, vol. 33, no. 11, pp. 3629–3635, Jun. 2005, doi: 10.1093/nar/gki678.

[107] R. Letra-Vilela *et al.*, "Can asymmetric post-translational modifications regulate the behavior of STAT3 homodimers?," *FASEB BioAdvances*, vol. 2, no. 2, pp. 116–125, Feb. 2020, doi: 10.1096/fba.2019-00049.

[108] S. Struk, A. Jacobs, E. Sánchez Martín-Fontecha, K. Gevaert, P. Cubas, and S. Goormachtig, "Exploring the protein-protein interaction landscape in plants: Protein-protein interaction landscape in plants," *Plant Cell Environ.*, vol. 42, no. 2, pp. 387–409, Feb. 2019, doi: 10.1111/pce.13433.

[109] S. Fields and O. Song, "A novel genetic system to detect protein–protein interactions," *Nature*, vol. 340, no. 6230, pp. 245–246, Jul. 1989, doi: 10.1038/340245a0.

[110] A. Brückner, C. Polge, N. Lentze, D. Auerbach, and U. Schlattner, "Yeast Two-Hybrid, a Powerful Tool for Systems Biology," *Int. J. Mol. Sci.*, vol. 10, no. 6, pp. 2763–2788, Jun. 2009, doi: 10.3390/ijms10062763.

[111] A. Paiano, A. Margiotta, M. De Luca, and C. Bucci, "Yeast Two-Hybrid Assay to Identify Interacting Proteins," *Curr. Protoc. Protein Sci.*, vol. 95, no. 1, p. e70, Feb. 2019, doi: 10.1002/cpps.70.

[112] J. De Las Rivas and C. Fontanillo, "Protein-protein interaction networks: unraveling the wiring of molecular machines within the cell," *Brief. Funct. Genomics*, vol. 11, no. 6, pp. 489–496, Nov. 2012, doi: 10.1093/bfgp/els036.

[113] J. J. Li and I. Herskowitz, "Isolation of *ORC6* , a Component of the Yeast Origin Recognition Complex by a One-Hybrid System," *Science*, vol. 262, no. 5141, pp. 1870–1874, Dec. 1993, doi: 10.1126/science.8266075.

[114] U. Putz, "A tri-hybrid system for the analysis and detection of RNA--protein interactions," *Nucleic Acids Res.*, vol. 24, no. 23, pp. 4838–4840, Dec. 1996, doi: 10.1093/nar/24.23.4838.

[115] E. J. Licitra and J. O. Liu, "A three-hybrid system for detecting small ligand-protein receptor interactions," *Proc. Natl. Acad. Sci.*, vol. 93, no. 23, pp. 12817–12821, Nov. 1996, doi: 10.1073/pnas.93.23.12817.

[116] S. Xing, N. Wallmeroth, K. W. Berendzen, and C. Grefen, "Techniques for the analysis of protein-protein interactions in vivo," *Plant Physiol.*, p. pp.00470.2016, Apr. 2016, doi: 10.1104/pp.16.00470.

[117] F. Ciruela, "Fluorescence-based methods in the study of protein–protein interactions in living cells," *Curr. Opin. Biotechnol.*, vol. 19, no. 4, pp. 338–343, Aug. 2008, doi: 10.1016/j.copbio.2008.06.003.

[118] V. S. Rao, K. Srinivas, G. N. Sujini, and G. N. S. Kumar, "Protein-Protein Interaction Detection: Methods and Analysis," *Int. J. Proteomics*, vol. 2014, pp. 1–12, Feb. 2014, doi: 10.1155/2014/147648.

[119] N. Johnsson and A. Varshavsky, "Split ubiquitin as a sensor of protein interactions in vivo.," *Proc. Natl. Acad. Sci.*, vol. 91, no. 22, pp. 10340–10344, Oct. 1994, doi: 10.1073/pnas.91.22.10340.

[120] M. G. Romei and S. G. Boxer, "Split Green Fluorescent Proteins: Scope, Limitations, and Outlook," *Annu. Rev. Biophys.*, vol. 48, no. 1, pp. 19–44, May 2019, doi: 10.1146/annurev-biophys-051013-022846.

[121] M. Morell, S. Ventura, and F. X. Avilés, "Protein complementation assays: Approaches for the in vivo analysis of protein interactions," *FEBS Lett.*, vol. 583, no. 11, pp. 1684–1691, Jun. 2009, doi: 10.1016/j.febslet.2009.03.002.

[122] D. Boassa *et al.*, "Split-miniSOG for Spatially Detecting Intracellular Protein-Protein Interactions by Correlated Light and Electron Microscopy," *Cell Chem. Biol.*, vol. 26, no. 10, pp. 1407-1416.e5, Oct. 2019, doi: 10.1016/j.chembiol.2019.07.007.

[123] P. Li, L. Wang, and L. Di, "Applications of Protein Fragment Complementation Assays for Analyzing Biomolecular Interactions and Biochemical Networks in Living Cells," *J. Proteome Res.*, vol. 18, no. 8, pp. 2987–2998, Aug. 2019, doi: 10.1021/acs.jproteome.9b00154.

[124] I. Ghosh, A. D. Hamilton, and L. Regan, "Antiparallel Leucine Zipper-Directed Protein Reassembly: Application to the Green Fluorescent Protein," *J. Am. Chem. Soc.*, vol. 122, no. 23, pp. 5658–5659, Jun. 2000, doi: 10.1021/ja994421w.

[125] C.-D. Hu, Y. Chinenov, and T. K. Kerppola, "Visualization of Interactions among bZIP and Rel Family Proteins in Living Cells Using Bimolecular Fluorescence Complementation," *Mol. Cell*, vol. 9, no. 4, pp. 789–798, Apr. 2002, doi: 10.1016/S1097-2765(02)00496-3.

[126] F. Herrera, S. Gonçalves, and T. F. Outeiro, "Imaging Protein Oligomerization in Neurodegeneration Using Bimolecular Fluorescence Complementation," in *Methods in Enzymology*, vol. 506, Elsevier, 2012, pp. 157–174. doi: 10.1016/B978-0-12-391856-7.00033-0.

[127] T. K. Kerppola, "Visualization of molecular interactions by fluorescence complementation," *Nat. Rev. Mol. Cell Biol.*, vol. 7, no. 6, pp. 449–456, Jun. 2006, doi: 10.1038/nrm1929.

[128] K. Ohashi, T. Kiuchi, K. Shoji, K. Sampei, and K. Mizuno, "Visualization of cofilin-actin and Ras-Raf interactions by bimolecular fluorescence complementation assays using a new pair of split

Venus fragments," *BioTechniques*, vol. 52, no. 1, pp. 45–50, Jan. 2012, doi: 10.2144/000113777.

[129] Y. Saka, A. I. Hagemann, and J. C. Smith, "Visualizing protein interactions by bimolecular fluorescence complementation in Xenopus," *Methods*, vol. 45, no. 3, pp. 192–195, Jul. 2008, doi: 10.1016/j.ymeth.2008.06.005.

[130] T. Nagai, K. Ibata, E. S. Park, M. Kubota, K. Mikoshiba, and A. Miyawaki, "A variant of yellow fluorescent protein with fast and efficient maturation for cell-biological applications," *Nat. Biotechnol.*, vol. 20, no. 1, pp. 87–90, Jan. 2002, doi: 10.1038/nbt0102-87.

[131] Y. J. Shyu, H. Liu, X. Deng, and C.-D. Hu, "Identification of new fluorescent protein fragments for bimolecular fluorescence complementation analysis under physiological conditions," *BioTechniques*, vol. 40, no. 1, pp. 61–66, Jan. 2006, doi: 10.2144/000112036.

[132] Y. Kodama and C.-D. Hu, "An improved bimolecular fluorescence complementation assay with a high signal-to-noise ratio," *BioTechniques*, vol. 49, no. 5, pp. 793–805, Nov. 2010, doi: 10.2144/000113519.

[133] Y. Kodama and C.-D. Hu, "Bimolecular fluorescence complementation (BiFC): A 5-year update and future perspectives," *BioTechniques*, vol. 53, no. 5, pp. 285–298, Nov. 2012, doi: 10.2144/000113943.

[134] M. Chen, C. Yan, Y. Ma, and X.-E. Zhang, "A tandem near-infrared fluorescence complementation system with enhanced fluorescence for imaging protein–protein interactions in vivo," *Biomaterials*, vol. 268, p. 120544, Jan. 2021, doi: 10.1016/j.biomaterials.2020.120544.

[135] D. Fang and T. K. Kerppola, "Ubiquitin-mediated fluorescence complementation reveals that Jun ubiquitinated by Itch/AIP4 is localized to lysosomes," *Proc. Natl. Acad. Sci.*, vol. 101, no. 41, pp. 14782–14787, Oct. 2004, doi: 10.1073/pnas.0404445101.

[136] J. Branco-Santos *et al.*, "Protein phosphatase 1 regulates huntingtin exon 1 aggregation and toxicity," *Hum. Mol. Genet.*, vol. 26, no. 19, pp. 3763–3775, Oct. 2017, doi: 10.1093/hmg/ddx260.

[137] F. Herrera and T. F. Outeiro, "α-Synuclein modifies huntingtin aggregation in living cells," *FEBS Lett.*, vol. 586, no. 1, pp. 7–12, Jan. 2012, doi: 10.1016/j.febslet.2011.11.019.

[138] W. Chun, G. S. Waldo, and G. V. W. Johnson, "Split GFP complementation assay: a novel approach to quantitatively measure aggregation of tau in situ: effects of GSK3β activation and caspase 3 cleavage," *J. Neurochem.*, vol. 103, no. 6, pp. 2529–2539, Dec. 2007, doi: 10.1111/j.1471-4159.2007.04941.x.

[139] J. Jeong *et al.*, "Monitoring of conformational change in maltose binding protein using split green fluorescent protein," *Biochem. Biophys. Res. Commun.*, vol. 339, no. 2, pp. 647–651, Jan. 2006, doi: 10.1016/j.bbrc.2005.11.056.

[140] A. A. Zamyatnin, A. G. Solovyev, P. V. Bozhkov, J. P. T. Valkonen, S. Yu. Morozov, and E. I. Savenkov, "Assessment of the integral membrane protein topology in living cells," *Plant J.*, vol. 46, no. 1, pp. 145–154, Apr. 2006, doi: 10.1111/j.1365-313X.2006.02674.x.

[141] Y. J. Shyu and C.-D. Hu, "Fluorescence complementation: an emerging tool for biological research," *Trends Biotechnol.*, vol. 26, no. 11, pp. 622–630, Nov. 2008, doi: 10.1016/j.tibtech.2008.07.006.

[142] M. M. Bradford, "A rapid and sensitive method for the quantitation of microgram quantities of protein utilizing the principle of protein-dye binding," *Anal. Biochem.*, vol. 72, no. 1–2, pp. 248–254, May 1976, doi: 10.1016/0003-2697(76)90527-3.

[143] A. Lachmann, H. Xu, J. Krishnan, S. I. Berger, A. R. Mazloom, and A. Ma'ayan, "ChEA: transcription factor regulation inferred from integrating genome-wide ChIP-X experiments," *Bioinformatics*, vol. 26, no. 19, pp. 2438–2444, Oct. 2010, doi: 10.1093/bioinformatics/btq466.

[144] M. Natsuizaka *et al.*, "IGFBP3 promotes esophageal cancer growth by suppressing oxidative stress in hypoxic tumor microenvironment," *Am. J. Cancer Res.*, vol. 4, no. 1, pp. 29–41, 2014.

[145] W. Chong, M. Shastri, and R. Eri, "Endoplasmic Reticulum Stress and Oxidative Stress: A Vicious Nexus Implicated in Bowel Disease Pathophysiology," *Int. J. Mol. Sci.*, vol. 18, no. 4, p. 771, Apr. 2017, doi: 10.3390/ijms18040771.

[146] J. T. Varughese, S. K. Buchanan, and A. S. Pitt, "The Role of Voltage-Dependent Anion Channel in Mitochondrial Dysfunction and Human Disease," *Cells*, vol. 10, no. 7, p. 1737, Jul. 2021, doi: 10.3390/cells10071737.

[147] N. Sumita, T. Bito, K. Nakajima, and C. Nishigori, "Stat3 activation is required for cell proliferation and tumorigenesis but not for cell viability in cutaneous squamous cell carcinoma cell lines," *Exp. Dermatol.*, vol. 15, no. 4, pp. 291–299, Apr. 2006, doi: 10.1111/j.0906-6705.2006.00407.x.

[148] M. M. Sherry, A. Reeves, J. K. Wu, and B. H. Cochran, "STAT3 Is Required for Proliferation and Maintenance of Multipotency in Glioblastoma Stem Cells," *Stem Cells*, vol. 27, no. 10, pp. 2383–2392, Oct. 2009, doi: 10.1002/stem.185.

[149] F. Laudisi, F. Cherubini, G. Monteleone, and C. Stolfi, "STAT3 Interactors as Potential Therapeutic Targets for Cancer Treatment," *Int. J. Mol. Sci.*, vol. 19, no. 6, p. 1787, Jun. 2018, doi: 10.3390/ijms19061787.

[150] V. Caldera, M. Mellai, L. Annovazzi, G. Valente, L. Tessitore, and D. Schiffer, "Stat3 Expression and Its Correlation with Proliferation and Apoptosis/Autophagy in Gliomas," *J. Oncol.*, vol. 2008, pp. 1–9, 2008, doi: 10.1155/2008/219241.

[151] H. Xu, G. Ma, F. Mu, B. Ning, H. Li, and N. Wang, "STAT3 Partly Inhibits Cell Proliferation via Direct Negative Regulation of FST Gene Expression," *Front. Genet.*, vol. 12, p. 678667, Jun. 2021, doi: 10.3389/fgene.2021.678667.

[152] R. Brigelius-Flohé and M. Maiorino, "Glutathione peroxidases," *Biochim. Biophys. Acta BBA - Gen. Subj.*, vol. 1830, no. 5, pp. 3289–3303, May 2013, doi: 10.1016/j.bbagen.2012.11.020.

[153] E.-G. Yoo *et al.*, "Insulin-Like Growth Factor-Binding Protein-3 Mediates High Glucose-Induced Apoptosis by Increasing Oxidative Stress in Proximal Tubular Epithelial Cells," *Endocrinology*, vol. 152, no. 8, pp. 3135–3142, Aug. 2011, doi: 10.1210/en.2010-1122.

[154] L. Zhou, H.-W. Koh, U.-J. Bae, and B.-H. Park, "Aggravation of post-ischemic liver injury by overexpression of insulin-like growth factor binding protein 3," *Sci. Rep.*, vol. 5, no. 1, p. 11231, Sep. 2015, doi: 10.1038/srep11231.

[155] C.-H. Jung, E. M. Kim, J.-Y. Song, J. K. Park, and H.-D. Um, "Mitochondrial superoxide

dismutase 2 mediates γ-irradiation-induced cancer cell invasion," *Exp. Mol. Med.*, vol. 51, no. 2, pp. 1–10, Feb. 2019, doi: 10.1038/s12276-019-0207-5.

[156] S. Damiano *et al.*, "Metabolism Regulation and Redox State: Insight into the Role of Superoxide Dismutase 1," *Int. J. Mol. Sci.*, vol. 21, no. 18, p. 6606, Sep. 2020, doi: 10.3390/ijms21186606.

[157] J. Bai and A. I. Cederbaum, "Mitochondrial Catalase and Oxidative Injury," *Neurosignals*, vol. 10, no. 3–4, pp. 189–199, 2001, doi: 10.1159/000046887.

[158] V. Shoshan-Barmatz, D. Ben-Hail, L. Admoni, Y. Krelin, and S. S. Tripathi, "The mitochondrial voltage-dependent anion channel 1 in tumor cells," *Biochim. Biophys. Acta BBA - Biomembr.*, vol. 1848, no. 10, pp. 2547–2575, Oct. 2015, doi: 10.1016/j.bbamem.2014.10.040.

[159] F. Tomasello *et al.*, "Outer membrane VDAC1 controls permeability transition of the inner mitochondrial membrane in cellulo during stress-induced apoptosis," *Cell Res.*, vol. 19, no. 12, pp. 1363–1376, Dec. 2009, doi: 10.1038/cr.2009.98.

[160] S. D. Catz and J. L. Johnson, "Transcriptional regulation of bcl-2 by nuclear factor κB and its significance in prostate cancer," *Oncogene*, vol. 20, no. 50, pp. 7342–7351, Nov. 2001, doi: 10.1038/sj.onc.1204926.

[161] D. Levens, "You Don't Muck with MYC," *Genes Cancer*, vol. 1, no. 6, pp. 547–554, Jun. 2010, doi: 10.1177/1947601910377492.

[162] Y. Xu, S. Porntadavity, and D. K. St Clair, "Transcriptional regulation of the human manganese superoxide dismutase gene: the role of specificity protein 1 (Sp1) and activating protein-2 (AP-2)," *Biochem. J.*, vol. 362, no. 2, pp. 401–412, Mar. 2002, doi: 10.1042/bj3620401.

[163] K. Kunisada *et al.*, "Activation of JAK-STAT and MAP Kinases by Leukemia Inhibitory Factor Through gp130 in Cardiac Myocytes," *Circulation*, vol. 94, no. 10, pp. 2626–2632, Nov. 1996, doi: 10.1161/01.CIR.94.10.2626.

[164] D. M. Morales-Prieto *et al.*, "Intranuclear Crosstalk between Extracellular Regulated Kinase1/2 and Signal Transducer and Activator of Transcription 3 Regulates JEG-3 Choriocarcinoma Cell Invasion and Proliferation," *Sci. World J.*, vol. 2013, pp. 1–10, 2013, doi: 10.1155/2013/259845.

[165] J. Sgrignani, M. Garofalo, M. Matkovic, J. Merulla, C. V. Catapano, and A. Cavalli, "Structural Biology of STAT3 and Its Implications for Anticancer Therapies Development," *Int. J. Mol. Sci.*, vol. 19, no. 6, p. 1591, May 2018, doi: 10.3390/ijms19061591.

[166] M. Tkach *et al.*, "p42/p44 MAPK-mediated Stat3Ser727 phosphorylation is required for progestin-induced full activation of Stat3 and breast cancer growth," *Endocr. Relat. Cancer*, vol. 20, no. 2, pp. 197–212, Apr. 2013, doi: 10.1530/ERC-12-0194.

[167] D. Kim *et al.*, "STAT3 activation in large granular lymphocyte leukemia is associated with cytokine signaling and DNA hypermethylation," *Leukemia*, vol. 35, no. 12, pp. 3430–3443, Dec. 2021, doi: 10.1038/s41375-021-01296-0.